POLYANHYDRIDE BLENDS AS DRUG DELIVERY MATRICES TO CONTROL BIOFILMS, BONE, AND NERVE REGENERATION

by

MICHELLE LINETTE JOHNSON

A Dissertation submitted to the

Graduate School-New Brunswick

Rutgers, The State University of New Jersey

in partial fulfillment of the requirements

for the degree of

Doctor of Philosophy

Graduate Program in Chemistry and Chemical Biology

written under the direction of

Professor Kathryn E. Uhrich

and approved by

_____

_____

_____

_____

New Brunswick, New Jersey

May, 2008

ABSTRACT OF THE DISSERTATION

Polyanhydride Blends for Drug Delivery, Biofilm Prevention, and Tissue Engineering

By MICHELLE LINETTE JOHNSON

Dissertation Director:

Kathryn E. Uhrich

Biodegradable polyanhydrides were fabricated into disks, coatings, microspheres, and tubes for controlled drug delivery as well as enhanced thermal and mechanical properties. The polymer systems were evaluated as potential treatments for periodontal disease, orthopedic injuries, nerve regeneration, and biofilm formation. The polymers contained the non-steroidal anti-inflammatory drug (NSAID), salicylic acid and the antibiotic, ampicillin, in the polymer backbone, which are subsequently released as the polymers degrade. Significantly, the polymers can be fabricated into these different geometries that would not be possible with the drug molecules alone.

This dissertation characterizes the *in vitro* degradation of the polyanhydrides specifically for the multiple applications. Polymer degradation was monitored by high pressure liquid chromatography (HPLC) for final degradation products. The effect of physically admixing additional drugs into the polymer matrix was studied as well, where the admixed drugs were delineated from the chemically incorporated drugs by HPLC. Accelerated *in vitro* degradation rates were developed using highly basic media.

Mechanical and thermal properties were examined for potential orthopedic and nerve applications. The compliance and modulus of polymer blends and composites were measured to characterize the flexibility and strength of each system. Additionally, properties, such as glass transition temperature (T_g) and decomposition temperature (T_d) were measured to monitor polymer changes as a result of processing and degradation.

Overall, the fundamental chemical, thermal and mechanical properties of each polyanhydride system were monitored. This dissertation describes the optimization of controlled drug release rates for specific applications through composites and blends of ceramics (hydroxyapatite), drugs (antimicrobials and NSAIDs), and polymers (polyanhydrides).

DEDICATION

To Jemal Jr., Jemir, Robert Jr., Jenelle, and Jada. Always strive to do your best and achieve your dreams. Thank you for making me laugh and giving me some much needed breaks throughout my graduate school years.

ACKNOWLEDGEMENTS

To my advisor, Kathryn Uhrich: Thank you for the advice and guidance you have given me to help me achieve my goals. Your support and encouragement have been paramount in my reaching this level. Thank you for your kind words of wisdom, which helped my development, and I will continue to carry them with me as I move into industry.

I would like to thank my committee members Jing Li, Ph.D., Dinesh Patwardhan, Ph.D., and John Taylor, Ph.D. for their suggestions and help with my experiments and writing. I would also like to give a special thank you to Ted Madey Ph.D. for helping me with fellowship applications and experiment planning, and allowing me access to his laboratory.

To my family, Mom, Dad, Rhonda, and Kimberly, thanks for supporting me through all these years in school. I'm finally finished!

Kehinde, thanks for always being there to answer my questions and help me. I really appreciate everything.

Tanya, thanks for being such a great friend and always being there to listen and give advice. I hope your graduate school is as enlightening for you as mine was for me.

I would like to thank all of the staff and students of the NSF-IGERT on Integratively Engineered Biointerfaces for a very stimulating interchange in which I learned a great deal. I would especially Linda Anthony, Ph.D. for all of her support and for taking the time to be a reference for me, and Prabhas Moghe, Ph.D. for pushing me to achieve more from my research and also providing references for external funding.

FDA/CDRH/OSEL/DCMS, thank you all for your help and advice during and after my internship.

Additionally, in no particular order, I would like to thank Kris Wetter, the Uhrich Group, Mark Reynolds DDS Ph.D., Mike Chikindas Ph.D. and Linda, Rick Riman Ph.D., Ana, Dan, Eugene, Rui, Melissa, Ann, Eileen, Bonnie, and last but not least NSF and NIH for funding.

TABLE OF CONTENTS

LIST OF TABLES

LIST OF FIGURES

CHAPTER 1: INTRODUCTION

1.1. Controlled Drug Delivery from Polymer Matrices

Historically, drugs were systemically administered with a short, uncontrolled release profile.[1,2] Recent drug delivery methods, such as polymeric drug carriers, were developed to sustain drug release with fewer doses and to stabilize sensitive drug compounds.[3-5] The polymeric drug delivery systems are often designed for localized release, which avoids the toxicity associated with systemic drug delivery.[4]

Two major mechanisms govern controlled release from biodegradable polymers, diffusion- and erosion- controlled mechanisms.[6] **Figures 1.1 and 1.2** depict how drugs are released from polymers in both mechanisms. **Figure 1.1** shows diffusion through a polymer matrix into the surrounding media over time. The diffusion-controlled method usually describes nondegradable polymer systems,[7] but can also influence drug release from degradable polymer systems. In this case, diffusion is driven by pore formation in the polymer matrix. **Figure 1.2** shows erosion-controlled drug delivery which describes drug release from degradable polymers. As the polymer matrix erodes into the surrounding media, the drug is released into the media as well.

Polymer matrix erosion can be further classified as either surface- or bulk-eroding (**Figure 1.3**).[8] Bulk erosion encompasses devices that erode from the "inside-out". The entire device erodes as media penetrates to form pores (**Figure 1.3 left**).

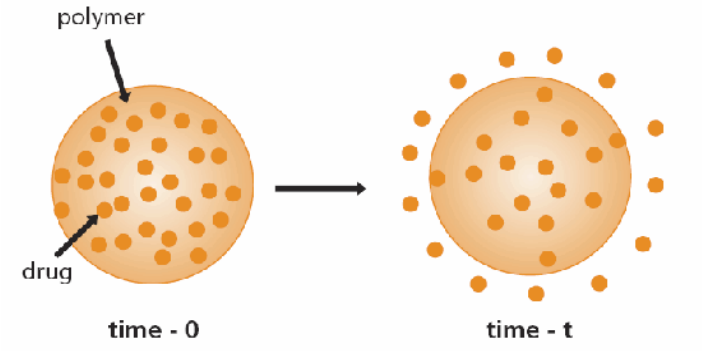

Figure 1.1. Schematic demonstrating the mechanism of diffusion-controlled release[6]

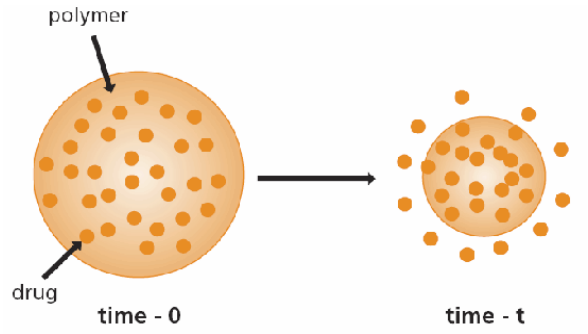

Figure 1.2. Schematic demonstrating the mechanism of erosion-controlled release[6]

In contrast, some devices only erode from the surface (**Figure 1.3 right**). The media only interacts with the surface of the device, while the device interior remains unaffected. The erosion mechanisms alter drug release profiles and polymer systems should be selected based on the desired drug release rate and profile.

Controlled drug delivery systems are often designed to achieve zero-ordered or near-zero ordered drug release,[9] as zero-ordered drug release is independent of time and

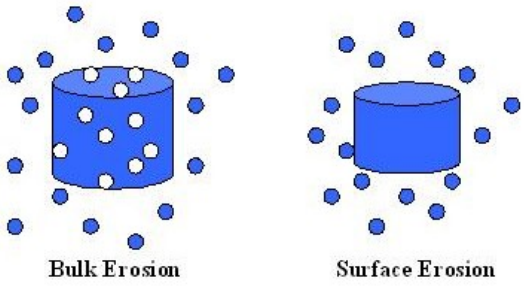

Figure 1.3. Schematic of bulk and surface erosion mechanisms.[6]

drug concentration remains constant. However, most systems do not achieve zero-ordered release and many are classified as near-zero ordered.[10] Additionally, many systems display a first-ordered release profile, which is defined as an initial high concentration of drug release followed by a linear decrease in drug release over time.[11]

Drug release profiles can also be defined by cumulative release profiles.[12] Cumulative release profiles show the total amount of drug released over time (**Figure 1.4**). The initial release phase can be characterized by a lag or burst phase. The lag phase is minimal drug release during the initial stages, while the burst phase is a very fast initial release. The initial stages are often followed by a linear increase in drug release. The final stage of cumulative drug release is often a plateau phase, where the drug release rate slows considerably and essentially levels off with no further increases.

With so many ways to describe drug release, it can be difficult to classify complicated systems. As a result, polymeric drug delivery rates are simulated using computer models to determine the effects the polymers and drugs have on the overall delivery system.[13,14] In this dissertation, experimental techniques were used to characterize release rates and profiles.

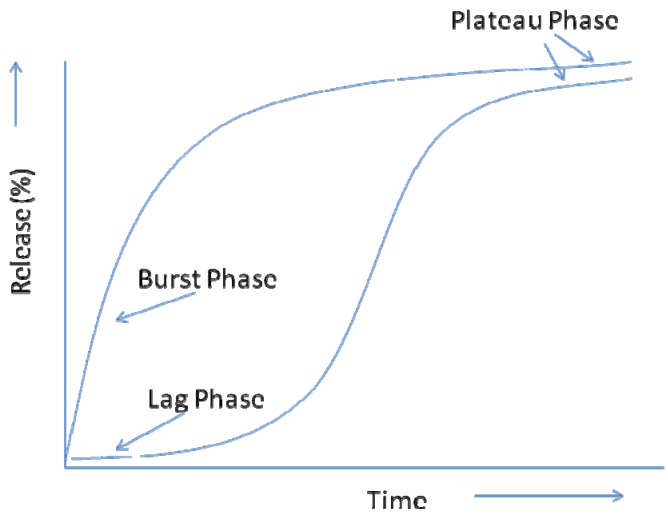

Figure 1.4. Schematic showing phases of cumulative drug release.

1.2. Polyanhydrides and Poly(anhydride-esters)

Polyanhydrides have been studied in detail over the past few decades, specifically for their potential as drug delivery vehicles.[15-17] Polyanhydrides have many desirable characteristics that make them amenable for drug delivery. For example, they surface-erode in media, which avoids the "inside-out" degradation profile observed in bulk-eroding materials, and ultimately better controls drug release rates (**Figure 1.5**).[18]

Initial *in vitro* degradation studies determined the general pathway of poly(anhydride-ester) degradation, as illustrated in **Scheme 1.1**.[19-21] First, the anhydride bonds between each repeat unit are cleaved to yield the diacid intermediate. Second, the ester bonds are cleaved within each repeat unit to release the active drug molecule, salicylic acid in this example, and the biocompatible linker.

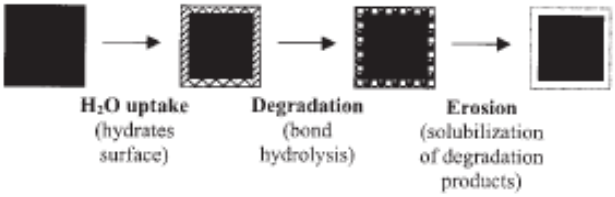

Figure 1.5. The mechanism of polyanhydride hydrolysis, which begins with water uptake, followed by degradation, and finally erosion of the polymer matrix.[20,22-25]

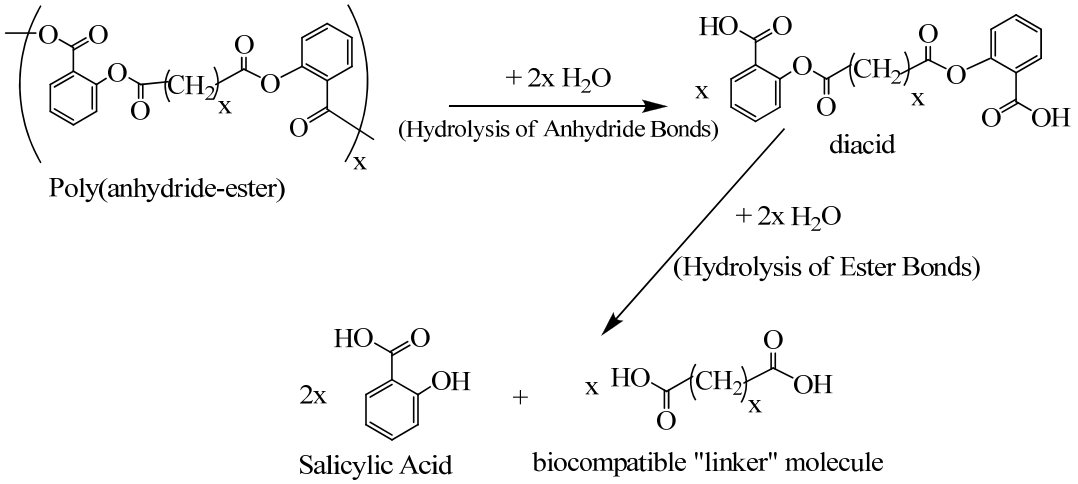

Scheme 1.1. Degradation mechanism of poly(anhydride-esters)[19-21]

The salicylic acid-based poly(anhydride-esters) (SA-based PAEs) have been synthesized by the melt-condensation and solution polymerization methods.[26] In the melt-condensation polymerization, the monomer is heated under vacuum to remove excess acetic anhydride and form anhydride linkages between the polymer repeat units, followed by precipitation from an organic solvent. The solution polymerization is prepared using triphosgene as coupling agent and triethylamine as acid acceptor,

requiring strictly stoichiometric amounts of each compound. Thermally sensitive drugs, such as ampicillin, must be prepared by solution polymerization because they would decompose in the melt-condensation polymerization. The resulting polymers from either

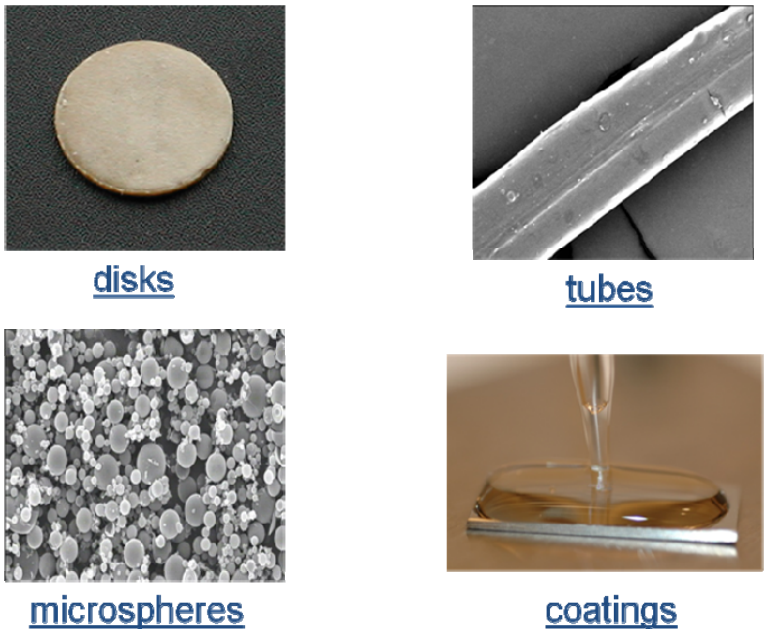

Figure 1.6. Fabrication methods of polyanhydrides into various geometries. [19,27,28]

polymerization method can be manipulated and fabricated into many geometries for various applications.[19,27,28] Specifically, disks and fibers are implanted to treat periodontal disease, tubes and microspheres direct nerve growth, and coatings prevent biofilm formation and restenosis.

The SA-based PAEs have been examined in animal studies and *in vitro* for related applications, such as localized release in bone to heal fractures and periodontal disease treatment.[26,29,30] The results showed that these polymers reduce inflammation and

prevent bone resorption, which is critical for implants to remain in place and prevent loosening and rejection.[29,30]

1.3. Significance of Drug Molecules Incorporated into the Polymer Backbone

Salicylic acid and ampicillin have been incorporated into polyanhydride backbones for release upon hydrolytic degradation of the polymer. Salicylic acid, the active ingredient in aspirin, has been used for over 3500 years as an anti-inflammatory agent, analgesic, and anti-pyretic.[31,32] Ampicillin is a common antibiotic based on penicillin and is active against Gram-positive and some Gram-negative bacteria.[32,33] These drug compounds are systemically administered to patients, yet localized release can reduce systemic toxicity, prevent bacterial resistance, and target the injury site.[34,35] Further, drug delivery from biodegradable polymers may be able to improve patient response to the implants due to reduced inflammation and foreign body response.[36]

1.4. Applications of Polyanhydride Blends

As previously mentioned, polyanhydrides can be adapted to a variety of applications. Here, the focus is on developing biomaterials to treat periodontal disease, promote bone growth, prevent biofilm formation, and regenerate nerves following injury. The polymer systems discussed are biodegradable and release drug compounds, such as salicylic acid and ampicillin, to treat each condition.

1.4.1. Drug Delivery for Periodontal Treatment

Periodontal disease is a common bacterial infection that causes the periodontium (gum tissue) and bone surrounding the teeth to erode and resorb (Figure **1.7.**), ultimately causing tooth loss.[37] Recent therapies include localized delivery of antibiotics to reduce the risk of adverse systemic drug reactions and increase patient compliance.[38-41] For example, PerioChip™ is implanted into the periodontal pocket and releases chlorhexidine into the gum tissue to treat the bacterial infection (**Figure 1.7.**). The system discussed in this dissertation is similar to PerioChip™ and was designed using SA-based PAEs loaded with antimicrobials, such as chlorhexidine, clindamycin, and minocycline to treat the pain and infection associated with periodontal disease. The polymer degrades into salicylic

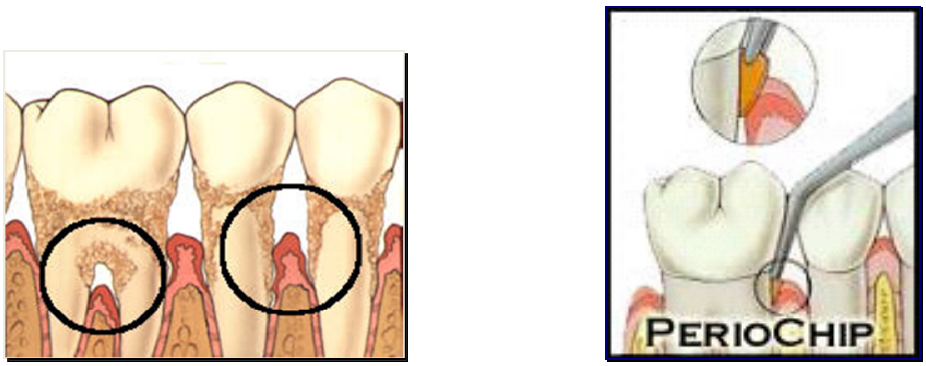

Figure 1.7. Progression of periodontal disease (left) and treatment with PerioChip™ (right).

acid while releasing antimicrobials to treat infections at the implant site for the first few weeks following surgery, or the critical healing period for the patient.

1.4.2. Polymer Coatings for Medical Devices

Polymer coatings on medical devices are becoming increasingly popular.[42] The most common polymer coatings were developed for cardiac stents to prevent restenosis.[43] Stent surfaces are believed to greatly influence stent properties and usage, so a polymer coating for controlled drug release may be extremely beneficial.[44] Various types of stent coatings from inorganic to polymeric have been developed for improved function.

Another novel coating development, which will be discussed in more detail in a following chapter, involves coating medical devices with antimicrobials to treat and prevent bacterial infections. Another issue in medical devices is bacterial resistance, the development of coatings to prevent biofilm formation is important as well.[45,46] An important finding has shown synergy between local and systemic delivery of antimicrobials.[47] Such developments will be significant to reducing the number of revision surgeries and increasing the overall success of metal implants.

1.4.3. Polymer:Hydroxyapatite Composites for Bone Growth

Hydroxyapatite can be synthesized as a porous, biocompatible material that is very similar to the minerals found in human bone and teeth. The ratio of calcium to phosphorous in the synthetic material must be very close to the theoretical value of 1.67 because the release of free Ca^{2+} and PO_4^{3-} is the driving force of pore formation upon erosion of hydroxyapatite.[48]

Yet, synthetic hydroxyapatite is unable to match the mechanical properties of natural hydroxyapatite and is still accepted for some non-load bearing bone implant

applications. Hydroxyapatite cannot be used alone for load-bearing applications because it is brittle, stiff and generally has poor mechanical strength.[49] Hydroxyapatite is too weak to dissipate the energy from the typical recurring impact in bone.[49] Hydroxyapatite composites can be made with polymers, fibers, and other materials to improve and optimize the mechanical properties for specific bone applications.[50,51]

1.4.4. Polyanhydrides for Nerve Regeneration

Nerve guidance conduits for tissue engineering can be enhanced with various compounds to enhance nerve growth, including biodegradable polymers and microsphere and collagen fillings.[52,53] Particularly, protein delivery is extremely promising for guiding nerve growth. In some cases, the conduit itself can be used as a drug delivery vehicle, but it may be more useful to load microspheres into the conduit to facilitate nerve growth.[54,55] In developing polyanhydrides for nerve regeneration, the thermal and mechanical properties were compared to other systems that have been studied, such as poly(glycolic acid) and collagen for similar flexibility and degradation rate.[56]

1.5. General Overview of the Dissertation

This dissertation has four general objectives. The first objective is to physically admix salicylic acid and antimicrobials into salicylic acid-based poly(anhydride-esters) (SA-based PAEs) to treat periodontal disease and optimize the *in vitro* drug release characteristics of the admixed drugs and from the polymer itself. The first objective is addressed in Chapters 2 and 8 and highlights the use of high performance liquid

chromatography (HPLC) to delineate the final degradation product (salicylic acid) from oligomers and other degradation products.

The second objective is outlined in Chapter 4; the objective is to develop an antibiotic-based poly(anhydride-amide) coating for drug release and biofilm resistance. Studies of biofilm growth are significant as bacteria, such as *Staphylococcus aureus* become increasingly resistant to traditional therapies.

The third objective of this dissertation is to optimize protein encapsulation in SA-based PAEs so that protein delivery can be controlled for nerve regeneration. The protein delivery system was developed to potentially be used to fill polyanhydrides tubes for directed nerve growth. The protein-loaded polymer microspheres are discussed in Chapter 5, whereas the thermal and mechanical properties of the polyanhydride tubes are described in Chapter 6.

The final objective is to develop polymer:hydroxyapatite composites and polyanhydride blends and characterize the mechanical properties (compliance and modulus) for medical devices or implants. These projects are discussed in Chapters 3 and 6, respectively.

All biomaterials are defined as a result of their function. It is important to characterize the fundamental chemical, mechanical, and thermal properties of a biomaterial prior to biological studies. This dissertation examines the fundamental properties of potential biomaterials to define their future uses.

1.6. References

1. Chien YW. Rate-control drug delivery systems: controlled release vs. sustained release. Medical Progress through Technology 1989;15:21-46.

2. Schacht EH. Using biodegradable polymers in advanced drug delivery systems. Medical Device Tech 1990;1(1):15-21.

3. Mills SN, Davis SS. Controlled drug delivery. In: Illum L, Davis SS., editor. Polymers in Controlled Drug Delivery. Bristol: Wright; 1987.

4. Vernon B, Wegner M. Controlled release. In: Wnek GE, Bowlin GL., editor. Encyclopedia of Biomaterials and Biomedical Engineering. New York: Marcel Dekkar; 2004.384-391.

5. Hanssen AD, Osmon DR, Patel R. Local antibiotic delivery systems. Clin Orthop Relat Res 2005;437:111-114.

6. Langer R. New methods of drug delivery. Science 1990;249(4976):1527-1553.

7. Heller J, Hoffman AS. Drug delivery systems in biomaterials. In: Ratner B, editor. Biomaterials Science. San Diego: Elsevier; 2004.628-648.

8. Uhrich KE, Cannizzaro SM, Langer RS. Polymeric systems for controlled drug release. Chem Rev 1999;99:3181-3198.

9. Landgraf W, Li N-H, Benson JR. New polymer enables near zero-order release of drugs. Drug Deliv Tech 2005;5(2):50-55.

10. DiColo G. Controlled drug release from implantable matrices based on hydrophobic polymers. Biomaterials 192;13(12):850-856.

11. Okana T, Bae YH, Jacobs H, Kim SW. Thermally on-off switching polymers for drug permeation and release. J Controlled Release 1990;11:255-265.

12. Li Y-H, Zhu J-B. Modulation of combined-release behaviors form a novel "tablets-in-capsule system". J Controlled Release 2004;95:381-389.

13. Larobina D, Mensitieri G, Kipper MJ, Narasimhan B. Mechanistic understanding of degradation in bioerodible polymers for drug delivery. AIChE Journal (Bioengineering, Food, and Natural Products) 2002;48(12):2960-2970.

14. Saylor DM, Kim C-S, Patwardhan DV, Warren JA. Diffuse-interface theory for structure formation and release behavior in controlled drug release systems. Acta Biomaterialia 2007;3:851-864.

15. Domb AJ, Amselem S, Shah J, Maniar M. Polyanhydrides: Synthesis and characterization. Adv in Polym Sci 1993;107:93-141.

16. Kumar N, Langer RS, Domb AJ. Polyanhydrides: an overview. Adv Drug Deliv Rev 2002;54:889-910.

17. Jain JP, Modi S, Domb AJ, Kumar N. Role of polyanhydrides as localized drug carriers. J Controlled Release 2005;103:541-563.

18. Langer R. Biopolymers in controlled release systems. NATO ASI Series E: Applied Science 1986;106(Polym. Biomater.):161-169.

19. Erdmann L, Uhrich KE. Synthesis and degradation characteristics of salicylic acid-derived poly(anhydride-esters). Biomaterials 2000;21(19):1941-1946.

20. Whitaker KA. Structure-property relationships of a degradable salicylate-based poly(anhydride-ester). New Brunswick: Rutgers University; 2006. 149 p.

21. Prudencio A, Schmeltzer RC, Uhrich KE. Effect of linker structure on salicylic acid-derived poly(anhydride-esters). Macromolecules 2005;38:6895-6901.

22. Gopferich A. Mechanisms of polymer degradaton and erosion. Biomaterials 1996;1996:103-114.

23. Gopferich A, Tessmar J. Polyanhydride degradation and erosion. Adv Drug Deliv Rev 2002;54:911-913.

24. Burkersroda F, Schedl L, Gopferich A. Why degradable polymers undergo surface erosion or bulk erosion. Biomaterials 2002;23:4221-4231.

25. Whitaker-Brothers K, Uhrich K. Investigation into the erosion mechanism of salicylate-based poly(anhydride-esters). J Biomed Mater Res 2006;76A:470-479.

26. Schmeltzer R, Johnson M, Griffin J, Uhrich KE. Comparison of salicylate-based poly(anhydride-esters) formed *via* melt-condensation *versus* solution polymerization. J Biomater Sci Polymer Edn 2008;in press.

27. Whitaker-Brothers K, Uhrich K. Poly(anhydride-ester) fibers: Role of copolymer composition on hydrolytic degradation and mechanical properties. J Biomed Mater Res 2004;70A:309-318.

28. Yeagy BA, Prudencio A, Schmeltzer RC, Uhrich KE, Cook TJ. Characterization and *in vitro* degradation of salicylate-derived poly(anhydride-ester microspheres). J Microencapsulation 2006;23(6):643-653.

29. Erdmann L, Macedo B, Uhrich KE. Degradable poly(anhydride-ester) implants: Effects of localized salicylic acid release on bone. Biomaterials 2000;21(24):2507-2512.

30. Harten RD, Svach DJ, Schmeltzer R, Uhrich KE. Salicylic acid-derived poly(anhydride-esters) inhibit bone resorption and formation in vivo. J Biomed Mater Res 2005;72A(4):354-362.

31. Vane JR, Botting RM. Anti-inflammatory drugs and their mechanism. Inflammation Research 1998;47(Supplement 2):S78-S87.

32. The Merck Index, Thirteenth Edition. Rahway, NJ: Merck & Co., Inc.; 2001.

33. Kirby WM, Bulger RJ. The new penicillins and cephalosporins. Annual Rev of Med 1964;15:393-412.

34. Graham GG, Champion GD, Day RO, Kaski AL, Hils LG, Paull PD., editor. Salicylates in rheumatoid arthritis: Pharmacokinetics and analgesic response. Bosel and Stuttgart: Birkhauser Verlag; 1976.

35. Nair LS, Laurencin CT. Biodegradable polymers as biomaterials. Prog Polym Sci 2007;32:762-798.

36. Anderson JM, et.al. Host reactions to biomaterials and their evaluation. Biomaterials Science 1996(165-214).

37. Schwach-Abdellaoui K, Vivien-Castioni N, Gurny R. Local delivery of antimicrobial agents for the treatment of periodontal diseases. Eur J Pharm Biopharm 2000;50:83-99.

38. Ciancio S. Site specific delivery of antimicrobial agents for periodontal disease. Gen Dent 1999(March-April 1999):172-181.

39. Killoy WJ, Saiki SM. A new horizon for the dental hygienist: Controlled local delivery of antimicrobials. J Dent Hygiene 1999;73(2):84-92.

40. Killoy WJ. The clinical significance of local chemotherapies. J Clin Periodontol 2002;29(Suppl 2):22-29.

41. Trombelli L, Tatakis DN. Periodontal diseases: current and future indications for local antimicrobial therapy. Oral Diseases 2003;9(Suppl. 1):11-15.

42. Siepmann F, Siepmann J, Walther M, MacRae RJ, Bodmeier R. Polymer blends for controlled release coatings. J Controlled Release 2008;125(1):1-15.

43. Ge L, Cosgrave J, Iokovou I, Sangiorgi GM, Colombo A. New drug-eluting stent technologies. Curr Cardio Rev 2005;1(3):189-193.

44. Wnek GE, Bowlin GL. Encyclopedia of Biomaterials and Biomedical Engineering. Marcel Dekkar 2004;New York, NY.

45. Costerton JW. Biofilm theory can guide the treatment of device-related orthopaedic infections. Clin Orthop Relat Res 2005;437:7-11.

46. Patel R. Biofilms and antimicrobial resistance. Clin Orthop Relat Res 2005;437:41-47.

47. Campoccia D, Montanaro L, Ariciola CR. The significance of infection related to orthopedic devices and issues of antibiotic resistance. Biomaterials 2006;27:2331-2339.

48. Tampieri A, Celotti G, Spiro S, Delcogliano A, Franzese. Porosity-graded hydroxyapatite ceramics to replace natural bone. Biomaterials 2001;22:1365-1370.

49. Orlovskii VP, Komlev VS, Barinov SM. Hydroxyapatite and hydroxyapatite-based ceramics. Inorganic Materials 2002;38(10):1159-1172.

50. Durucan C, Brown PW. Biodegradable hydroxyapatite-polymer composites. Adv Eng Mater 2001;3(4):227-231.

51. Katti KS. Biomaterials in total joint replacement. Colloids and Surfaces B: Biointerfaces 2004;39:133-142.

52. Ma PX. Biomimetic materials for tissue engineering. Adv Drug Deliv Rev 2008;60:184-198.

53. Ciardelli G, Chiono V. Materials for peripheral nerve regeneration. Macromolecular Bioscience 2005;6:13-26.

54. Piotrowicz A, Shoichet MS. Nerve guidance channels as drug delivery vehicles. Biomaterials 2006;27:2018-2027.

55. Goraltchouk A, Scanga V, Morshead CM, Shoichet MS. Incorporation of protein-eluting microspheres into biodegradable nerve guidance channels for controlled release. J Controlled Release 2006;110:400-407.

56. Tanaka S, Takigawa T, Ichihara S, Nakamura T. Mechanical properties of the bioabsorbable polyglycolic acid-collagen nerve guide tube. Polym Eng Sci 2006;46:1461-1467.

CHAPTER 2: CONCURRENT RELEASE OF ADMIXED ANTIMICROBIALS AND SALICYLIC ACID FROM SALICYLATE-BASED POLY(ANHYDRIDE-ESTERS)

2.1. Abstract

A polymer blend consisting of antimicrobials (chlorhexidine, clindamycin, and minocycline) physically admixed at 10 % by weight into a salicylic acid-based poly(anhydride-ester) (SA-based PAE) were developed as an adjunct treatment for periodontal disease. The SA-based PAE/antimicrobial blends were characterized by multiple methods, including contact angle measurements and differential scanning calorimetry (DSC). Static contact angle measurements showed no significant differences in hydrophobicity between the polymer/antimicrobial matrix surfaces. Notable decreases in the polymer glass transition temperature (T_g) and the antimicrobials' melting points (T_m) were observed, indicating that the antimicrobials act as plasticizers within the polymer matrix. *In vitro* drug release of salicylic acid from the polymer matrix and for each physically admixed antimicrobial was concurrently monitored by high pressure liquid chromatography (HPLC) during the course of polymer degradation and erosion. Although the polymer/antimicrobial blends were immiscible, the initial 24 hours of drug release correlated to the erosion profiles. The SA-based PAE/antimicrobial blends are being investigated as an improvement on current localized drug therapies used to treat periodontal disease.

2.2. Introduction

Polyanhydrides have been studied by many researchers over the past two decades as drug carriers.[1-3] Particularly, polyanhydrides exhibit nearly zero-order drug release profiles *in vitro* [2,3] because they primarily erode by a surface-erosion mechanism that excludes water from the polymer matrix during degradation.[4-7] Polyanhydride matrices have been examined for the delivery of multiple bioactive agents, such as hydrophobic drugs, anticancer agents, and DNA.[8-11]

Building upon the success of the polyanhydrides, our laboratory synthesized salicylic acid-based poly(anhydride-ester) (SA-based PAEs)[12-14] that degrade into active drug molecules and may also act as drug carrier matrices. Salicylic acid is particularly relevant because it is a non-steroidal anti-inflammatory drug (NSAID) that can treat inflammation and the pain associated with periodontal disease.[15,16] In an early example, the SA-based PAEs were fabricated into fibers, then the degradation and mechanical properties examined.[17] Based upon our early results, we evaluated the SA-based PAEs as drug delivery systems to concurrently deliver physically admixed antimicrobials and chemically incorporated salicylic acid, both of which are released upon hydrolytic degradation of the polymer matrix.[18] The combined delivery of an antimicrobial and anti-inflammatory is of particular interest for treating periodontal disease.

Periodontal disease is a very common bacterial infection that causes the periodontium (gum tissue) and bone surrounding the teeth to erode and resorb, ultimately causing tooth loss.[19] Typically, periodontal disease is treated with scaling and root planing to physically remove plaque below the gum line. Scaling and root planing is

usually followed with additional treatments, including systemic administration of antibiotics to ensure bacterial destruction.[20] Recent therapies include localized delivery of antibiotics to reduce the risk of adverse systemic drug reactions and to decrease concerns of patient compliance.[21-24] Examples of such commercially available products include Arestin®, a microsphere system based on poly(glycolide-*co*-dl-lactide) (PGLA) for minocycline release and Atridox®, a poly(lactic acid) (PLA)-based system for doxycycline release. Notably, the current approach to localized delivery utilizes PGLA and PLA which have been shown to cause inflammation and a foreign body response.[25,26] In comparison, the SA-based PAEs in this paper do not cause inflammation, compared to PLA-based systems which show pronounced inflammation in a rat defect model.[27] Nonetheless, the PLA and PGLA systems enable a prolonged release of the antimicrobials over 1-3 weeks without a lag phase rather than immediate release of the antibiotic without polymer. The polymer/antimicrobial system described herein is designed for implantation into the pockets formed in the periodontium (gum tissue) such that both the NSAID and antimicrobials are simultaneously and locally released into the periodontal pocket.

Three antimicrobials (chlorhexidine·2HCl, clindamycin·HCl, and minocycline·HCl) were physically admixed into the polymer matrix at 10 weight %, at approximately the current therapeutic levels used in similar periodontal products.[23,28-30] The antimicrobials have different octanol/water partition coefficient (logP)[31] and pKa[32] values which correlate to each drug's hydrophobicity, charge (**Table 2.1)** and potential release rate from the biodegradable polymer matrix. Further, the three antimicrobials provide a range of options to prevent contraindications in patients, are clinically relevant,

and have been examined for their potential use in other delivery systems throughout the literature.[19,28,33-35]

Table 2.1. LogP, pKa, solubility, T_m, and T_d values of antimicrobial agents and salicylic acid.

Antimicrobial	(calc) logP value[31]	pKa values[31]	Solubility in PBS (mg/mL)	T_m (°C)	T_d (°C)
Chlorhexidine·2HCl 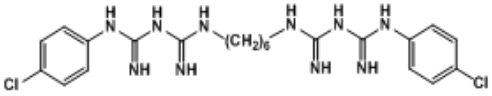	4.55	10.8	0.446	187	280
Clindamycin·HCl 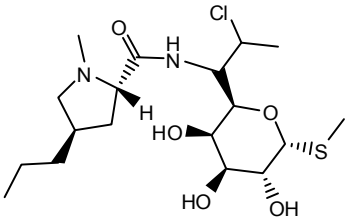	1.82	7.5	19.1	144	190
Minocycline·HCl 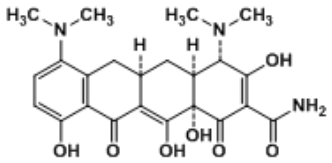	-0.55	2.8 5.0 7.8 9.5	27.1	136	138
Salicylic Acid 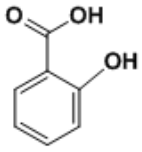	2.06	2.97 13.4	145	158	211

This chapter describes the physical polymer degradation characteristics and the controlled, concurrent *in vitro* release of clinically relevant antimicrobials and a NSAID from a biodegradable polymer matrix. The localized drug delivery system described herein may enhance the benefits of localized antimicrobial delivery systems by providing localized pain relief and anti-inflammatory effects due to the concurrent release of an NSAID,[28] in addition to the release of antimicrobials to reduce microbial growth.

2.3. Materials and Methods

2.3.1. Materials

Poly[1,6-bis(*o*-carboxyphenoxy)hexanoate] was prepared using previously described methods.[13,14] The polymer had M_w = 20,600, PDI = 1.2, and T_g = 65°C. Chlorhexidine·2HCl, clindamycin·HCl, and minocycline·HCl were purchased from MP Biomedicals (Irvin, CA) and used as received. Potassium phosphate dibasic and potassium phosphate monobasic and HPLC grade-acetonitrile were obtained from Aldrich.

2.3.2. Polymer Disk Preparation

The antimicrobials were separately incorporated into the polymer at 10% (w/w). Polymer (900 mg) was heated in a 150 mL PTFE beaker (FisherBrand, Pittsburg, PA) with a heat gun for approximately 2 minutes or until the polymer began to flow at 65°C. Each antimicrobial agent (100 mg) was added to the molten polymer and stirred for one

minute with a glass stirring rod. The mixture was then cooled to room temperature and then ground for 30 seconds in a coffee grinder (Mr. Coffee, Rye, NY).

The ground antimicrobial-polymer mixture (50.0 ± 5.0 mg) was placed into an IR pellet die (International Crystal Laboratories, Garfield, NJ) and pressed at 4,000 psi at room temperature for 5 minutes in a Carver Press (Carver, Wabash, IN). The resulting disks were 6.0±0.2 mm diameter and 1.0±0.2 mm thick, as determined by vernier caliper measurements (Mitutoyo, Japan).

2.3.3. Differential Scanning Calorimetry (DSC) Studies

DSC was performed on polymer/antimicrobial samples in triplicate following admixing but prior to pressing into disks. Up to 15 mg of each sample was placed in a TA instruments aluminum hermetic pan and analyzed on a TA Instruments Q200 DSC (New Castle, DE). The samples were tested using a heat- cool- heat scan from 0°C to 200°C at 10°C/minute under N_2. The polymer's T_g values were obtained from the second heat cycle and determined as the inflection point for all samples. Each antimicrobial's T_m was obtained from the first heat cycle. All DSC data analysis was completed using TA Universal Analysis software on a Dell Dimension 3000 computer with a Windows XP operating system.

2.3.4. Contact Angle Measurements

Static contact angle measurements were performed on polymer samples in triplicate on three separate samples prior to degradation using deionized water on a model 100 goniometer (Rame-Hart, Mountain Lakes, NJ). The contact angle was determined

digitally with a camera attachment and the measuring system on the DROPimage Advanced software on a Dell Dimension 3000 computer with a Windows XP operating system.

2.3.5. *In Vitro* Degradation Studies

The sample disks (40.0±1.4 mg) were placed in 20 mL scintillation vials containing 10 mL 0.1 M phosphate buffer solution (PBS) at pH 7.4. The vials were stored in a New Brunswick Scientific Series 25 Controlled Environment Incubator Shaker at 37°C and constantly shaken at 65 rpm. The degradation media was decanted from the vial and replaced with 10 mL fresh PBS at pre-determined time intervals. The spent degradation media was stored at room temperature until further analysis. The degradation study was conducted twice with an n=3 for both sets of experiments. All data shown are the average of at least 3 samples.

2.3.6. Determination of Mass Loss and Water Uptake

Water uptake and mass loss were determined by obtaining the mass of each sample using an analytical balance (Mettler Toledo Columbus, OH). At predetermined time points during the degradation study, the samples were removed from the degradation media, rinsed in deionized water to remove residual phosphate salts, and patted with Kimwipes® (Kimberly-Clark, Neenah, WI). Each sample was lyophilized in a Freezone Freeze Dry System (Labconco, Kansas City, MO) for 48 hours to ensure a constant mass. The water uptake was calculated using Equation (1) [7,36]:

$$WA(\%) = \frac{W_h - W_r}{W_r} \times 100 \qquad (1)$$

where *WA* is water absorbed by the sample or water uptake, W_h is the mass of the hydrated sample, and W_r is the residual mass of the lyophilized sample. The mass loss was calculated using Equation (2) [7,36]:

$$ML(\%) = \frac{W_0 - W_r}{W_0} \times 100 \qquad (2)$$

where *ML* is the mass loss of the sample and W_0 is the mass of the sample prior to degradation. Three samples were measured and averaged for each time point ($n = 3$).

2.3.7. High Pressure Liquid Chromatography (HPLC) Analysis of Degradation Media

Free salicylic acid release and antimicrobial (chlorhexidine·2HCl, minocycline·HCl, and clindamycin·HCl) release were quantified using a Gemini C18 column (150 x 4.6 mm, Phenomenex, Torrance, CA) on a Perkin Elmer (PE) HPLC system consisting of a Series 200 UV detector, a Series 200 pump, and an ISS 200 autosampler. The HPLC system was connected to a Dell computer running PE TotalChrom software via PE-Nelson 900 Interface and 600 LINK. Samples were diluted using PBS if needed to ensure measurements within the calibration curve and filtered through 0.45 μm poly(tetrafluoroethylene) (PTFE) syringe filters (Nalgene, Rochester, NY). Salicylic acid release was monitored at 210 nm, while chlorhexidine, clindamycin, and minocycline were monitored at 254 nm, 210 nm, and 298 nm respectively, with a

mobile phase of 75% 20 mM dibasic and monobasic potassium phosphate pH 2.5 using 1N HCl to adjust the pH and 25% acetonitrile. Five point calibration curves were generated for each compound with concentrations ranging between 0.0025 mg/ml and 0.5 mg/ml. Complete recovery (100 weight % of incorporated antimicrobials) of the antimicrobials was ensured by dissolving any remaining solid at the end of the *in vitro* degradation study and running the dissolved samples on the HPLC with the same running conditions.

2.4. Results and Discussion

2.4.1. Influence of Admixed Antimicrobials on Polymer Matrix Properties

The incorporation of molecules into a polymer's matrix may alter the inherent properties of the matrix. Static contact angle and DSC measurements were performed to determine the effect of the admixed antimicrobials on polymer **1 (Figure 2.1)** properties.

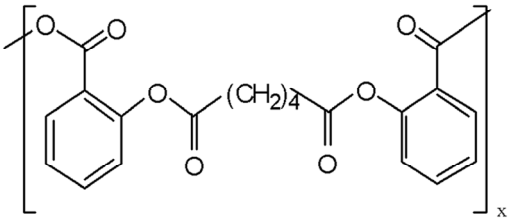

Figure 2.1. Chemical structure of poly[1,6-bis(*o*-carboxyphenoxy)hexanoate] (**Polymer 1**).

Primarily, the static contact angle was used to identify any changes to the hydrophobic nature of the polymer surface. Compression-molded disks of the polymer **1** alone showed a static contact angle of 56° in deionized water. The contact angles

decreased slightly to 54° when the antimicrobials were added to the compression-molded polymer at 10 weight %. Based on the minimal change in the contact angle measurement, the antimicrobials are not influencing the hydrophobic surface of polymer **1**.

DSC measurements were conducted to determine the extent of mixing between the antimicrobials and the polymer chains through changes in the glass transition temperature of polymer **1**. DSC has been used for decades as a method to measure the interaction or mixing of drugs within polymeric matrix systems.[37] The DSC results are summarized in **Table 2.2**. The T_g of the polymer alone is 65 °C, and a noticeable

Table 2.2. Thermal Properties of Antimicrobial:Polymer Blends.

Sample	Polymer T_g (°C)	Antimicrobial T_m (°C)
Polymer	65	*
10% Chlorhexidine in Polymer	54	152
10% Clindamycin in Polymer	40	144
10% Minocycline in Polymer	39	138

*Thermal transition not observed

decrease in the polymer T_g is observed with each antimicrobial admixture. For the admixture, the polymer's glass transition (39-65 °C) is clearly separated from the

antimicrobials' melting transition (138-152 °C). A sample DSC curve for minocycline is displayed in **Figure 2.2**. Additionally, a significant decrease in the T_m of chlorhexidine was observed from 187 °C for chlorhexidine alone to 152 °C in the chlorhexidine/polymer blend. The DSC results show that there is a characteristic lowering of the polymer's T_g for each of the polymer:antimicrobial blends that is consistent with previously reported results on diffusion-controlled drug release from polymers[38]. Each of the antimicrobials acts as a plasticizer within the polymer matrix, which indicates an increase in the free volume of the polymer.

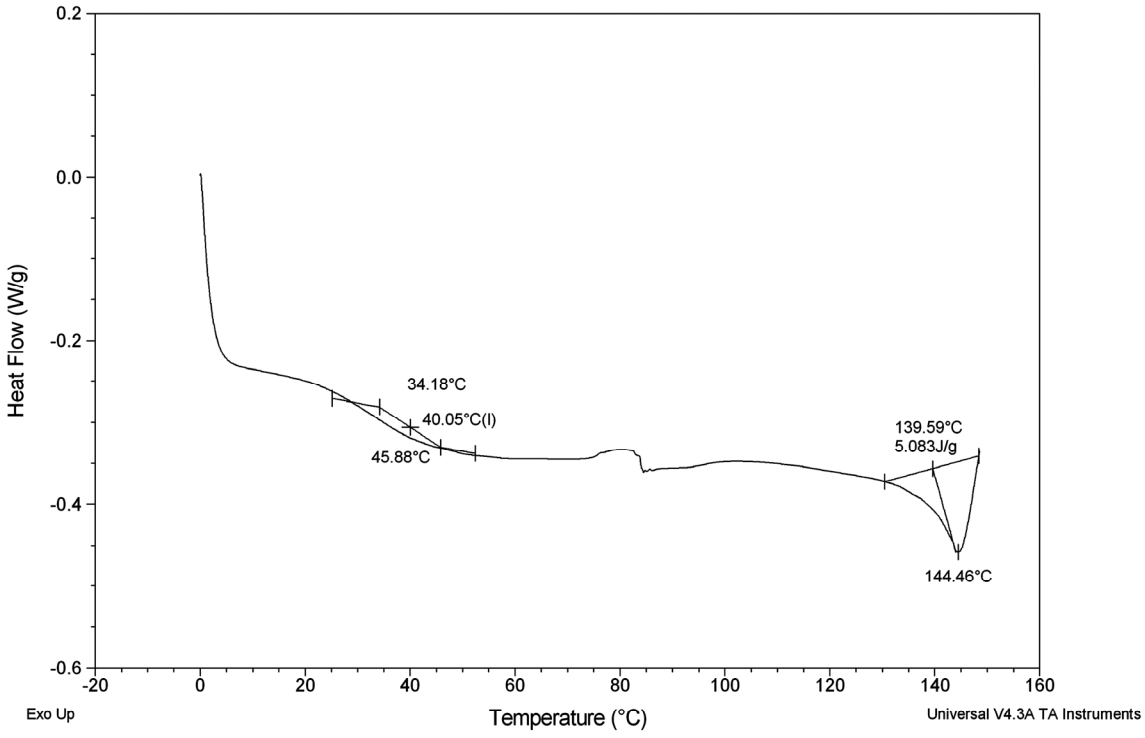

Figure 2.2. Representative DSC curve of 10% clindamycin HCl in Polymer **1** (polymer T_g shown at 40 °C and clindamycin T_m shown at 144 °C).

2.4.2. Salicylic Acid and Antimicrobial Release

The retention time of each compound separated by HPLC is shown in **Table 2.3**; note that each compound is distinct. The cumulative release of salicylic acid from the SA-based PAE (Polymer **1**) matrix is shown in **Figures 2.3 and 2.4** for each of the admixed antimicrobial matrices. Compared to polymer alone, the overall rate of salicylic acid release resulting from hydrolytic degradation of the polymer backbone was not significantly influenced by the presence of each admixed antimicrobial. Even though the differences in the release profiles are not statistically significant, a strong trend is observed: *the amount of salicylic acid released into the media decreases with increased antimicrobial hydrophobicity* **(Table 2.1, Figures 2.3 and 2.4)**. In addition, all release profiles exhibit a lag phase of approximately 15 hours. After the lag phase, the release profile is linear, faster, nearly zero-order, and ultimately reaches a plateau. Polymers were 50% degraded ($t_{1/2}$) at times ranging from 25 hours for the polymer alone, to 30

Table 2.3. HPLC Retention Times for Chlorhexidine, Clindamycin, Minocycline, and Salicylic Acid.

Compound	Retention Time (min)
Chlorhexidine	29.6
Clindamycin	5.1
Minocycline	2.3
Salicylic Acid	8.1

hours for minocycline (most hydrophilic at logP -0.55), and 42 hours for chlorhexidine (most hydrophobic at logP 4.55).

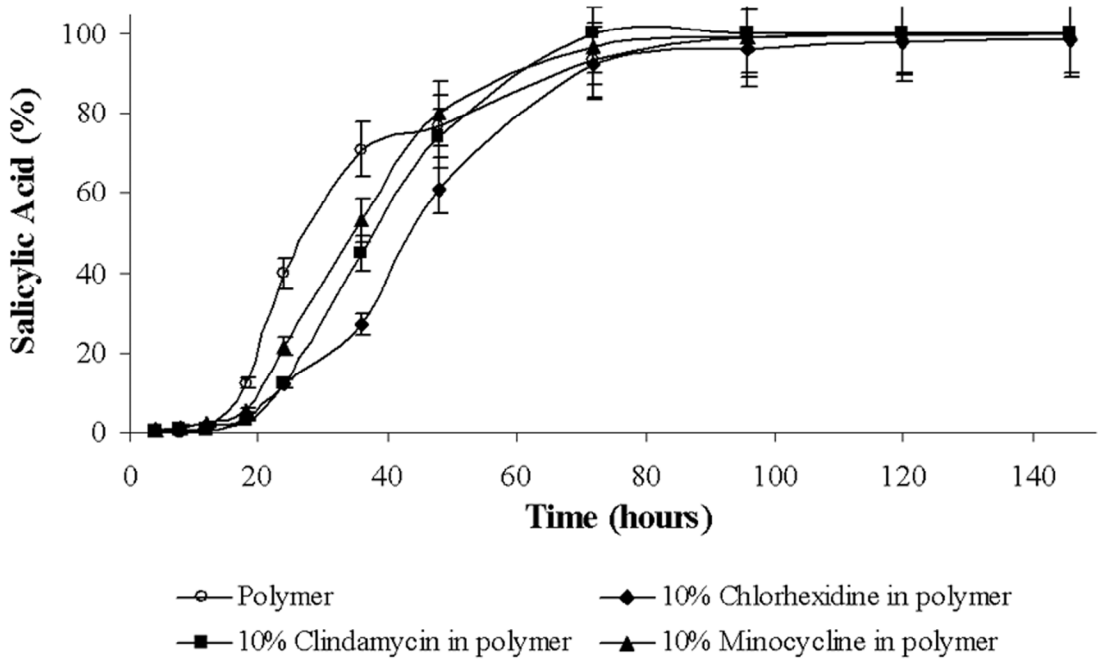

Figure 2.3. Cumulative release profiles of salicylic acid generated from four different polymer matrices, ranging from the salicylic acid-based polymer alone and the three antimicrobials (10 wt%) admixed within the polymer at 140 hours.

The release profiles of the three admixed antimicrobials from each polymer/antimicrobial matrix are compared in **Figures 2.5** (140 hours) and **2.6** (24 hours). The antimicrobial release generally corresponds to the logP values: chlorhexidine

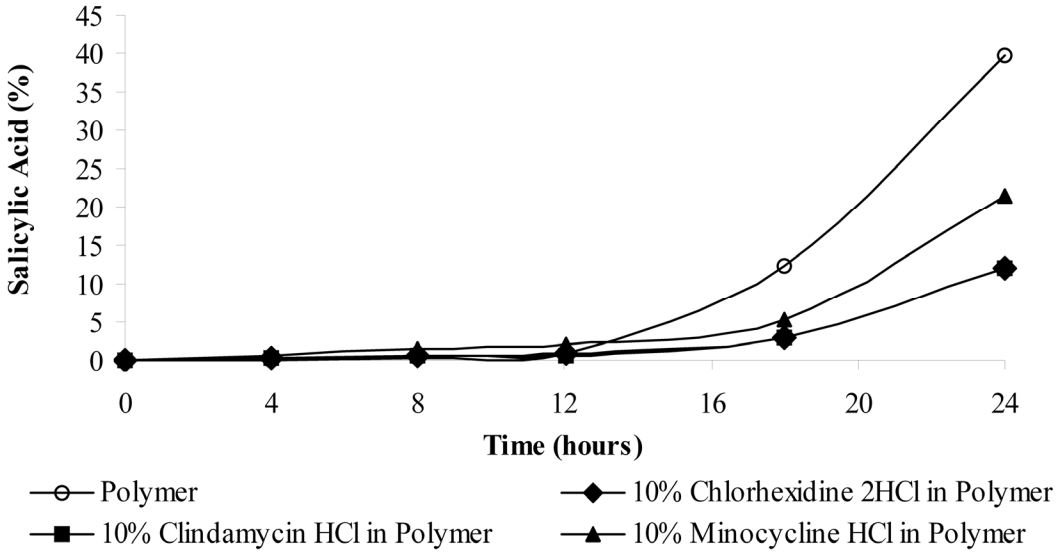

Figure 2.4. Cumulative release profiles of salicylic acid generated from four different polymer matrices, ranging from the salicylic acid-based polymer alone and the three antimicrobials (10 wt%) admixed within the polymer at 24 hours.

(logP 4.55) exhibited a longer lag phase and minimal release into the media before the matrix lost its integrity, whereas minocycline (logP -0.55), and clindamycin (logP 1.82) are quickly released into the degradation media. Given the large disparity between more hydrophobic drugs (e.g., chlorhexidine) and the SA-based PAE, the release of drugs with logP values and solubilities equal to or less than that of salicylic acid are better controlled. These studies were conducted using the SA-based PAE with an adipic linker (Figure 2.1), but antimicrobial release may be tailored with other SA-based PAEs with different linkers, as shown from their varied degradation rates.[14]

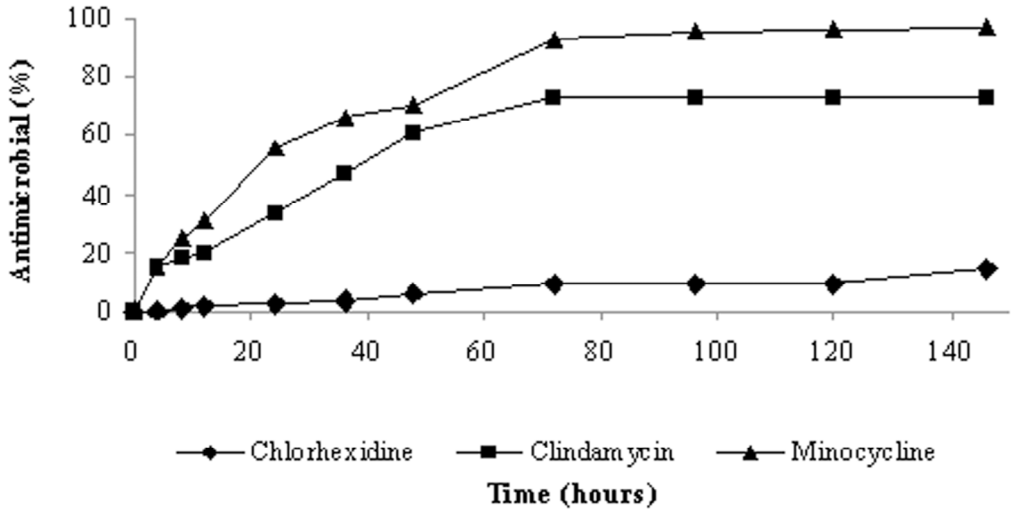

Figure 2.5. Cumulative release profiles of admixed antimicrobials from the salicylic acid-based polymer matrices at 140 hours.

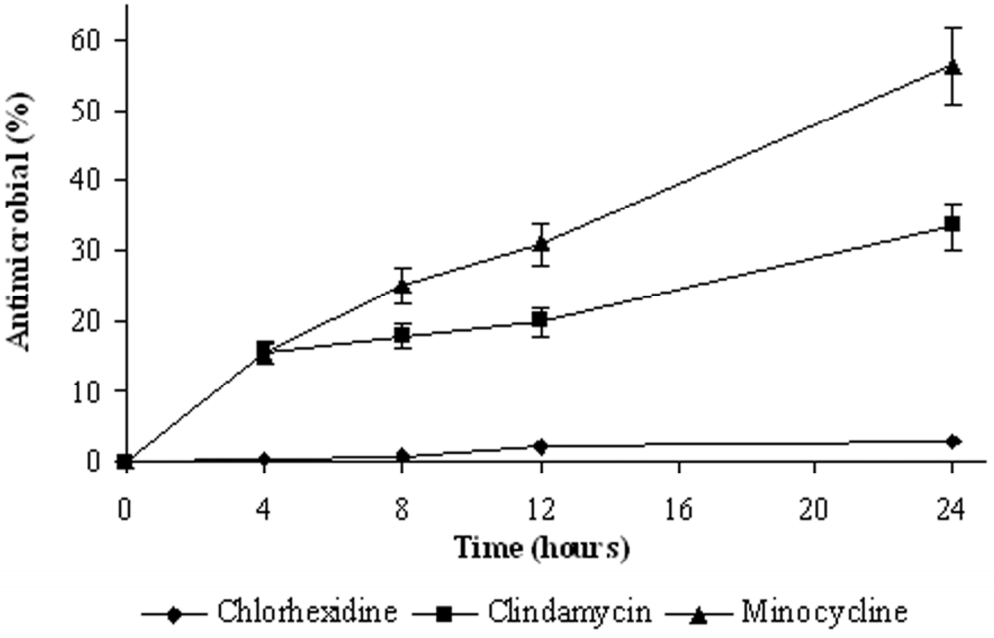

Figure 2.6. Cumulative release profiles of admixed antimicrobials from the salicylic acid-based polymer matrices at 24 hours.

Additionally, the pKa values (**Table 2.1**) for each compound are expected to affect the release rate. Based on the pH of the PBS (7.4), each drug molecule will have different charge states. While the salicylic acid will be ionized in the PBS, the three admixed drugs will either be neutral or protonated. Chlorhexidine has a very high pKa (10.3) and is a cation in the PBS buffer pH 7.4.[32,39] Clindamycin is basic also, with a pKa of 7.6,[32,40] and is expected to be in ionized form for these experiments.[41] Although the hydrophobicity of the drugs has the most influence on the drug release rate, the possibility remains for ion-pairing between salicylic acid and the basic drugs, chlorhexidine and clindamycin, ultimately, chlorhexidine's release from the matrix is noticeably slower. However, clindamycin's release rate is only slightly affected as its pKa is very close to the media pH and is only partially ionized. Minocycline is acidic with pKa values at 2.8, 5.0, 7.8, and 9.5, and is mostly a zwitterion at pH 7.4.[32,42] The mostly neutral minocycline may not interact with the salicylic acid, especially considering its very hydrophilic logP value. As a result, the major factor affecting drug release is the logP value, but the pKa value can also affect the drug interactions and the overall release rate.

2.4.3. Mass Loss and Water Uptake

Mass loss and water uptake of the polymer disks were also monitored for the first 24 hours of hydrolytic degradation, then compared to the drug release rates to determine how water permeation influences polymer degradation and ultimately drug release. These experiments were limited to 24 hours because the matrix shape changes and

integrity decreases after this time point. The mass loss data is shown in **Figure 2.7**, and the water uptake data in **Figure 2.8**. The polymer alone has the fastest rate of mass loss; the minocycline and chlorhexidine also have significant mass loss in the first 24 hours of degradation. However, clindamycin has very little mass loss, which may be due to the similar logP values of clindamycin (1.82) and salicylic acid (2.06) creating an equilibrium with little driving force for physical degradation of the admixed clindamycin samples. The admixed clindamycin samples had the least amount of mass loss and water uptake, and an intermediate release rate. The minocycline admixed samples had the most similar mass loss and water uptake profiles compared to the polymer alone. In general, the presence of admixed antimicrobials slowed down the matrices mass loss and water uptake.

The water uptake results (**Figure 2.8)** depict the same trend as the mass loss results **(Figure 2.7)**. The polymer alone has the greatest amount of water uptake, followed by the hydrophobic chlorhexidine and hydrophilic minocycline. After 24 hours, the minocycline- and chlorhexidine-containing disks absorbed more water than clindamycin-admixed disks. These observations correlate with our salicylic acid release in that salicylic acid release from the polymer alone is fastest, followed by minocycline, chlorhexidine, and clindamycin, respectively **(Figure 2.4)**.

2.5. Conclusions

Polyanhydrides are often defined as surface-eroding materials[4] with tunable erosion mechanisms for tissue engineering and sensitive compounds, such as

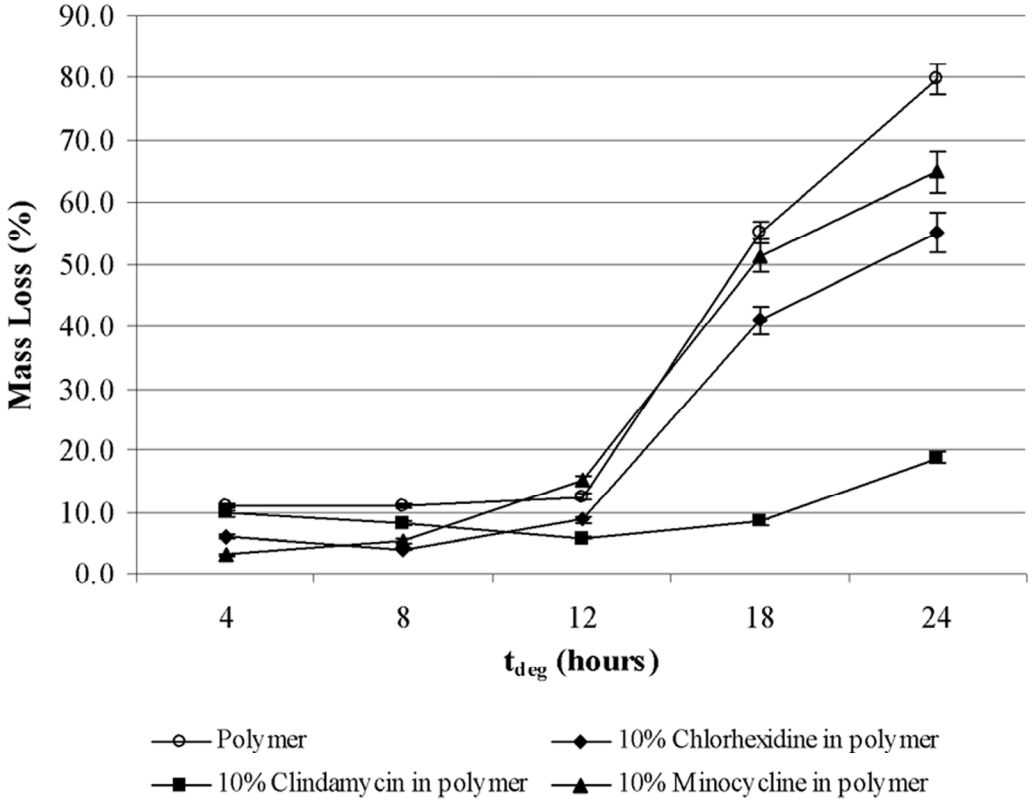

Figure 2.7. Percentage of mass loss from the polymer matrices during the degradation study (up to 24 hours)

proteins. [43,44] This research sought to correlate drug release rate to polymer matrix erosion profiles, based on water uptake and mass loss. The varied solubility parameters and immiscibility of the polymer:antimicrobial blends were observed to influence drug release as demonstrated in related studies.[45,46] Most importantly, salicylic acid release profiles were not influenced by the incorporated drugs. The SA-based PAEs release antimicrobials after a 12 hour lag phase, which may be more useful than the PLA

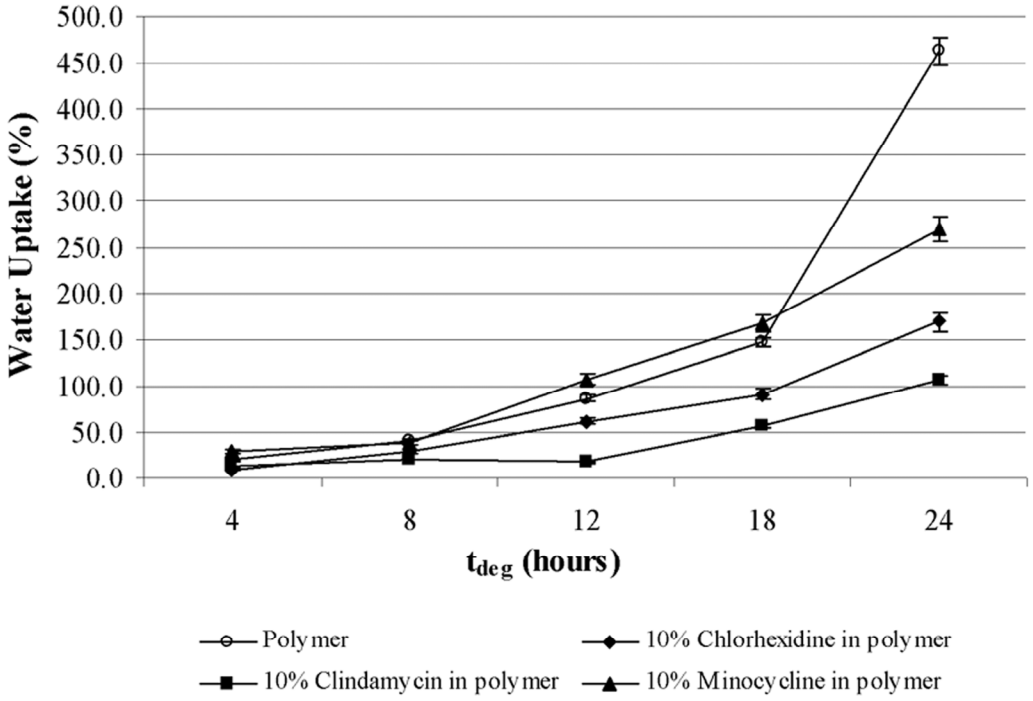

Figure 2.8. Percentage water uptake from the polymer matrices during the degradation study (up to 24 hours).

and PLGA-based systems for sustaining the overall drug release. Typically, drug release from the Arestin® system occurs immediately with drug release percentages at 99 % after the first 72 hours.[47] Upon analysis of the initial 24 hours of drug release, the trend for salicylic acid and antimicrobial release correlates with the mass loss and water uptake findings **(Figures 2.4, 2.6-2.8)**. Based on the results, the release of three antimicrobials may be primarily controlled by drug diffusion from the polymer matrix. The antimicrobials (chlorhexidine·2HCl, clindamycin·HCl, and minocycline·HCl) were successfully admixed into the poly(anhydride-ester) matrix and their subsequent release sustained for at least 3 days. The antimicrobial release generally slowed with increasing

hydrophobicity of the antimicrobials as based on the logP values. In summary, a range of antimicrobials with varying properties can be released from the SA-based PAE matrices without affecting the chemical degradation of the polymer.

2.6. References

1. Kumar N, Langer RS, Domb AJ. Polyanhydrides: an overview. Adv Drug Deliv Rev 2002;54:889-910.

2. Jain JP, Modi S, Domb AJ, Kumar N. Role of polyanhydrides as localized drug carriers. J Control Release 2005;103:541-563.

3. Uhrich K, Cannizzaro S, Langer R, Shakesheff K. Polymeric systems for controlled drug release. Chem Rev 1999;99:3181-3198.

4. von Burkersroda F, Schedl L, Gopferich A. Why degradable polymers undergo surface erosion or bulk erosion. Biomaterials 2002;23:4221-4231.

5. Gopferich A, Tessmar J. Polyanhydride degradation and erosion. Adv Drug Deliv Rev 2002;54:911-931.

6. Akbari H, D'Emanuele A, Atwood D. Effect of geometry on the erosion characteristics of polyanhydride matrices. Int J Pharm 1998;160:83-89.

7. Akbari H, D'Emanuele A, Atwood D. Effect of fabrication technique on the erosion characteristics of polyanhydride matrices. Pharm Dev Technol 1998;3(2):251-259.

8. Berkland C, Kipper MJ, Narasimhan B, Kim K, Pack DW. Microsphere size, precipitation kinetics and drug distribution control drug release from biodegradable polyanhydride microspheres. J Control Release 2004;94:129-141.

9. Shikanov A, Vaisman B, Krasko MY, Nyska A, Domb A. Poly(sebacic acid-co-ricinoleic acid) biodegradable carrier for paclitaxel: in vitro release and in vivo toxicity. J Biomed Mater Res 2004;69A:47-54.

10. Quick D, Macdonald KK, Anseth KS. Delivering DNA from photocrosslinked, surface eroding polyanhydrides. J Control Release 2004;97:333-343.

11. Brem H. Biodegradable polymer implants to treat brain tumors. J Control Release 2001;74(1-3):63-67.

12. Erdmann L, Uhrich, K. Synthesis and degradation characteristics of salicylic acid derived poly(anhydride-esters). Biomaterials 2000;21:1941-1946.

13. Schmeltzer R, Anastasiou TJ, Uhrich KE. Optimized synthesis of salicylate-based poly(anhydride-esters). Polym Bull 2003;49(6):441-448.

14. Prudencio A, Schmeltzer RC, Uhrich KE. Effect of linker structure on salicylic acid-derived poly(anhydride-esters). Macromolecules 2005;38:6895-6901.

15. Vane J, Botting RM. Anti-inflammatory drugs and their mechanism of action. Inflammation Res 1998;47(Supplement 2):S78-S87.

16. Drouganis A, Hirsh R. Low-dose aspirin therapy and periodontal attachment loss in ex- and non-smokers. J Clin Periodontol 2001;28:38-45.

17. Whitaker-Brothers K, Uhrich K. Poly(anhydride-ester) fibers: Role of copolymer composition on hydrolytic degradation and mechanical properties. J Biomed Mater Res 2004;70A:309-318.

18. Johnson ML, Uhrich KE. In vitro release characteristics of antimicrobials admixed into salicylic acid-based poly(anhydride-esters). Polym Mater Sci Eng 2006;95:979-980.

19. Schwach-Abdellaoui K, Vivien-Castioni N, Gurny R. Local delivery of antimicrobial agents for the treatment of periodontal diseases. Eur J Pharm Biopharm 2000;50:83-99.

20. Slots J, Ting M. Systemic antibiotics in the treatment of periodontal disease. Periodontol 2000 2002;28:106-176.

21. Trombelli L, Tatakis DN. Periodontal diseases: current and future indications for local antimicrobial therapy. Oral Diseases 2003;9(Suppl. 1):11-15.

22. Killoy W, Saiki SM. A new horizon for the dental hygienist: controlled local delivery of antimicrobials. J Dent Hygiene 1999;73(2):84-92.

23. Cianco S. Site specific delivery of antimicrobial agents for periodontal disease. General Dentistry 1999(March-April 1999):172-181.

24. Killoy WJ. The clinical significance of local chemotherapies. J Clin Periodontol 2002;29(Suppl 2):22-29.

25. Tatakis D, Trombelli L. Adverse effects associated with a bioabsorbable guided tissue regeneration device in the treatment of human gingival recession defects. J Periodontol 1999;70(5):542-547.

26. Tatakis D, Trombelli, L. Adverse effects associated with a bioabsorbable guided tissue regeneration device in the treatment of human gingival recession defects. A clinicopathologic case report. J Periodontol 1999;70(5):542-547.

27. Reynolds M, Prudencio A, Aichelman-Reidy ME, Woodward K, Uhrich KE. Non-steroidal anti-inflammatory drug (NSAID)-derived poly(anhydride-esters) in bone and periodontal regeneration. Curr Drug Delivery 2007;4(3):1-7.

28. Greenwell H, Bissada NF. Emerging concepts in periodontal therapy. Drugs 2002;62(18):2581-2587.

29. Addy M. Chlorhexidine compared with other locally delivered antimicrobials: A short review. J Clin Periodontol 1986;13:957-964.

30. Schulz M, Schmoldt A. Therapeutic and toxic blood concentrations of more than 800 drugs and other xenobiotics. Pharmazie 2003;58(7):447-474.

31. LogP Calculation: SciFinder Scholar ACD/Labs Software v8.14 for Solaris; ©1994-2005 ACD/Labs.

32. Williams DA, Lemke TL. Foye's Principles of Medicinal Chemistry. Philadelphia: Lippincott, Williams, and Wilkins; 2002.

33. Yue IC, Poff J, Cortes ME, Sinisterra RD, Faris CB, Hilden P, Langer R, Shastri VP. A novel polymeric chlorhexidine delivery device for the treatment of periodontal disease. Biomaterials 2004;25:3743-3750.

34. Walker C, Gordon J. The effect of clindamycin on the microbiota associated with refractory periodontitis. J Periodontol 1990;61(11):692-698.

35. Park YJ, Lee JY, Yeom HR, Kim KH, Lee SC, Shim IK, Chung CP, Lee SJ. Injectable polysaccharide microcapsules for prolonged release of minocycline for the treatment of periodontitis. Biotechnol Lett 2005;27(22):1761-1766.

36. Whitaker-Brothers K, K. Uhrich. Investigation into the erosion mechanism of salicylate-based poly(anhydride-esters). J Biomed Mater Res 2006;76A:470-479.

37. Theeuwes F, Hussain A, Higuchi T. Quantitative analytical method for determination of drugs dispersed in polymers using differential scanning calorimetry. J Pharm Sci 1974;63(3):427-429.

38. Siepmann F, Le Brun V, Siepmann J. Drugs acting as plasticizers in polymeric systems: A quantitative treatment. J Control Release 2006;115:298-306.

39. Akaho E, Fukumori, Y. Studies on Absorption Characteristics and Mechanism of Adsorption of Chlorhexidine Mainly by Carbon Black. J Pharm Sci 2001;90(9):1288-1297.

40. Wan H, Holmen AG, Wang Y, Lindberg W, Englund M, Nagard MB, Thompson RA. High-throughput screening of pKa values of pharmaceuticals by pressure-assisted capillary electrophoresis and mass spectrometry. Rapid Commun Mass Spectrom 2003;17:2639-2648.

41. Sabath LD, Toftegaard I. Rapid Microassays for Clindamycin and Gentamicin When Present Together and the Effect of pH and of Each on the Antibacterial Activity of the Other. Antimicrob Agents and Chemother 1974;6(1):54-59.

42. Colaizzi JL, Klink PR. pH-Partition Behavior of Tetracyclines. J Pharm Sci 1969;58(10):1184-1189.

43. Burkoth AK, Burdick J, Anseth KS. Surface and bulk modifications to photocrosslinked polyanhydrides to control degradation behavior. J Biomed Mater Res 2000;51:352-259.

44. Torres MP, Vogel BM, Narasimhan B, Mallapragada SK. Synthesis and characterization of novel polyanhydrides with tailored erosion mechanisms. J Biomed Mater Res 2006;76A:102-110.

45. Lyu S-P, Sparer R, Hobot C, Dang K. Adjusting drug diffusivity using miscible polymer blends. JControl Release 2005;102:679- 687.

46. Karavas E, Georgarakis E, Bikiaris D. Adjusting drug release by using miscible polymer blends as effective drug carries. J Therm Anal Cal 2006;84(1):125-133.

47. OraPharma. Data on file. 2005.

CHAPTER 3: SALICYLIC ACID-BASED POLY(ANHYDRIDE-ESTER):HYDROXYAPATITE COMPOSITES FOR BONE APPLICATIONS

3.1. Abstract

Composites of salicylic acid-based poly(anhydride-ester) (SA-based PAE) and hydroxyapatite have been examined for rebuilding bone at implant interfaces. The composites were made at three ratios of polymer to hydroxyapatite (90:10, 50:50, and 10:90). The bulk mechanical properties of hydroxyapatite, the SA-based PAE, and each composite were examined. The composites were degraded in media over one week, during which time, the pH, water uptake, mass loss, and salicylic acid release were measured. The *in vitro* degradation of 50:50 poly(lactic-*co*-glycolic acid) (PLGA) composites was used as a polymer control with salicylic acid admixed within the PLGA matrix. Ultimately, SA-based PAE:hydroxyapatite composites may have to ability to promote new bone growth while also minimizing the inflammatory response and pain for the patient.

3.2. Introduction

Composites of hydroxyapatite and polymers are very important to the advancement of biomaterials for bone growth. Specifically, polymer:hydroxyapatite composites have been a significant influence for bone regeneration because of enhanced mechanical properties.[1-3] The mechanical properties of polymer:hydroxyapatite

composites change according to various factors such as molecular weight distribution, particle size, thermal properties and interfacial interactions.[4-9]

Hydroxyapatite is a biocompatible material that breaks down into mineral ions, calcium and phosphate, which can thus be used to promote bone growth. Hydroxyapatite has the chemical formula, $(Ca)_{10}(PO4)_6(OH)_2$,[10] a calcium/phosphate ratio of 1.67, and can release free calcium and phosphate ions to increase bone growth and implant integration.[11-13] However, synthetic hydroxyapatite does not have the mechanical strength needed for load-bearing implant applications.[12] Hydroxyapatite has been studied as a coating for titanium alloy (Ti_6Al_4V) implant materials,[14-17] but a major problem with hydroxyapatite is that it becomes very brittle and weak over time.[2,12,18] The addition of polymer to the hydroxyapatite may protect the hydroxyapatite from the surrounding media during degradation and further promote bone growth.

Biodegradable polymers are commonly used for drug delivery, but some polymers, such as poly(lactic acid) (PLA) and poly(glycolic acid) (PGA) break down into acids that have undesirable, non-therapeutic effects in the patient, including pain, inflammation, and toxicity.[19] For preparing polymer composites with other materials, such as hydroxyapatite, the polymer must remain stable during composite processing.[20] Researchers have demonstrated some success with polymer:hydroxyapatite composites containing PLA, PGA, and copolymers of the two, as well as poly(ε-caprolactone).[21-26] Some researchers have focused on the physical changes that occur as polymers interact with hydroxyapatite.[9,27-29] Others have shown that using poly(3-hydroxybutyrate-*co*-3-hydroxyvalerate) reduced the inflammatory response.[30] Therefore, with proper design,

hydroxyapatite:polymer composites may be a safer, more effective way to promote bone growth through mechanical strength and drug delivery.

In this chapter, SA-based PAE:hydroxyapatite composites at ratios of 90:10 50:50, and 10:90 were analyzed for potential use in orthopedic applications such as bone fillers and implant fixation aids. Based on the previous success of the SA-based PAEs in promoting bone growth in periodontal disease applications,[31,32] the addition of hydroxyapatite may enhance such an effect. Simultaneous release of salicylic acid may further enhance the composite effectiveness by reducing the foreign body response. The potential for synergy between the two composite components, biodegradable polymers and hydroxyapatite, extends new possibilities to the areas of metal implant fixation and bone growth and regeneration.

3.3. Materials and Methods

3.3.1. Materials

The salicylic acid-based poly(anhydride-ester) (SA-based PAE) was prepared using previously described methods.[33,34] 50:50 PLGA, commercial hydroxyapatite (calcium phosphate tribasic), dichloromethane, and all other reagents and organic solvents were purchased from Aldrich (Milwaukee, WI). Only the initial characterization studies (physical properties and peel test) were conducted using synthetic hydroxyapatite received as a gift from Prof. Riman's laboratory.

3.3.2. Preparation of Polymer:Hydroxyapatite Composites

The polymer:hydroxyapatite composites were prepared by weighing appropriate amounts of polymer and hydroxyapatite, mixed with 10 mL dichloromethane and sonicated for ten minutes. The dichloromethane was evaporated, and the remaining composite dried in the vacuum oven at room temperature overnight.

The polymer:hydroxyapatite mixtures (40.0 ± 5.0 mg) were placed into an IR pellet die (International Crystal Laboratories, Garfield, NJ) and pressed at 4,000 psi at room temperature for 5 minutes in a Carver Press (Carver, Wabash, IN). The resulting disks were 6.0 mm diameter and 1.0 mm thick, as determined by vernier caliper measurements (Mitutoyo, Japan). Three disks (n=3) were prepared for each time point at each composite ratio and stored at 4 °C until the *in vitro* degradation study.

3.3.3. Hydroxyapatite Characterization

Prior to making the composites, hydroxyapatite was characterized alone. The density was measured with a Micrometrics Accupyc II 1340 Pycnometer (Norcross, GA). Hydroxyapatite (200 mg) was weighed into a metal cup and placed in the pycnometer for density measurement. The results are the average of three measurements taken per sample.

The surface area of the hydroxyapatite samples was measured using the Brunauer, Emmett, and Teller (BET) method.[35,36] Hydroxyapatite (500 mg) was placed in a glass tube and thoroughly dried prior to analysis. The surface area measurement was completed using nitrogen gas as the adsorbant and liquid nitrogen as the coolant in a

Micrometrics Gemini 2365 Surface Area Analyzer (Norcross, GA). The density and surface area measurements were used to calculate the hydroxyapatite particle size.

The American Society for Testing and Materials (ASTM) method D3359-97 was used to measure hydroxyapatite adhesion to titanium metal by tape test.[37] Test Method A, named the X-cut tape test, was completed on a total of three samples, where an X was cut into the coatings using a sharp blade. Permacel P-99 tape (New Brunswick, NJ) was placed over the x and removed within 30 seconds at a 180 ° angle. Any removal of the coating surrounding the X-cuts, or change in the X-cuts was an indicator that the coating was weakly bound to the substrate. Digital images were taken to monitor changes before and after the tape test.

3.3.4. Composite Characterization

Gel permeation chromatography (GPC) was performed using Waters Breeze GPC system (Milford, MA), which consisted of a 1500 series isocratic pump running THF at 1 mL/min, 717plus autosampler, and a 2414 refractive index (RI) detector. Samples were dissolved in dichloromethane and filtered through 0.45 um PTFE syringe filters.

Static contact angle measurements were performed on the composite disks, as well as the polymers alone, in triplicate using deionized water on a model 100 goniometer (Rame-Hart, Mountain Lakes, NJ). The contact angle was determined digitally with a camera attachment and the measuring system on the DROPimage Advanced software on a Dell Dimension 3000 computer with a Windows XP operating system. The reported values are the average of at least three angle measurements per drop.

3.3.5. Mechanical Analysis of Polymer: Hydroxyapatite Composites

Disks of SA-based PAE: hydroxyapatite composites were examined with compression testing (0 – 8000 mN) on a PE DMA 7e with a TAC 7/DX instrument controller (Waltham, MA). PE Pyris version 3.81 software was used for data collection and processing on a Dell Optiplex GX110 computer. The experiments were conducted using 10 mm parallel plates for each composition. Compressive modulus values for each blend were calculated by taking the slope of each stress vs. strain curve in the linear region at 2 % strain.

3.3.6. *In Vitro* Degradation of Polymer: Hydroxyapatite Composites

The sample disks (40.0±5.0 mg) were placed in 20 mL scintillation vials containing 10 mL 0.1 M phosphate buffer solution (PBS) at pH 7.4. The vials were stored in a New Brunswick Scientific Series 25 Controlled Environment Incubator Shaker (Edison, NJ) at 37°C and constantly shaken at 65 rpm. The degradation media was decanted from the vial and replaced with 10 mL fresh PBS at pre-determined time intervals; 24, 72, and 168 hours. The pH of the spent degradation media was measured using an Accumet digital pH meter (Fisher, Fairlawn, NJ), and then stored at 4 °C until further analysis. All data shown are the average of at least 3 samples.

3.3.7. Water Uptake and Mass Loss Measurements

Water uptake and mass loss were determined by obtaining the mass of each sample using an analytical balance (Mettler Toledo Columbus, OH). At predetermined

time points during the degradation study, the samples were removed from the degradation media, rinsed in deionized water to remove residual phosphate salts, and patted with Kimwipes® (Kimberly-Clark, Neenah, WI). Each sample was lyophilized in a Freezone Freeze Dry System (Labconco, Kansas City, MO) for 48 hours to ensure a constant mass. The water uptake was calculated using Equation (1) [38,39]:

$$WA(\%) = \frac{W_h - W_r}{W_r} \times 100 \qquad (1)$$

where *WA* is water absorbed by the sample or water uptake, W_h is the mass of the hydrated sample, and W_r is the residual mass of the lyophilized sample. The mass loss was calculated using Equation (2) [38,39]:

$$ML(\%) = \frac{W_0 - W_r}{W_0} \times 100 \qquad (2)$$

where *ML* is the mass loss of the sample and W_0 is the mass of the sample prior to degradation. Three samples were measured and averaged for each time point ($n = 3$). Statistical error was shown by error bars denoting the standard deviation of the three measurements.

3.3.8. Salicylic Acid Release by High Pressure Liquid Chromatography (HPLC)

All hydroxyapatite:polymer composite degradation media were analyzed for salicylic acid release on a Waters 2695 HPLC Separations System with a 2487 Dual

Wavelength UV detector (Milford, MA). The degradation media was filtered through 0.45 μm PTFE filters (Nalgene, Rochester, NY) and put into vials for HPLC analysis. A six point calibration curve for salicylic acid was prepared with concentrations ranging from 0.01 mg/mL to 0.4 mg/mL. Salicylic acid was separated on a C18 column (150×4.6 mm, 5 μm, Phenomenex, Torrance, CA, USA) with a flow rate of 1 ml/min in an isocratic mobile phase of 75% 20 mM monobasic potassium phosphate (KH_2PO_4) at pH 2.5 and 25% acetonitrile. The UV detector measured salicylic acid release at both 210 and 298 nm.

3.4. Results and Discussion

3.4.1. Hydroxyapatite Physical Properties

The hydroxyapatite was first characterized alone to determine its physical properties and potential to adhere to metal implants. First, the Brunauer, Emmett, and Teller (BET) method was used to measure surface area (SUA).[35,36] The BET method is based on the amount of nitrogen adsorbed on the particle surface to determine the surface area. A pycnometer was used to measure the density (ρ) of the powder. Finally, the diameter (D) of the particles was calculated using $D=6/(SUA\cdot \rho)$. The final results are shown in **Table 1.** Although the commercially available (Sigma Aldrich) hydroxyapatite does not necessarily have a uniform, well defined morphology, its particle size is an order-of-magnititude smaller than the more uniform hydroxyapatite prepared in the Riman lab. For the purpose of this dissertation, the bulk properties of the hydroxyapatite in disk form are the primary focus, while the specific physical properties of the

hydroxyapatite in powder form provided insight on the most efficient ways to prepare the composites.

Table 3.1. Physical Properties of Hydroxyapatite

Sample (source)	Surface Area (m^2/g)	Density (g/cm^3)	Diameter (μm)
Hydroxyapatite (synthetic Riman Lab)	1.8589	2.6897	1.2000
Hydroxyapatite (commercial Sigma Aldrich)	16.0942	2.9207	0.12764

Subsequently, the synthetic hydroxyapatite was analyzed as a potential coating on metal implants using an ASTM.[37] The peel test was performed on hydroxyapatite-coated titanium disks, shown in **Figure 3.1**, to measure the adhesivity of the hydroxyapatite coating to the titanium substrates. This method provided qualitative information about adhesivity from digital photographs and SEM images before and after the test. This method has been used to measure the adhesivity of other hydroxyapatite coatings as well.[40]

The digital images in **Figure 3.1** showed that the X-cuts on the hydroxyapatite coated samples remained the same after tape removal. The scanning electron microscopy (SEM) images in the lower half of **Figure 3.1** showed that the hexagonal morphology of the hydroxyapatite crystals was also unchanged after the tape test. Overall, hydroxyapatite adheres tightly to the titanium alloy surface.

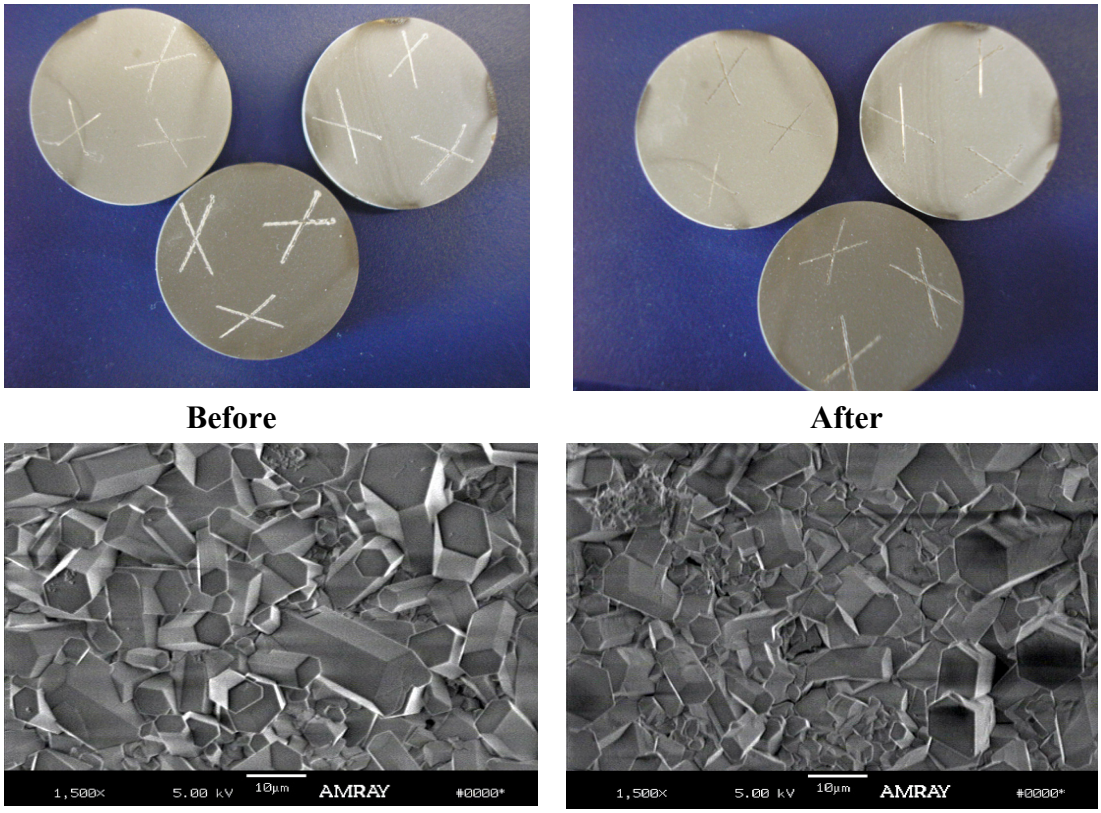

Figure 3.1. Peel test results for hydroxyapatite coated on sandblasted Ti alloy disks

3.4.2. SA-based PAE: Hydroxyapatite Composites

After the composites were compression-molded into 6 mm disks, their bulk properties were examined, including polymer molecular weight (M_w) and contact angle measurements. The composites were analyzed for any changes in M_w to ensure that polymer did not degrade or decompose during the composite preparation. **Figure 3.2** shows overlaid gel permeation chromatography (GPC) plots comparing the elution of the polymer alone and the two composite ratios. The plot shows no difference in the polymer

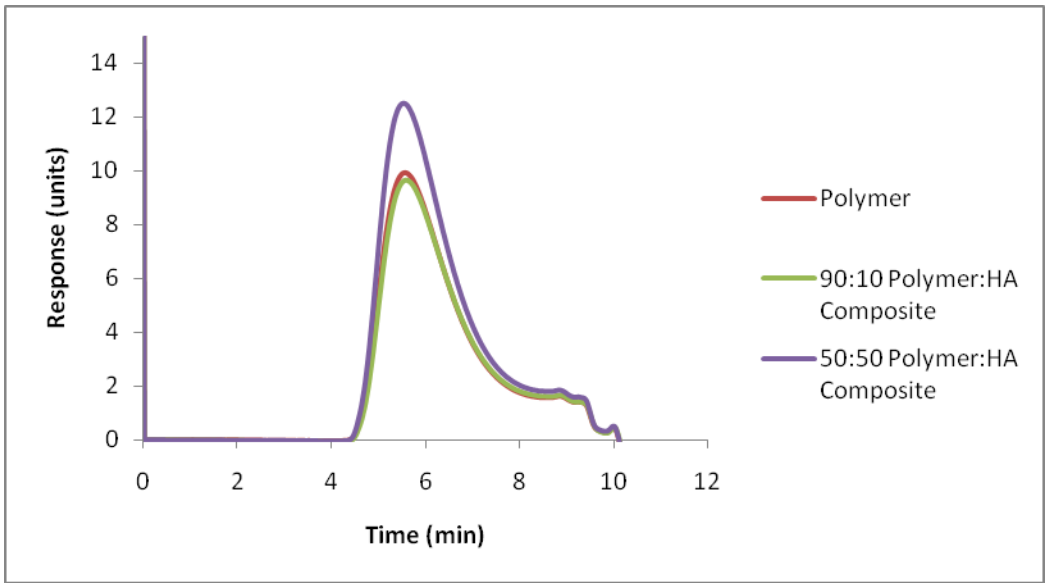

Figure 3.2. Gel Permeation Chromatography Plot Showing the Comparison of polymer M_w before and after composite preparation

M_w after the composite preparation. The actual M_w values are exhibited in **Table 3.2**; no significant change, in degradation or decomposition is observed upon preparation of the polymer:hydroxyapatite composites.

Table 3.2. M_w of the SA-based PAE before and after composite preparation

Sample	M_w
SA-based PAE	16,500
90:10 SA-based PAE:Hydroxyapatite Composite	16,200
50:50 SA-based PAE:Hydroxyapatite Composite	17,000

Hydroxyapatite is more hydrophilic[41] than the polymers (SA-based PAE and PLGA) used to make the composites. As a result, the static contact angle of the composites was measured to elucidate the relative hydrophobicity of each composition. The hydroxyapatite surface was unstable to the sessile water droplet, so the contact angle

for hydroxyapatite alone was not measured. Sessile contact angle measurements are shown in **Table 3.3.** As expected, the contact angle decreased as the amount of hydroxyapatite increase; in other words, increasing hydroxyapatite content increased

Table 3.3. Contact Angle of Polymer:Hydroxyapatite Composites

Sample	Contact Angle
PLGA	69.0°
90:10 PLGA:HA	56.3°
90:10 PLGA:HA:SA	67.0°
50:50 PLGA:HA	60.0°
SA-based PAE	71.5 °
90:10 SA-based PAE:HA	69.4°
50:50 SA-based PAE:HA	65.0°

hydrophilicity. However, when salicylic acid is admixed into the PLGA, the contact angle increases significantly. This effectively nullifies the effect of hydroxyapatite on the PLGA hydrophobicity. This effect was not seen in the SA-based PAE composites because the salicylic acid is already chemically bound within the polymer backbone.

3.4.3. Mechanical Analysis of Poly(anhydride-ester):Hydroxyapatite Composites

The compressive moduli of the SA-based PAE composites were compared to determine the effect of the hydroxyapatite content. A representative stress vs. strain curve of hydroxyapatite alone is shown in **Figure 3.3**.

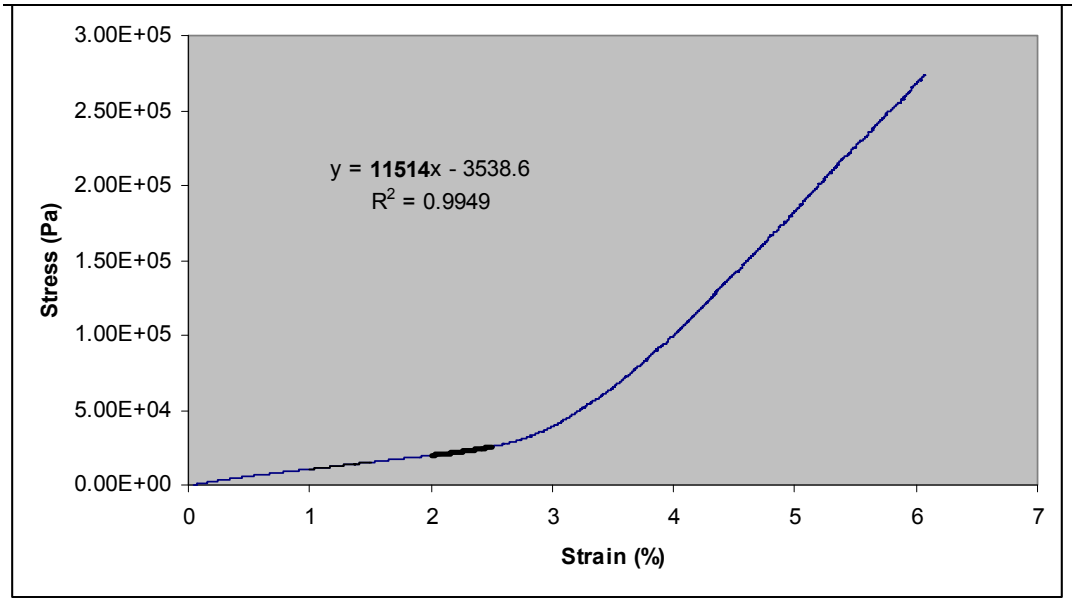

Figure 3.3. Representative stress vs. strain curve of hydroxyapatite (commercial). The compressive modulus is represented as the slope at 2% strain.

For all samples, the compressive modulus was calculated by measuring the slope at 2 % strain. The final results for the compressive moduli are depicted in **Table 3.4**. The modulus increases as the ratio of hydroxyapatite increases, and with linear dependence on the hydroxyapatite content.

Table 3.4. Compressive Modulus of Polymer:Hydroxyapatite Composites

Sample	Compressive Modulus at 2% Strain (Pa)
SA-based PAE	1,845.0
90:10 SA-based PAE: HA	6,631.0
50: 50 SA-based PAE: HA	21,926
10:90 SA-based PAE: HA	35,866
HA	121,010

3.4.4. *In Vitro* Degradation of Polymer: Hydroxyapatite Composites

The composites were degraded in PBS to simulate physiological conditions, and pH changes, mass loss, water uptake, and salicylic acid release rates were monitored over the course of one week. As hydroxyapatite is extremely brittle, the samples with 90 wt % hydroxyapatite were too brittle for the degradation study, and it was concluded that these samples have no potential as implant materials using the disk fabrication method.

3.4.4.1. pH of Degradation Media

The pH of the degradation media was monitored during the degradation study, and summarized in **Table 3.5**. The pH values ranged from 7.33 to 7.64. Overall, no significant change in the pH was observed; the hydroxyapatite may be neutralizing the acidic polymer degradation products. The pH began to decrease more noticeably at the 7 day time point.

Table 3.5. pH of Polymer:Hydroxyapatite Composites Degradation Media

Sample	pH after 1 day	pH after 3 days	pH after 7 days
90:10 PLGA:HA	7.55	7.48	7.47
90:10 PLGA:HA:SA	7.54	7.41	7.43
50:50 PLGA:HA	7.60	7.61	7.45
90:10 SA-based PAE:HA	7.63	7.64	7.37
50:50 SA-based PAE:HA	7.40	7.46	7.46

3.4.4.2. Mass Loss and Water Uptake Measurements

Mass loss and water uptake measurements provide information about the general degradative and erosion mechanisms of polymer:hydroxyapatite composites. Mass loss is a measure of the amount of composite material lost at each degradation study time point. The mass loss results for the 90:10 and 50:50 polymer:hydroxyapatite composites are shown in **Figures 3.4 and 3.5**, respectively. The 50:50 SA-based PAE: hydroxyapatite composites had a slightly higher mass loss percentage than the 50:50 PLGA:hydroxyapatite composites. PLGA tends to have a longer initial lag phase, due to its crystalline domains, that is quickly overcome during the linear degradation phase. The results for the 90:10 composites in **Figure 3.4** show that the SA-based PAE composites were solubilized much faster than the PLGA composites. However, when salicylic acid was physically admixed within the PLGA composite matrix, similar mass loss rates were observed. A similar trend was observed in the water uptake experiments.

Water uptake is the amount of water able to penetrate into the sample matrix, and also a qualitative measure of sample swelling. Water uptake measurements provide general information about sample degradation profiles, as well. The water uptake results comparing the SA-based PAE composite to the PLGA composite with and without admixed salicylic acid are shown in **Figure 3.6**. Water penetrates into the PLGA with

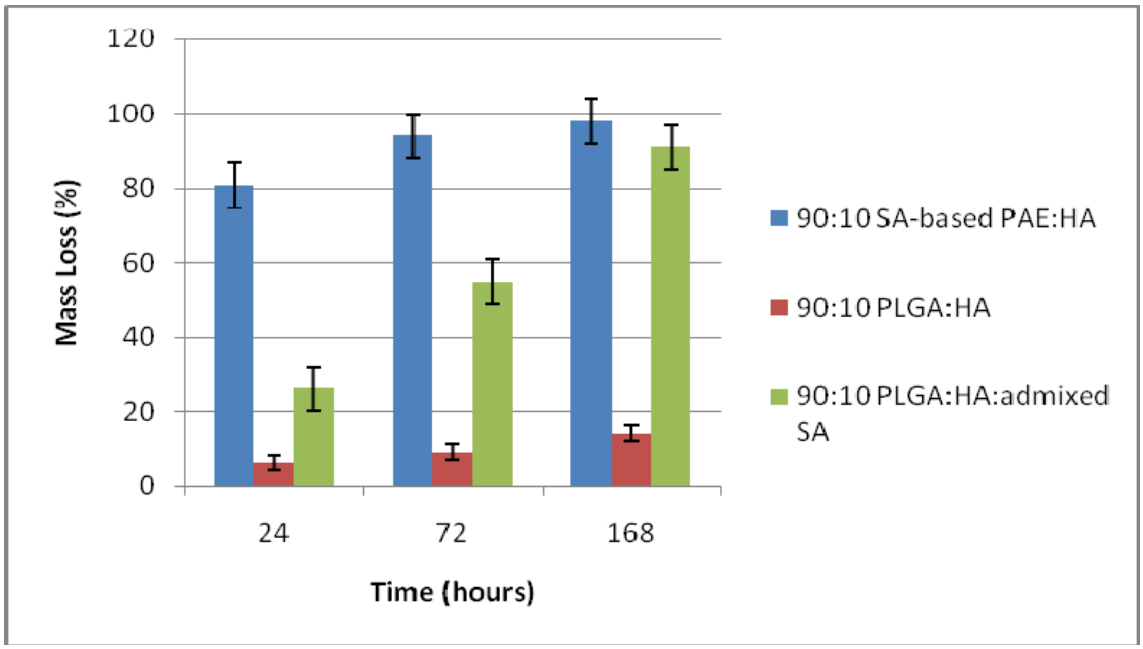

Figure 3.4. Mass Loss from Polymer:Hydroxyapatite Composites (90:10 ratios).

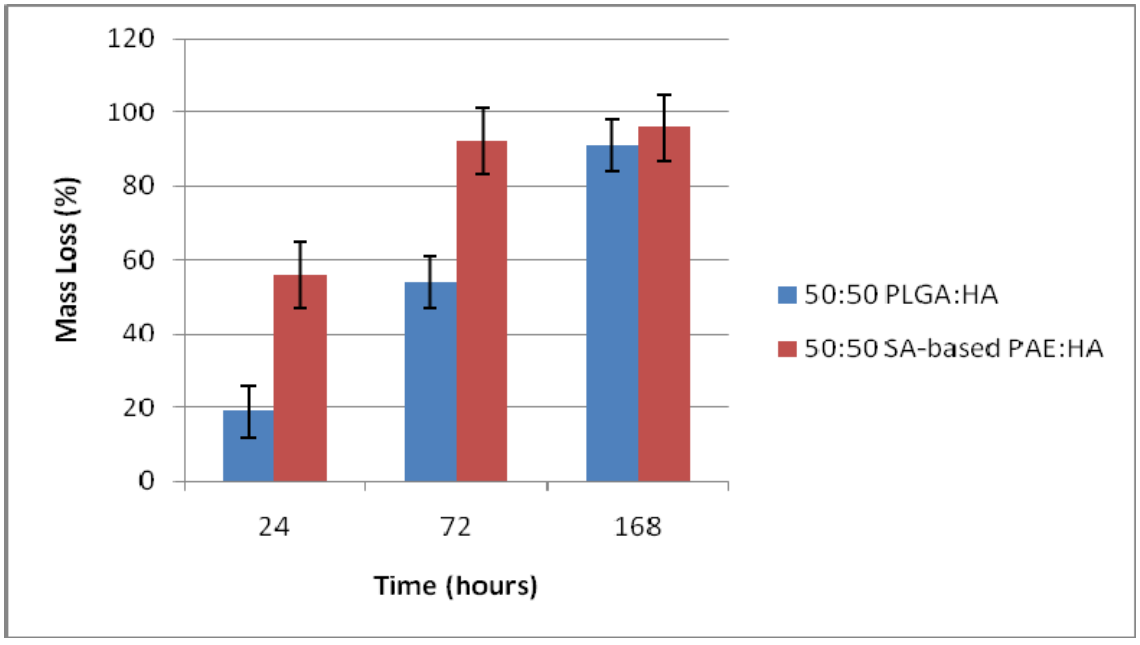

Figure 3.5. Mass Loss from Polymer:Hydroxyapatite Composites (50:50 ratios).

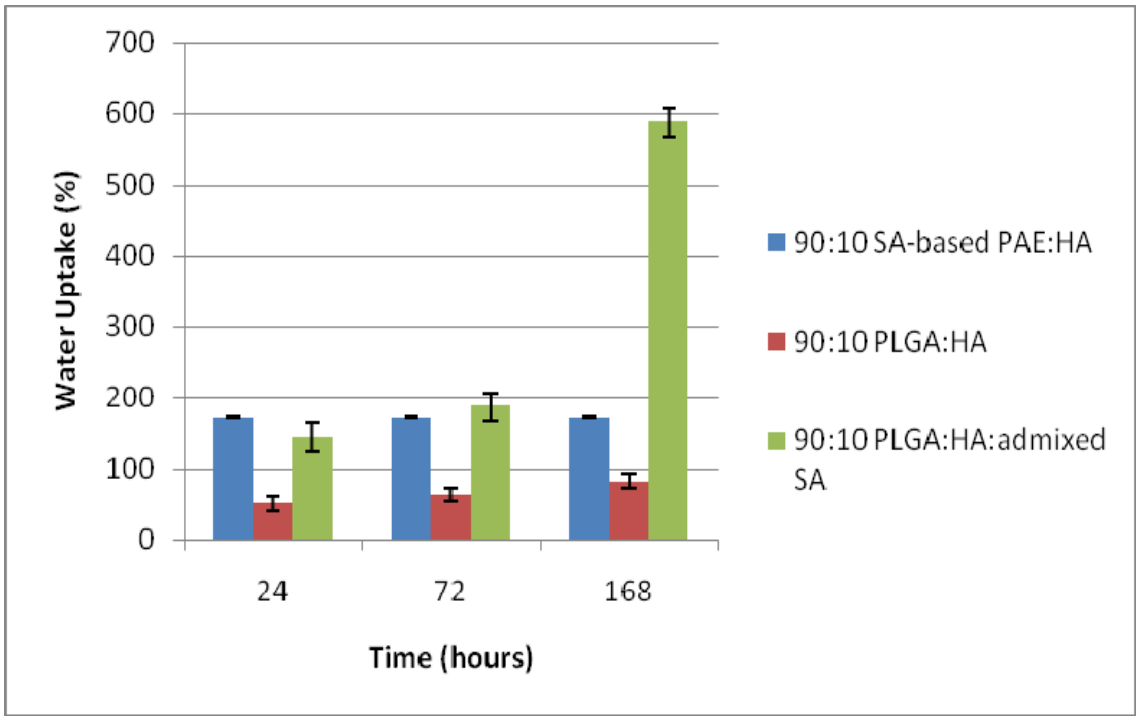

Figure 3.6. Water Uptake from Polymer:Hydroxyapatite Composites

admixed salicylic acid and the SA- based PAE matrices more rapidly than PLGA:HA composites. After 24 hours, both composites have absorbed more than 100 % their mass in water. On the other hand, the PLGA composite without admixed salicylic acid absorbs less than 50% its mass in water. PLGA is partially crystalline, while the SA-based PAE is completely amorphous. The crystalline domains are more effective at preventing water penetration into the polymer matrix. However, the SA-based PAE's water uptake is more controllable than the PLGA with admixed salicylic acid.

3.4.4.3. Salicylic Acid Release During Polymer Degradation

Salicylic acid release was monitored for its possible use to prevent the inflammation and pain associated with the foreign body response. **Figure 3.7** depicts the

cumulative salicylic acid release from the SA-based PAE compared to each of the SA-based PAE:hydroxyapatite composites, 50:50 and 90:10. The addition of hydroxyapatite

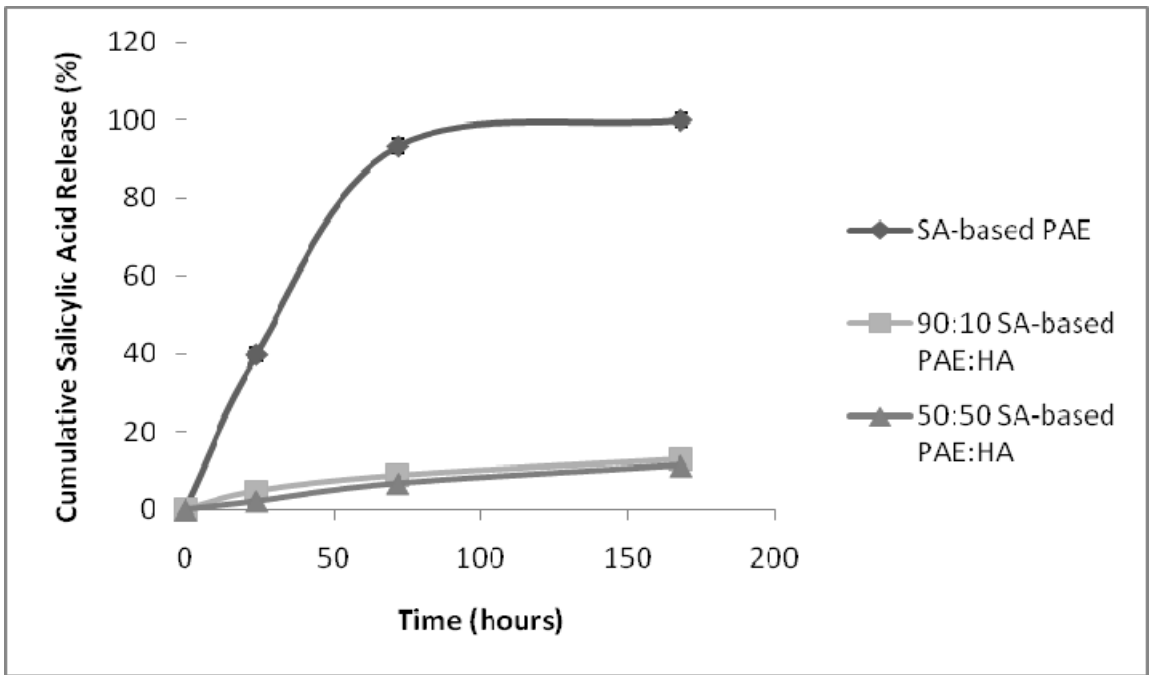

Figure 3.7. Cumulative Salicylic Acid Release from Polymer:Hydroxyapatite Composites During 1 week

greatly slows down the salicylic acid release. Thus, the salicylic acid release is more controllable and it eliminates both lag and burst phases. The composite with 90 wt % SA-based PAE has a slightly faster release rate than the composite with 50 wt % SA-based PAE.

Figure 3.8 shows the cumulative release of salicylic acid from the 90:10 SA-based PAE:hydroxyapatite composite and the 90:10 PLGA:hydroxyapatite composite admixed with salicylic acid. The release curves show that salicylic acid release is better controlled when it is chemically bonded within the polymer backbone, as opposed to

physically admixed within the polymer matrix. The salicylic acid release from the PLGA admixed with salicylic acid shows more of a burst release phase, but the salicylic acid release from the chemically bonded SA-based PAE is first order.

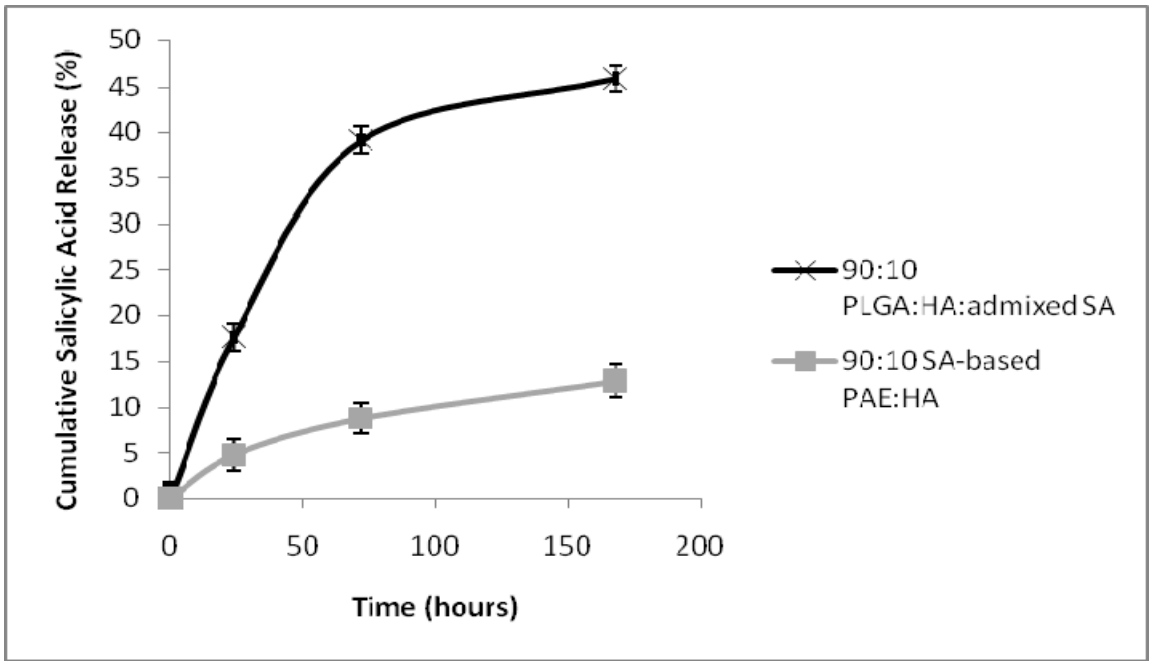

Figure 3.8. Cumulative Salicylic Acid Release from Polymer:Hydroxyapatite Composites (comparing release profiles of physically admixed SA and chemically bonded SA)

3.5. Conclusions

The SA-based PAE:HA composites had properties comparable to or better than PLGA:HA composites with the same ratios. No significant change was observed in the pH of the degradation media and SA-based PAE composites appear to have no lag phase based on water uptake and mass loss studies. SA-based PAE:hydroxyapatite composites

are more stable during the release of salicylic acid, while the PLGA-based composites degraded very quickly and did not control the salicylic acid release rate. Overall, the SA-based PAE:hydroxyapatite composites may have more potential as biomaterials for bone applications due to their controlled release of salicylic acid.

3.6. Acknowledgements

I would like to acknowledge Dr. Richard Riman (Department of Materials Science and Engineering, Rutgers University) and his research group, specifically, Ana Sever, Dan Haders, Eugene and Rui Zhou, who helped me with materials, access to instruments, and general questions. I would also like to acknowledge Yamalia Roberts, who was the undergraduate summer student who helped with much of the work in this chapter.

3.7. References

1. Durucan C, Brown PW. Biodegradable Hydroxyapatite-Polymer Composites. Adv Eng Mater 2001;3(4):227-231.

2. Katti KS. Biomaterials in total joint replacement. Colloids and Surfaces B: Biointerfaces 2004;39:133-142.

3. Ma PX. Biomimetic materials for tissue engineering. Adv Drug Deliv Rev 2008;60:184-198.

4. Nazhat SN, Kellomaki M, Tormala P, Tanner KE, Bonfield W. Dynamic Mechanical Characterization of Biodegradable Composites of Hydroxyapatite and Polylactides. J Biomed Mater Res 2001;58:335-343.

5. Ural E, Kesenci K, Fambri L, Migliaresi C, Piskin E. Poly(D,L-lactide/ε-caprolactone)/hydroxyapatite composites. Biomaterials 2000;21:2147-2154.

6. Russias J, Saiz E, Nalla RK, Gryn K, Ritchie RO, Tomsia AP. Fabrication and mechanical properties of PLA/HA composites: A study of in vitro degradation. Mater Sci Eng C 2006;26:1289-1295.

7. Kasuga T, Ota Y, Nogami M, Abe Y. Preparation and mechanical properties of polylactic acid composites containing hydroxyapatite fibers. Biomaterials 2001;22:19-23.

8. Kikuchi M, Koyama Y, Takakuda K, Miyairi H, Shirahama N, Tanaka J. *In vitro* change in mechanical strength of B-tricalcium phosphate/copolymerized poly-L-lactide composites and their application for guided bone regeneration. J Biomed Mater Res 2002;62:265-272.

9. Chen B, Sun K. Poly (ε-caprolactone)/hydroxyapatite composites: effects of particle size, molecular weight distribution and irradiation on interfacial interaction and properties. Polym Test 2005;24:64-70.

10. Kay MI, Young RA. Crystal Structure of Hydroxyapatite. Nature 1964;204:1050-1052.

11. Skrtic D, Antonucci JM, Eanes ED. Amorphous Calcium Phosphate-Based Bioactive Polymeric Compostites for Mineralized Tissue Regeneration. J. Res. Natl. Inst. Stan. 2003;108(3):167-182.

12. Orlovskii VP, Komlev VS, Barinov SM. Hydroxyapatite and Hydroxyapatite-Based Ceramics. Inorganic Materials 2002;38(10):1159-1172.

13. Raikar GN, Ong JL, Lucas LC. Hydroxyapatite Characterization by XPS. Surf Sci Spectra 1997;4(1):9-13.

14. Wang J, Layrolle P, Stigter M, de Groot K. Biomimetic and electrolytic calcium phosphate coatings on titanium alloy: physicochemical characteristics and cell attachment. Biomaterials 2004;25:583-592.

15. Ishikawa K, Miyamoto Y, Nagayama M, Asaoka K. Blast Coating Method: New Method of Coating Titanium Surface with Hydroxyapatite at Room Temperature. J Biomed Mater Res (Appl Biomater) 1997;38:129-134.

16. Casaletto MP, Kaciulis S, Mattogno G, Mezzi A, Ambrosio L, Branda F. XPS characterization of biocompatible hydroxyapatite-polymer coatings. Surf. Interface Anal. 2002;34:45-49.

17. Yang YC, Chang E, Lee SY. Mechanical properties and Young's modulus of plasma-sprayed hydroxyapatite coating on Ti substrate in simulated body fluid. J Biomed Mater Res 2003;67A:886-899.

18. Haddock SM, Debes JC, Nauman EA, Fong KE, Arramon YP, Keaveny TM. Structure-function relationships for coralline hydroxyapatite bone substitute. J Biomed Mater Res 1999;47:71-78.

19. Li H, Chang J. pH-compensation effect of bioactive inorganic fillers on the degradation of PLGA. Composites Sci and Tech 2005;65:2226-2232.

20. Sigmund WM, Bell NS, Bergstrom L. Novel Powder-Processing Methods for Advanced Ceramics. J Am Cerem Soc 2000;83(7):1557-1574.

21. Marra K.G. SJ, Kumta PN, DiMilla PA, Weiss LE. *In vitro* analysis of biodegradable polymer blend/hydroxyapatite composites for bone tissue engineering. J Biomed Mater Res 1999;47:324-335.

22. Rizzi SC, Heath DJ, Coombes AGA, Bock N, Textor M, Downes S. Biodegradable polymer/hydroxyapatite composites: Surface analysis and initial attachment of human osteoblasts. J Biomed Mater Res 2001;55:475-486.

23. Causa F, Netti PA, Ambrosia L, Ciapetti G, Baldini N, Pagani S, Martini D, Giunti A. Poly-ε-caprolactone/hydroxyapatite composites for bone regeneration: in vitro characterization and human osteoblast response. J Biomed Mater Res 2006;76A:151-162.

24. Kim H-W. Biomedical nanocomposites of hydroxyapatite/polycaprolactone obtained by surfactant mediation. J Biomed Mater Res 2007;83A:169-177.

25. Kim S-S, Park MS, Jeon O, Choi CY, Kim B-S. Poly(lactide-co-glycolide)/hydroxyapatite composite scaffolds for bone tissue engineering. Biomaterials 2006;27:1399-1409.

26. Devin JE, Attawia MA, Laurencin CT. Three-dimensional degradable polymer-ceramic matrixes for use in bone repair. J Biomater Sci: Polym Edit 1996;7(8):661-669.

27. Chen J, Chu B, Hsiao BS. Mineralization of hydroxyapatite in electrospun nanofibrous poly(L-lactic acid) scaffolds. J Biomed Mater Res 2006;79A:307-317.

28. Moharram MA, Allam MA. Study of the Interaction of Poly(acrylic acid) and Poly(acrylic acid-Poly acrylamide) Complex with Bone Powders and Hydroxyapatite by Using TGA and DSC. J Appl Polym Sci 2007;105:3220-3227.

29. Cushnie EK, Khan YM, Laurencin CT. Amorphous hydroxyapatite-sintered polymeric scaffolds for bone tissue regeneration: Physical characterization studies. J Biomed Mater Res 2008;84A:54-62.

30. Cool SM, Kenny B, Wu A, Nurcombe V, Trau M, Cassady AI, Grondahl L. Poly(3-hydroxybutyrate-co-3-hydroxyvalerate) composite biomaterials for bone tissue regeneration: *In vitro* performance assessed by osteoblast proliferation, osteoclast adhesion and resorption, and macrophage proinflammatory response. J Biomed Mater Res 2007;82A:599-610.

31. Whitaker-Brothers K, Uhrich K. Poly(anhydride-ester) fibers: Role of copolymer composition on hydrolytic degradation and mechanical properties. J Biomed Mater Res 2004;70A:309-318.

32. Reynolds MA, Prudencio A, Aichelmann-Reidy ME, Woodward K, Uhrihc KE. Non-steroidal anti-inflammatory drug (NSAID)-derived poly(anhydride-esters) in bone and periodontal regeneration. Curr Drug Deliv 2007;4(3):233-239.

33. Schmeltzer R, Anastasiou TJ, Uhrich KE. Optimized synthesis of salicylate-based poly(anhydride-esters). Polym. Bull. 2003;49(6):441-448.

34. Prudencio A, Schmeltzer RC, Uhrich KE. Effect of linker structure on salicylic acid-derived poly(anhydride-esters). Macromolecules 2005;38:6895-6901.

35. Fagerlund G. Determination of specific surface by the BET [Brunauer, Emmett, Teller] method. Materiaux et Constructions (Paris) Materials and Structures 1973;6(33):239-245.

36. Salvador F, Sanchez-Jimenez C, Sanchez-Montero MJ, Salvador A. A review of the application of the BET equation to experimental data. The C parameter. Studies in Surface Scienct and Catalysis 2002;144:379-386.

37. ASTM D 3359. West Conshohocken, PA: ASTM International; 1998.

38. Akbari H, D'Emanuele A, Atwood D. Effect of fabrication technique on the erosion characteristics of polyanhydride matrices. Pharm. Dev. Technol. 1998;3(2):251-259.

39. Whitaker-Brothers K, K. Uhrich. Investigation into the erosion mechanism of salicylate-based poly(anhydride-esters). J. Biomed. Mater. Res. 2006;76A:470-479.

40. Wei M, Swain MV, Ruys AJ, Milthorpe BK, Sorrell CC. Adhesive strength testing of hydroxyapatite coatings. II. The adhesive tape test and Rockwell indentation. Materials Engineering 1998;9(1):19-30.

41. Henriques M, Azeredo J, Oliveira R. Adhesion of *Candida albicans* and *Candida dubliniensis* to acrylic and hydroxyapatite. Colloids and Surfaces B: Biointerfaces 2004;33:235-241.

CHAPTER 4: NOVEL POLY(ANHYDRIDE-AMIDE) COATINGS FOR METAL DEVICES

4.1. Abstract

The goal of this research was to create uniform polymer coatings with consistent amounts of ampicillin for localized, controlled drug delivery. A biodegradable ampicillin-based poly(anhydride-amide) coating was solvent-cast onto stainless steel substrates. The *in vitro* polymer degradation was monitored to determine the release rates of the ampicillin diacid intermediate as well as the free ampicillin. At physiological conditions (in PBS pH 7.4 and 37 °C) only the ampicillin diacid was observed because free ampicillin release requires amide bond cleavage that does not occur under these experimental conditions. The coatings were further tested for activity against biofilm growth in *Staphylococcus aureus*. The ampicillin diacid prevented biofilm formation, whereas the polymer itself was inactive. Based upon these results, the ampicillin-based poly(anhydride-amide) may be useful, upon hydrolytic degradation, to prevent and treat bacterial infections in medical devices following implantation.

4.2. Introduction

Due to increased life expectancy, improved medical implant materials are needed to repair damaged tissue.[1] Further, an increasing need to prevent bacterial infections from occurring following implantation of medical devices exists. Metal implants,

especially stainless steel, provide a surface amenable to bacteria growth which exacerbates the problem.[2,3] Improvements in the performance and safety of metal implant materials have been made, but a relatively high occurrence of revision surgeries are needed due to biofilm formation and bacterial resistance.[4-6] Stainless steel has been used in medical devices such as cardiac stents and hip implants because of its corrosion resistance and mechanical properties.[7]

Bacterial infections have consistently been a safety issue with medical implants, including stainless steel materials and are becoming extremely difficult to treat due to the development of resistant biofilm networks that are not susceptible to traditional antibiotics.[8] Such infections often lead to multiple revision surgeries, and in some cases, death.[9]

Typically, bacterial infections are systemically treated with a course of antibiotics. However, systemic treatments expose the entire body to the drug such that the implant site may not receive the dosage necessary to kill the bacteria.[5] Often, this lowered dose results in the development of resistant bacteria, and ultimately biofilm formation.[10] Unfortunately, systemic antibiotics are rendered ineffective upon biofilm formation and, as a result, increased numbers of antibiotic resistant strains of bacteria. [10-12] Biofilms can cause the deterioration of the systems designed to control them, such as antibiotic-loaded cement, thus it is extremely important to develop effective systems to prevent biofilm formation.[13,14]

The most commonly studied localized antibiotic therapy is the physical admixture of antimicrobials within polymer matrices to treat bacterial infections.[15-18] However, novel drug delivery vehicles have widened the options for treatment.[19] Specifically, the

development of a device coating to mediate the initial bacterial infection may be beneficial. Polymer coatings for medical device applications have been characterized throughout the literature.[20-24] Motivation for device coatings originates from the need to reduce bacterial attachment while concurrently increasing cell attachment and bone growth.[25] Implant coatings with the added benefit of controlled antibacterial compound release is an important advancement.

Comparatively, current treatments for medical device-related bacterial infections are somewhat effective in preventing biofilm adhesion, but do not prevent the initial bacterial contamination.[26] For orthopedic applications, the antibiotic can be locally delivered at the time of surgery by antibiotic-loaded cement.[27] Localized antibiotic delivery ensures effective delivery without exposure to the patient's entire body. Other novel treatment options being studied include anti-adhesive surface modifications with heparin, albumin, and poly(ethylene oxide).[26]

Biodegradable polymers as drug delivery vehicles, with and without the drug chemically bonded in the polymer, have been under examination as a novel way to treat and prevent bacterial infections and biofilm formation.[28-32] This research highlights an ampicillin-based poly(anhydride-amide)[33] as a novel coating for controlled, localized delivery of antibiotics at the implant site. This drug-based polymer may better control and sustain drug release compared to other polymer systems because of the aliphatic linker covalently linked through amide bonds to each ampicillin molecule. Ultimately, ampicillin-based polymer coatings may facilitate new bone growth and integrate into the surrounding tissue.

4.3. Materials and Methods

4.3.1. Materials

Ampicillin was purchased from MP Biomedicals (Solon, OH). N,N-Dimethylformamide (DMF), acetic anhydride, dichloromethane, diethyl ether, pyridine, and triethylamine were purchased from Aldrich (Milwaukee, WI). All other reagents and solvents were purchased from Fisher Scientific (Fair Lawn, NJ) and used as received. Triethylamine was dried over calcium hydride, all other reagents were used without further purification.

4.3.2. Ampicillin-based Poly(anhydride-amide) Synthesis

The solution polymerization method used to prepare the ampicillin-based poly(anhydride-amide) (**1** in **Figure 4.1**) was published elsewhere.[33] Briefly, the ampicillin-based diacid (**2** in **Figure 4.3**) was prepared in DMF with pyridine as a base at 0°C. The polymer (**1**) was synthesized using triphosgene as a coupling agent and triethylamine as an acid acceptor at 0 °C under nitrogen. The resulting polymer (**1**) was isolated by pouring over diethyl ether, drying under vacuum at room temperature, and had a M_w = 86,000 and PDI = 1.1.

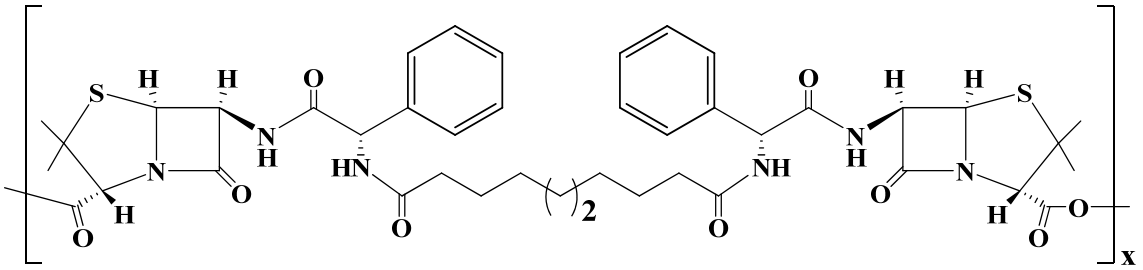

Polymer (1)

Figure 4.1. Structure of the ampicillin-based poly(anhydride-amide).

4.3.3. Coating Preparation and Characterization

A 5 % (w/v) ampicillin-based poly(anhydride-amide) (**1**) solution was prepared in DMF for solvent-casting. The polymer solution (150 µL) was pipetted onto 316L stainless steel coupons (McMaster-Carr, cut to 10 x 30 mm by Rutgers Physics Department Machine Shop). The solvent was evaporated using one of three methods: i) ambient conditions overnight; ii) heating samples to 60 °C for two hours; and iii) heating under vacuum to 60 °C for 45 minutes. Additionally, the ampicillin-based diacid precursor was precipitated onto stainless steel substrates for comparison to the polymer coatings.

Peel tests were conducted using the x-cut method in American Standard Test Method (ASTM) D 3359-02 (n=5).[34] Two 10 mm X-cuts were scratched into coated coupons using a fresh razor blade. Permacel P-99 tape was adhered to the surface and peeled away at a 180° angle after 90 seconds. Each sample was examined for coating removal and ranked according to the following scale: 5A-no peeling or removal; 4A-trace peeling or removal; 3A-jagged removal along incisions; 2A-jagged removal along most of the incisions; 1A-removal from most of the area of the X under the tape; and 0A-removal beyond the area of the X.

Sessile contact angle measurements were completed using deionized water on a model 250 Rame-Hart goniometer (Mountain Lakes, NJ) with DROPimage software. One water drop was placed on each coating and measured in real time with a camera. The contact angle was measured as the average value from five water droplets with three angle measurements taken for each drop. The final contact angle value is the average of at least 15 measurements.

Digital microscope images were taken using a Keyence VHX-100 Digital Microscope (Woodcliff Lake, NJ). The coating surfaces were examined up to a magnification of 3000x to monitor coating uniformity.

4.3.4 *In Vitro* Degradation Study

[*In vitro degradation studies were conducted at the Office of Science and Engineering Labs in the Division of Chemistry and Materials Science at the Food and Drug Administration in Rockville, MD*]

Polymer-coated stainless steel coupons were placed into individual chambers and degraded in the SOTAX USP 4 CE 7 Drug Dissolution Testing System (Allschwil, Switzerland) with a CP 7 ceramic pump, Agilent 8453 UV detection, and WinSOTAX software.[35,36] The samples were degraded at 37 °C in 0.1 M phosphate buffer solution (PBS) pH 7.4. In-line UV detection measurements were taken every five minutes for 4 hours and every hour subsequently at 210 nm. Preliminary experiments were done on a Varian 400-DS USP 7 Dissolution Instrument (Palo Alto, CA) under the same conditions outlined above and with the degradation media separated by HPLC with UV detection.

4.3.5. Bacterial Adherence

[Bacterial adherence studies were conducted by Innovotech Inc., Calgary, Alberta, Canada]

Bacterial adherence testing was completed at Innovotech Inc. (Calgary, Alberta, Canada) using the Biofilm Eradication Surface Testing (BEST) Assay method. *Staphylococcus aureus* (ATCC 29213) was obtained from ATCC (Manassas, VA). The coatings were exposed to the *Staphylococcus aureus* bacteria cells at the required density for biofilm formation (10^6 colony forming units (CFU)/mL) for 24 hours at 37 °C. Adherent bacteria cells were recovered and quantified compared to negative uncoated controls.

4.3.6. *In Vitro* Degradation with Bacteria Present

Polymer-coated coupons were degraded in BHI (Brain Heart Infusion) media (Fisher, Fair Lawn, NJ) with *S. aureus* cells for five days (cells were maintained by Linda Rosenberg, Department of Food Science, Rutgers University). The media was sampled at each time point, filtered through 0.45 μm surfactant-free cellulose acetate (SFCA) syringe filters (Nalgene, Rochester, NY), and stored at room temperature until HPLC analysis. The samples were transferred to HPLC vials and analyzed on a Waters 2695 Separations module with a 2487 Dual Wavelength UV Detector and Empower 2 software. The HPLC method was developed to separate the free ampicillin released from the ampicillin diacid at 210 nm on a Gemini C18 column (150 x 4.6 mm, 5 μm, Phenomenex, Torrance, CA). The method was a linear gradient with a mobile phase consisting of 20 mM monobasic potassium phosphate pH 4.0 and methanol. Five point

calibration curves were generated for both the ampicillin and the ampicillin diacid with concentrations ranging from 0.005 mg/mL to 0.5 mg/mL. The degradation media was diluted in monobasic potassium phosphate, if needed, to calculate release within the calibration curve. Before HPLC analysis, the samples were filtered once more through 0.45 μm PTFE syringe filters (Nalgene, Rochester, NY). Full system automation and data analysis were completed using Empower 2 software Build 2154. Complete ampicillin release was ensured by observing complete polymer degradation and calculating the total ampicillin content in the polymer.

4.3.7. *In Vitro* Cytotoxicity

[Cell studies were performed by Natasha Piracha, Department of Cell Biology and Neuroscience, Rutgers University]

Cytotoxicity of the polymer coatings was analyzed by culturing cells in media containing degraded polymer. Individual ampicillin-based polymer-coated stainless steel plates were placed in 50 mL of cell culture media for 48 hours. Media consisted of Dulbecco's Modified Eagle's Medium (DMEM; Sigma, St. Louis, MO), 10% v/v fetal bovine serum (Atlanta Biologicals, Lawrenceville, GA), penicillin/streptomycin, and L-glutamine.

L929 mouse areolar/adipose fibroblasts (Department of Biomedical Engineering, Rutgers University, Piscataway, New Jersey) were sustained in a cell culture incubator at 37°C and an atmosphere containing 5% CO_2. Confluent fibroblasts were removed from the cell culture flask via trypsinization. After media removal, trypsin (2 mg/mL, Sigma, St. Louis, MO) was placed on cells and incubated at 37°C for five minutes to allow cell

detachment from the surface of the flask. Trypsin activity was ceased with addition of media and the solution centrifuged for 2 min at 2000 rpm (Thermo Electron 5682 3L GP, Franklin, MA). Cells were seeded at a concentration of 100,000 cells/well in media containing polymer degradation media and analyzed after 24, 48, and 72 hours. All samples were studied in triplicate. A standard curve was generated with cells seeded at 25,000, 50,000, 100,000, and 500,000 cells/well in cell culture media without polymer, analyzed after 24 hours.

Imaging was performed with a fluorescent microscope (Olympus IX81, Center Valley, PA) with a 10x phase-contrast objective and cell morphology assessed by observation at 24, 48, and 72 hours.

Cell growth was quantified using Calcein AM staining as a live cell assessment every 24 hours for 72 hours. At each time point, cell culture media was removed and cells washed twice with phosphate buffered saline (PBS, pH 7.4, MP Biomedical, Aurora, OH) and refrigerated with 200 μL Calcein AM stain (8 μM, Molecular Probe, Carsbad, CA) for 30 minutes at 4°C. Fluorescent intensity was quantified using a fluorescence plate reader (Cytofluor ® Series 4000, Applied Biosystems, Woodinville, CA) at 485 nm excitation and 530 nm emission. For the three days, live cell numbers were quantified against the standard curve using Microsoft Excel ®.

4.4. Results and Discussion

4.4.1. Coating Preparation and Characterization

Smooth, uniform polymer coatings containing an average of 12 mg ampicillin-based poly(anhydride-amide) were solvent-cast onto 316L stainless steel. Several parameters were investigated to produce uniform polymer coatings: solvent evaporation rate, time, and temperature. Of these processing factors, we focused on two solvents (DMF and methanol) and three solvent evaporation rates. Optical microscope images of the processes are compared in **Figure 4.2**. Coatings with solvent evaporation at ambient conditions (room temperature and atmospheric pressure) produced cracked surfaces

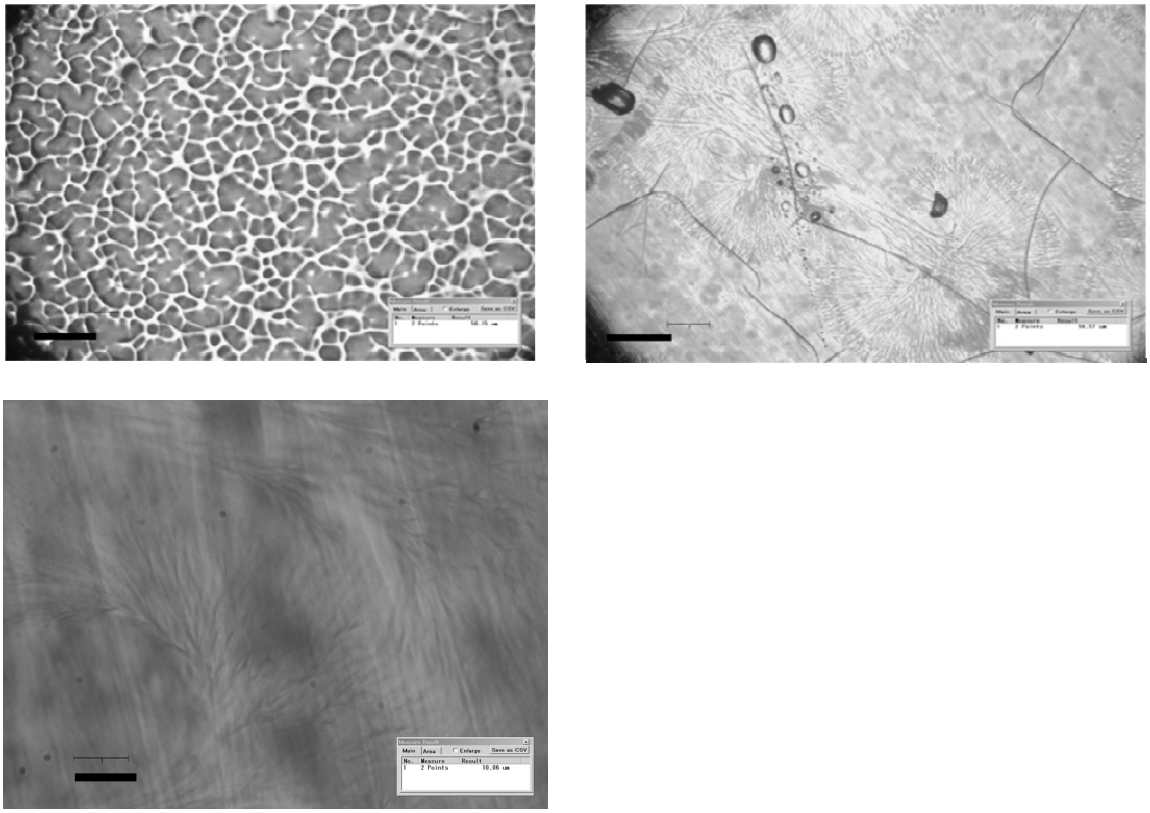

Figure 4.2. Digital images of coating surfaces showing solvent evaporation at a) ambient conditions, b) with heat to 60 °C, and c) with heat to 60 °C and vacuum. (Scale bars equal 50 μm (a and b) and 10 μm (c).

(**Figure 4.2a**). Solvent evaporation with heat produced fewer cracks than ambient evaporation (**Figure 4.2b**), but the faster evaporation rate produced a more uniform coating (**Figure 4.2c**). Solvent evaporation with heat and vacuum was deemed most successful because it reproducibly produced smooth, uniform polymer coatings.

The quality of the polymer coatings was further assessed by an ASTM peel test.[34] The results from the qualitative peel test are summarized in **Table 4.1**. The X-cut peel test[34] examines the adhesion strength of polymer-coated stainless steel substrates. Peel

Table 4.1. Peel Test Analysis of Coating Stability

Sample	Peel Test Results (Result Code)
PolyAmpicillin (vacuum and heat processing)	Trace peeling along incisions (4A)
PolyAmpicillin (heat only processing)	Jagged removal along most of incisions (3A)

ASTM Peel Test Scale
5A-no peeling or removal
4A-trace peeling or removal
3A-jagged removal along incisions
2A-jagged removal along most of the incisions
1A-removal from most of the area of the X under the tape
0A-removal beyond the area of the X

results showed trace coating removal along x-cut incisions, but overall, the coatings strongly adhere to the stainless steel substrates. These results may be due to a nonspecific chemical interaction between the steel and the coating, ultimately causing the coating to strongly adhere to the stainless steel surface without modification. To our knowledge, this work is the first example of a polymer adhering to a metal substrate without a pre-coating or surface modification prior to applying the polymer.

Upon examination of the heat-processed samples, a jagged removal along the x-cut incisions was noted. Thus, the heat-processed samples produce a weaker coating.

This result correlates with the dissolution data in which these coatings flaked off the metal substrate soon after immersion in degradation media (see **Section 4.4.2.**). Alternatively, the vacuum and heat processed samples are the most promising, as these coatings are strong enough to withstand the standard peel test.

The contact angle of the polymer coatings was about 45°, regardless of the solvent evaporation method. These coatings have intermediate contact angles, which are amenable to degradation, yet not immediately solubilized in aqueous media.

The decomposition temperatures of the polymer coatings prepared by various processing methods were measured by TGA to ensure polymer stability during processing (**Table 4.2**). Polymer (**1**) displayed a slight increase in the decomposition temperature following the coating preparation, increasing to a T_d of about 210 °C. Most importantly, during the coating process, the polymer does not decompose.

4.4.2. *In Vitro* Degradation Study

The hydrolytic degradation scheme for the polymer (**1**) is shown in **Figure 4.3**. The anhydride bonds are most labile, whereas the amide bonds in the diacid (**2)** intermediate are expected to hydrolyze slowly and require enzymatic degradation. Initially, the samples were degraded in the SOTAX USP 4 Dissolution system, which measures cumulative degradation products with real-time UV detection. Digital images of coated stainless steel during a dissolution experiment are shown in **Figure 4.4**. Note that the coatings prepared with the fast solvent evaporation (**Fig. 4c**, heat and vacuum) degrade uniformly compared to the coatings prepared with the slower solvent evaporation (**Fig. 4b**, heat only).

Table 4.2. Decomposition temperatures as measured by TGA (n=3) for each coating condition to ensure no polymer decomposition during processing. A fast evaporation rate indicates solvent evaporation under vacuum at 60 °C and a slow evaporation rate indicates solvent evaporation at 60 °C.

Ampicillin-based Polymer Coating Type	Solvent	Solvent Evaporation	T_d (°C)
1 (unprocessed polymer)			**195**
2	DMF	heat and vacuum	211
3	DMF	heat only	210
4	MeOH	heat and vacuum	208
5	MeOH	heat only	208

The *in vitro* degradation results of the ampicillin-based polymer (**1**) coatings are compared in **Figure 4.5**. Polymer **1** hydrolyzed in a more controlled manner with more than 70 % of the ampicillin-based polymer (**1**) coating degraded by 60 hours.

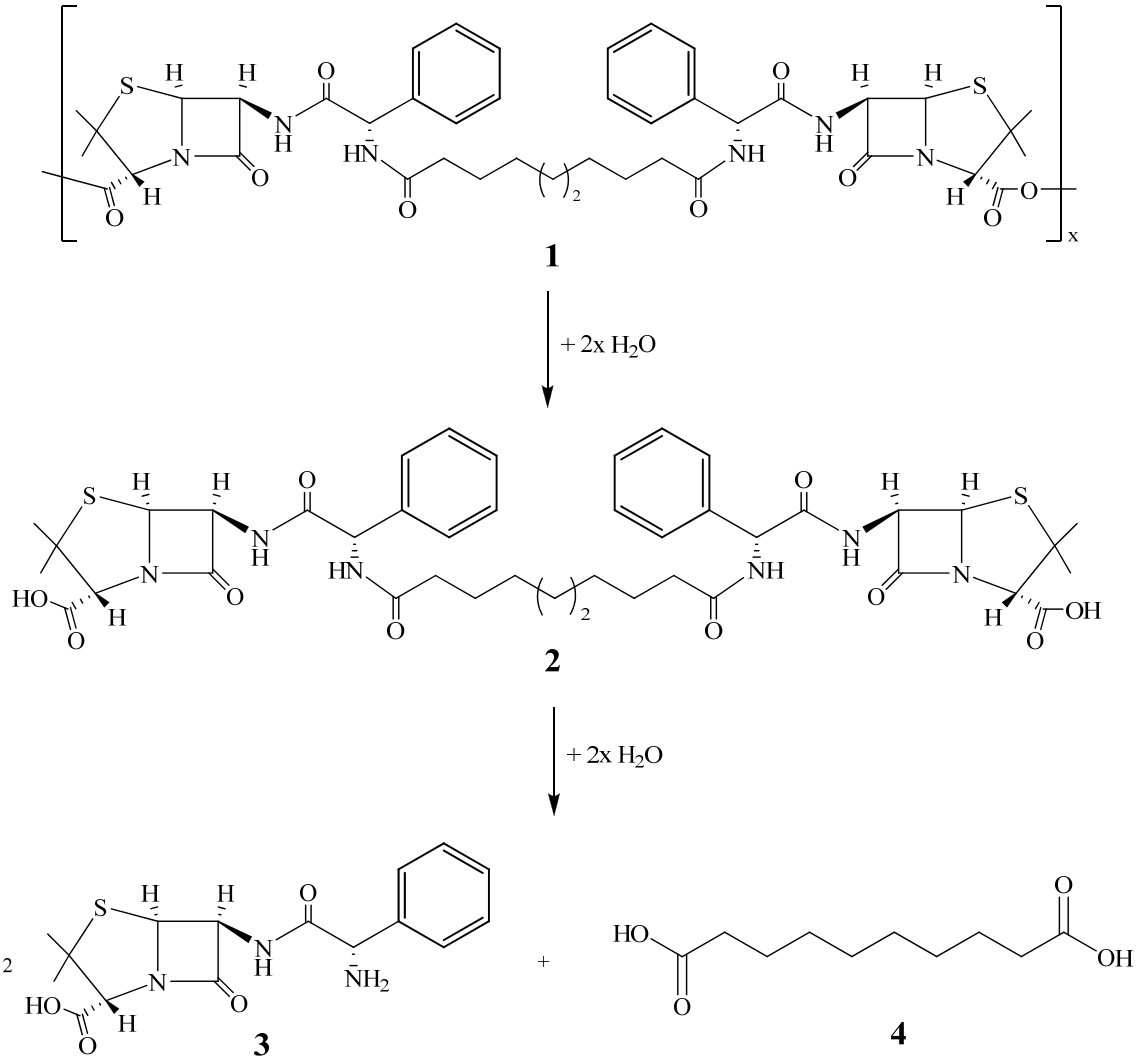

Figure 4.3. Proposed degradation scheme of ampicillin-based poly(anhydride-amide) (**1**). The polymer is expected to hydrolyze quickly at the anhydride bonds and under basic conditions the amide bond will hydrolyze to yield free ampicillin (**3**) and sebacic acid (**4**).

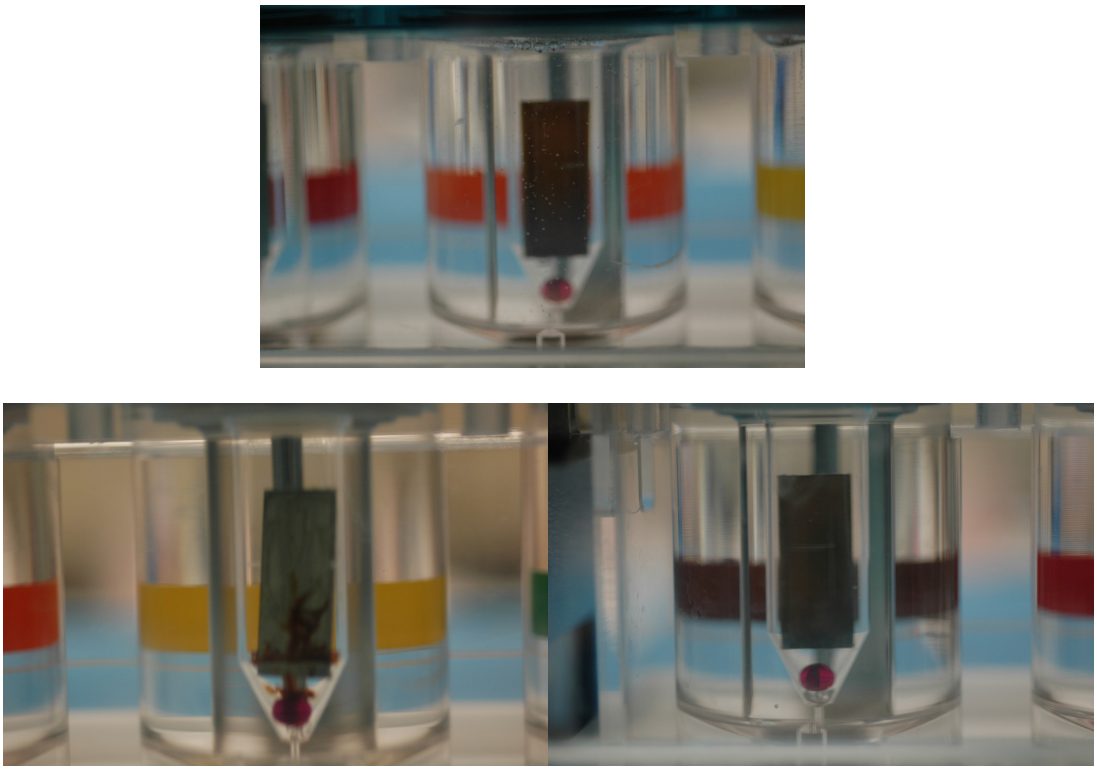

Figure 4.4. Representative images of coating degradation. Image 4a (top) shows a representative coating prior to degradation. Image 4b (bottom left) shows a coating prepared with solvent evaporation with heat to 60 °C only after 2 hours degradation. Image 4c (bottom right) shows a coating prepared with relatively fast solvent evaporation under vacuum and with heat to 60 °C after 2 hours degradation.

Additional release data was obtained from a Varian USP 7 Dissolution Instrument with the ability to separate degradation products by HPLC. In these studies, the free ampicillin drug was not detected because the degradation media was PBS at pH 7.4. The conditions were not amenable to amide bond hydrolysis such that ampicillin was not observed in the HPLC chromatogram (results not shown). Again, the diacid intermediate (**2**) was the final degradation product released from the coatings.

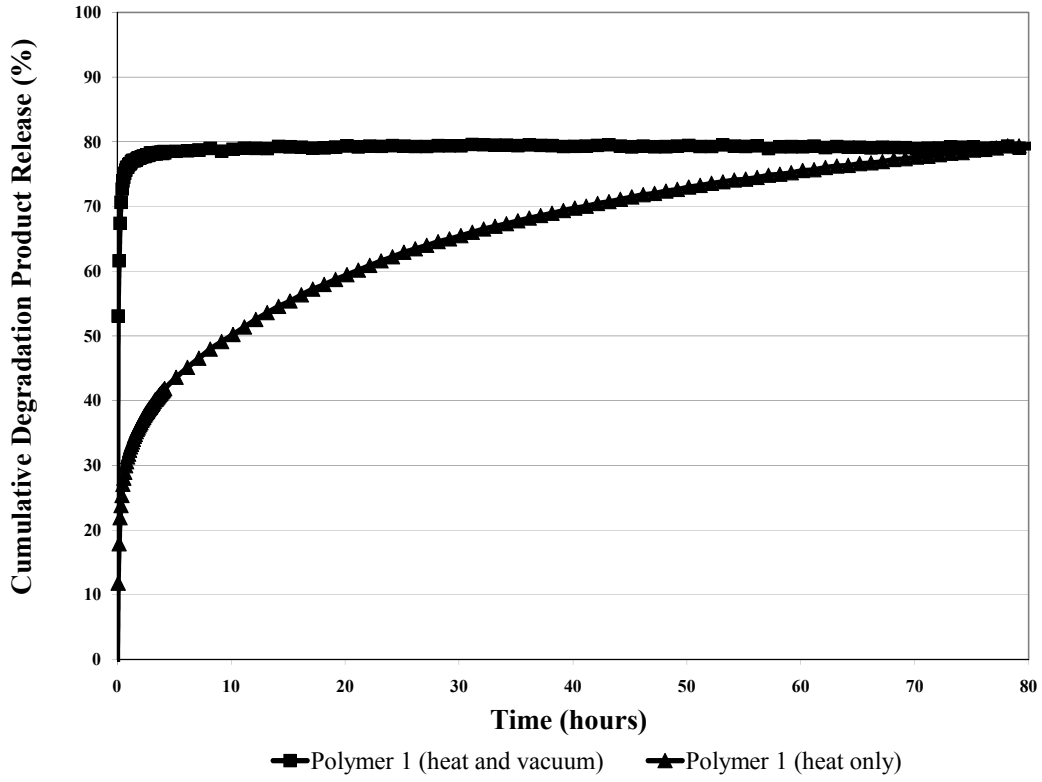

Figure 4.5. Cumulative degradation product release from coatings of polymer **1** prepared with heat and vacuum and heat alone with real-time UV detection.

4.4.3. Bacterial Adherence Study

Staphylococcus aureus growth was monitored during exposure to diacid (**2**) and polymer (**1**) coatings, as well as uncoated stainless steel controls. The bacteria were seeded to facilitate biofilm growth and were exposed to the coatings for 24 hours. The results of the study are shown in **Table 4.3**. The ampicillin-based diacid **(2)** demonstrated complete prevention of *Staphylococcus aureus* biofilm. In contrast, polymer **1** itself did not inhibit biofilm formation, indicating that the diacid **2** is one of the

bioactive compounds. No significant difference in bacterial growth was observed between the uncoated control and the polymer samples. Given that *Staphylococcus aureus* does not grow on the diacid (**2**) coating over longer time periods the diacid intermediate release from degrading polymer will prevent bacteria cell growth and biofilm formation.

Table 4.3. *Staphylococcus aureus* growth following exposure to ampicillin-based diacid (**2**) and polymer (**1**) coating for 24 hours.

Coating (n=3)	Log $_{10}$(Average Cell Count (CFU/mm^2))	± Std. Dev.	Log R	*S. aureus* Biofilm Prevention
Uncoated Control	1.79	0.69	Control	N/A
Polymer 1 (heat and vacuum	2.38	0.04	-0.59	no
Polymer 1 (heat only)	1.71	0.31	0.08	no
Diacid 2	0	0	1.79	yes

4.4.4. *In Vitro* Degradation in the Presence of Bacteria

The degradation profile was studied in more detail by measuring the degradation media following exposure of the coatings to *Staphylococcus aureus* for 5 days. The HPLC method yields ampicillin with a retention time of 17 minutes and the diacid (**2**) with a retention time of 6.5 minutes (**Figure 4.6**). The bacteria should aid in the complete degradation of the ampicillin-based poly(anhydride-amide) (**1**) to free

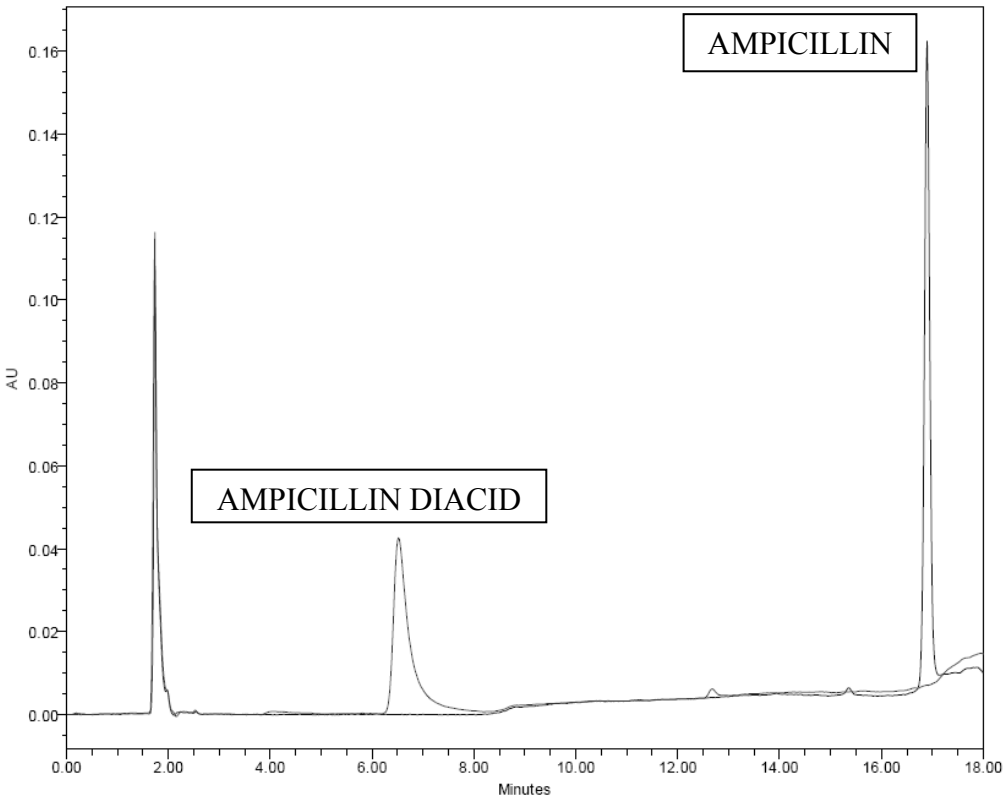

Figure 4.6. Representative HPLC chromatogram showing separation of ampicillin diacid and ampicillin.

ampicillin, but the HPLC results only showed the release of the diacid (**2**). The diacid release profile is shown in **Figure 4.7** and is similar to the cumulative release profile obtained from the SOTAX USP 4 Dissolution System (**Section 4.4.2.**).

4.4.5. Cytotoxicity Assessment

Fibroblasts were tested in media containing degraded polymer coatings through heat or through a heat and vacuum methods. Cell proliferation was quantified through 72 hours of culture. Fibroblast culture growth was not impeded by the use of polyampicillin

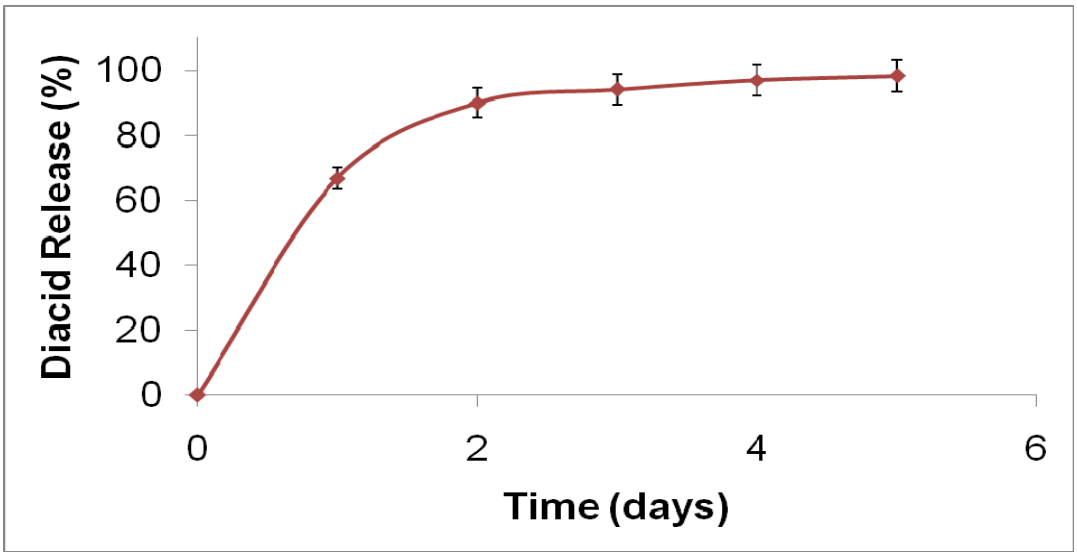

Figure 4.7. *In vitro* release profile from ampicillin-based polymer coatings exposed to *Staphylococcus aureus* for 5 days.

in the cell culture medium, as shown by the graph in **Figure 4.8**. All samples showed positive growth throughout the duration of testing with neither polymer impeding cell proliferation and amplification.

Cell morphology was compared to cells cultured in the control, which contained media without any polymer present (**Figure 4.9**). The cells displayed their natural, heterogeneous morphology. Generally, the fibroblasts readily attached and remained attached to the surface despite washing and showed characteristic spreading and extensions. However, cells cultured in media containing polymer **1** coatings prepared with fast solvent evaporation (heat and vacuum) do not extend and spread fibers as frequently as the control and polymer **1** coatings prepared with slow solvent evaporation (heat). Nonetheless, cells showed stellate morphology through 72 hours, proving a low cytotoxicity to the polymer degradation products.

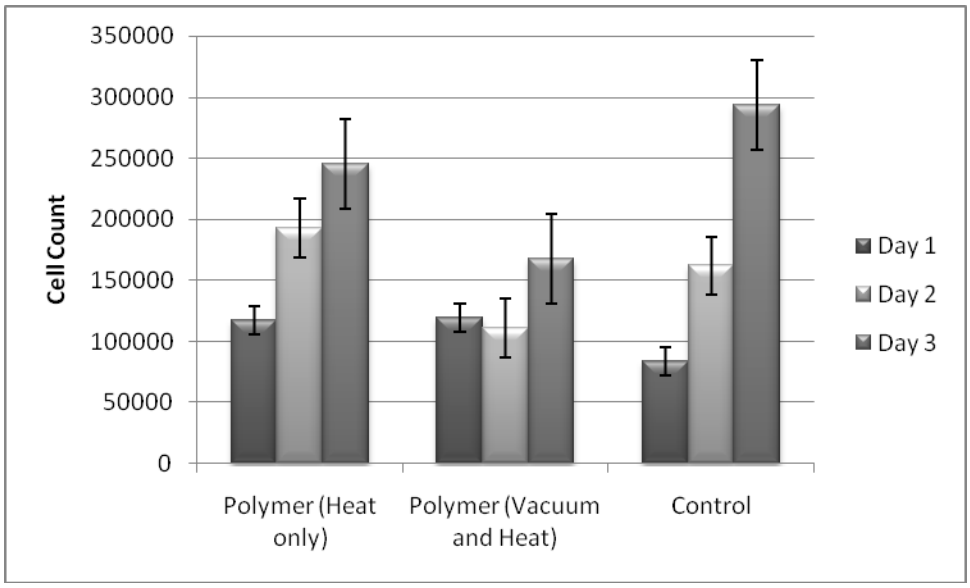

Figure 4.8. *In vitro* cytotoxicity of ampicillin-based polymer coatings

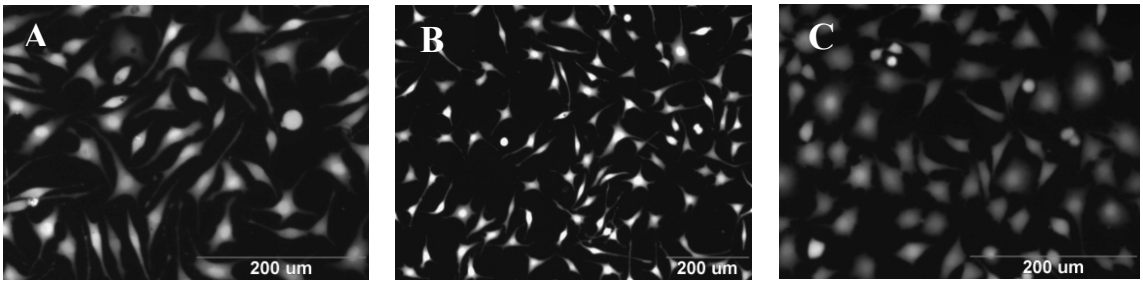

Figure 4.9. L929 fibroblasts samples of control (A), polyampicillin-heat only (B), and polyampicillin-heat and vacuum (C)

4.5. Conclusions

Ampicillin-based poly(anhydride-amide) coatings are a novel development that may improve current clinical therapies for bacterial infections. The coatings had strong adhesion properties to 316L stainless steel which had not been demonstrated in any other polymer system without first modifying the metal surface. The *in vitro* degradation

studies yielded the ampicillin-based diacid as the final degradation product, in PBS pH 7.4. The detection of the ampicillin-based diacid (**2**) in degradation media indicates that the biodegradable polymer coating is useful in preventing biofilm formation upon hydrolytic degradation, which is not possible with free ampicillin. Although the polymer (**1**) itself is inactive against bacteria growth, it degrades to the more hydrophilic diacid (**3**), which completely eradicates *Staphylococcus aureus* growth and biofilm formation. Overall, these poly(anhydride-amide) coatings may be able to circumvent the need for systemic administration and may also reduce bacterial resistance through the controlled release mechanism.

4.6. Acknowledgements

The authors would like to acknowledge Benita J. Dair, Ph.D. (FDA) and Martin K. McDermott, Ph.D. (FDA) for training and scientific discussions, FDA/CDRH/OSEL/DCMS for internship opportunity and Innovotech for bacterial testing. The authors acknowledge NSF-IGERT on Integratively Engineered Biointerfaces (DGE 033196) graduate fellowship for M.J. and National Institutes of Health (DE 013207) for funding.

4.7. Disclaimer

Statements in this chapter reflect the opinions of the authors and do not necessarily reflect the opinions of the US Food and Drug Administration. The mention of

commercial products, their source, or their use in connection with the material reported herein is not to be construed as either an actual or implied endorsement of the US Food and Drug Administration.

4.8. References

1. Habibovic P, deGroot K. Osteoinductive biomaterials-properties and relevance in bone repair. J Tissue Eng Regen Med 2007;1:25-32.

2. Sheehan E, McKenna J, Mulhall KJ, Marks P, McMormack D. Adhesion of *Staphylococcus* to orthopaedic metals, an in vivo study. J Orthop Res 2004;22:39-43.

3. Verheyen CCPM, Dhert WJA, de Blieck-Hogervorst JMA, van der Reijden TJK, Petit PLC, deGroot K. Adherence to a metal, polymer and composite by *Staphylococcus aureus* and *Staphylococcus epidermis*. Biomaterials 1993;14(5):383-391.

4. Costerton JW. Biofilm theory can guide the treatment of device-related orthopaedic infections. Clin Orthop Relat Res 2005;437:7-11.

5. Burrows LL, Khoury AE. Infection of medical devices. In: Wnek GE, Bowlin GL., editor. Encyclopedia of Biomaterials and Biomedical Engineering. New York: Marcel Dekkar; 2004.839-848.

6. Furno F, Bayston R. Antimicrobial/Antibiotics (infection resistance) materials. In: Wnek GE, Bowlin GL., editor. Encyclopedia of Biomaterials and Biomedical Engineering. New York: Marcel Dekkar; 2004.34-42.

7. Williams D. Concise Encyclopedia of Medical and Dental Materials. Oxford: Pergamon Press; 1990. 232-240 p.

8. Patel R. Biofilms and antimicrobial resistance. Clin Orthop Relat Res 2005;437:41-47.

9. Campoccia D, Montanaro L, Ariciola CR. The significance of infection related to orthopedic devices and issues of antibiotic resistance. Biomaterials 2006;27:2331-2339.

10. Hanssen AD, Osmon DR, Patel R. Local antibiotic delivery systems. Clin Orthop Relat Res 2005;437:111-114.

11. Ratner BD, Hoffman, AS, Schoen, FJ, Lemons, LE, editor. Biomaterials Science. San Diego: Elsevier Academic Press; 1996.

12. von Eiff C, Heilmann C, Peters G. New aspects in the molecular basis of polymer-associated infections due to Staphylococci. Eur J Clin Microbiol Infect Dis 1999;18:843-846.

13. Verran J, Whitehead K. Factors affecting microbial adhesion to stainless steel and other materials used in medical devices. Int J Artif Organs 2005;28:1138-45.

14. Flemming H-C. Relevance of biofilms for the biodeterioration of surfaces of polymeric materials. Polym Degrad Stab 1998;59:309-315.

15. von Eiff C, Kohnen W, Becker K, Jansen B. Modern strategies in the prevention of implant-associated infections. Int J Artif Organs 2005;28:1146-56.

16. Garvin K, Feschuk, C. Polylactide-polyglycolide antibiotic implants. Clin Orthop Relat Res 2005;437:105-110.

17. Gollwitzer H, Ibrahim K, Meyer H, Mittelmeier W, Busch R, Stemberger A. Antibacterial poly(D,L-lactic acid) coating of medical implants using a biodegradable drug delivery technology. J Antimicrob Chemother 2003;51:585-591.

18. Sharkawi T, Leyni-Barbaz D, Chikh N, McMullen JN. Evaluation of the *in vitro* drug release from resorbable biocompatible coatings for vascular stents. J Bioact and Compat Pol 2005;20:153-168.

19. Smith AW. Biofilms and antibiotic therapy: Is there a role for combating bacterial resistance by the use of novel drug delivery systems. Adv Drug Deliv Rev 2005;57(10):1539-1550.

20. Roosjen A, de Vries J, van der Mei HC, Norde W, Busscher HJ. Stability and effectiveness against bacterial adhesion of poly(ethylene oxide) coatings in biological fluids. J Biomed Mater Res Part B: Appl Biomater 2005;73B:347-354.

21. Tedjo C, Neoh KG, Kang ET, Fang N, Chan V. Bacteria-surface interaction in the presence of proteins and surface attached poly(ethylene glycol) methacrylate chains. J Biomed Mater Res 2007;82A:479-491.

22. Song R, Chiang MYM, Crosby AJ, Karim A, Amis EJ, Eidelman N. Combinatorial peel tests for the characterization of adhesion behavior of polymeric films. Polymer 2005;46:1643-1652.

23. Sarisuta N, Kumpugdee M, Muller BW, Puttipipatkhachorn. Physico-chemical characterization of interactions between erythromycin and various film polymers. Int J Pharm 1999;186:109-118.

24. Ruggeri V, Francolini I, Donelli G, Piozzi A. Synthesis, characterization, and *in vitro* activity of antibiotic releasing polyurethanes to prevent bacterial resistance. J Biomed Mater Res 2007;81A:287-298.

25. Lappalainen R, Santavirta SS. Potential of coatings in total hip replacement. Clin Orthop Relat Res 2005;430:72-79.

26. Arciola C, Alvi FI, An YH, Campoccia D, Montanaro L. Implant infection and infection resistant materials: A mini review. Int J Artif Organs 2005;28:1119-25.

27. Shi Z, Neoh KG, Kang ET, Wang W. Novel strategies for conferring antibacterial properties to bone cement. New Research on Biomaterials. Hauppauge: Nova Science; 2007.

28. Bryers JD, Jarvis RA, Lebo J, Prudencio A, Kyriakides TR, Uhrich K. Biodegradation of poly(anhydride-esters) into non-steroidal anti-inflammatory drugs and their effect on Pseudomonas aeruginosa biofilms in vitro and on the foreign-body response in vivo. Biomaterials 2006;27(29):5039-5048.

29. Krasko MY, Golenser J, Nyska A, Nyska M, Brin YS, Domb AJ. Gentamicin extended release from an injectable polymeric implant. J Controlled Release 2007;117(1):90-96.

30. Yoo JY, Shin JH, Khang G, Shin HS, Yuk SH, Kim YS, Kim MS, Rhee JM, Lee HB. Effect of glycolide monomer on release behavior of gentamicin sulfate-loaded PLGA microparticles. J Appl Polym Sci 2007;104(2):1019-1025.

31. Woo GLY, Mittelman MW, Santerre JP. Synthesis and characterization of a novel biodegradable antimicrobial polymer. Biomaterials 2000;21:1235-1246.

32. Kenawy E-R, Abdel-Hay FI, Shahada L, El-Raheen A, El-Shanshoury R, El-Newehy MH. Biologically active polymers. IV. Synthesis and antimicrobial activity of tartaric acid polyamides. J Appl Polym Sci 2006;102:4780-4790.

33. Prudencio A, Song, M, Uhrich KE. Synthesis of novel antimicrobial-based poly(anhydride-amides) and antibacterial assessment. Biomacromolecules 2007(under review).

34. ASTM D 3359. West Conshohocken, PA: ASTM International; 1998.

35. Brown W. Apparatus 4 flow through cell: Some thoughts on operational characteristics. Diss Tech 2005;12(2):28-30.

36. Beyssac E, Lavigne J. Dissolution study of active pharmaceutical ingredients using the flow through apparatus USP 4. Diss Tech 2005;12(2):23-25.

CHAPTER 5: CONTROLLED RELEASE OF NERVE GROWTH FACTOR (NGF) FROM SALICYLIC ACID-BASED POLY(ANHYDRIDE-ESTER) MICROSPHERES

5.1 Abstract

Salicylic acid-based poly(anhydride-ester) (SA-based PAE) microspheres containing encapsulated nerve growth factor (NGF) were evaluated with respect to their influence on nerve regeneration. The NGF-loaded SA-based PAE microspheres have the potential to increase nerve growth as a result of the novel SA-based PAE properties to relieve pain and inflammation. The morphology of the microspheres was analyzed before and during degradation using scanning electron microscopy (SEM). Nerve growth factor release was quantified with an enzyme-linked immunosorbent assay (ELISA). The NGF-loaded SA-based PAE microspheres showed comparable results to NGF-loaded PLGA microspheres, except for increased acidity of the SA-based PAE media during degradation. The microspheres, which simultaneously release a non-steroidal anti-inflammatory drug (NSAID), salicylic acid, and a growth-promoting factor, NGF, can be combined into nerve guidance conduits prior to insertion in the injured site and may decrease current recovery times.

5.2 Introduction

Polymeric microspheres have been studied in depth for their ability to encapsulate and release various drugs and proteins in a controlled manner.[1-6] Research has shown that poly(lactic acid) (PLA), poly(glycolic acid) (PGA) and/or copolymers of the two (PLGA) can be used as microspheres to deliver various growth factors.[7-13] However, PLGA has been reported to create an acidic environment, eventually causing a foreign body response with increased macrophage activity, inflammation, etc.[14,15] Based on favorable *in vivo* studies,[16,17] salicylic acid-based poly(anhydride-esters) (SA-based PAEs) (**Figure 5.1)** have been formulated into microspheres.[18] In addition to a physical encapsulation of actives, these polymers have the added benefit of releasing a non-steroidal anti-inflammatory drug (NSAID) that reduces inflammation and prevents the foreign body response upon hydrolytic degradation.[19]

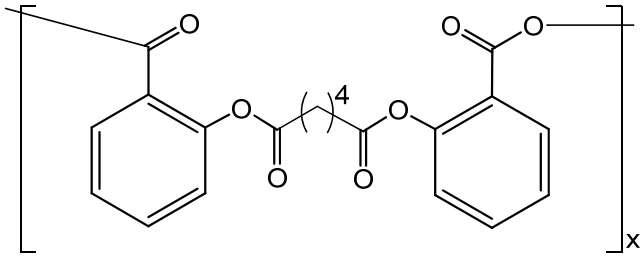

Figure 5.1. Chemical structure of the SA-based PAE with adipic linker.

In the past decade, controlled delivery from polymeric microspheres has been more focused on protein delivery.[20,21] From growth factors to bone morphogenic proteins (BMPs), researchers have studied ways to protect and sustain delivery of sensitive proteins.[13,22-29] However, controlled protein delivery has proven to be extremely difficult

because of the thermal, solvent, and enzymatic sensitivity of proteins. Researchers have studied ways to alter the microsphere preparation methods to better stabilize the proteins with polymer matrices.[30,31]

Nerve growth factor (NGF) is particularly interesting for controlled release studies because it enhances nerve differentiation and growth.[32-34] Recently, NGF was found to cause inflammation and pain following injury.[35,36] As excess NGF is needed to heal nerve damage, an anti-inflammatory agent may help stop the inflammation and pain caused by the increased NGF. Neurons respond favorably to SA-based PAEs,[37] as such, these polymers may be useful for the encapsulation and controlled release of NGF.

In this study, NGF was loaded into an SA-based PAE using a solvent evaporation microsphere preparation technique. The microspheres were characterized, degraded *in vitro* and the release of NGF and salicylic acid monitored. 50:50 PLGA was loaded with NGF and used as a polymer control for this study. Neurons grown on the SA-based PAEs with NGF dissolved in the media have shown positive axonal growth profiles.[37] Therefore, NGF-loaded SA-based PAE microspheres may provide similar results in future studies with nerve guidance conduits.

5.3. Materials and Methods

5.3.1. Materials

Recombinant rat β-NGF and the corresponding enzyme-linked immunosorbent assay (ELISA) kit were purchased from R&D Systems (Minneapolis, MN). 50:50 poly(lactic-co-glycolic acid) (PLGA) was received as a gift (BPI, Cupertino, CA) and

purchased from Sigma-Aldrich (St. Louis, MO). The salicylic acid-based poly(anhydride-ester) (SA-based PAE) was prepared using previously described methods.[38,39] Dulbecco's phosphate buffered saline (PBS) without Ca and Mg was purchased from MP Biomedicals (Solon, OH). All other reagents were purchased from Aldrich (Milwaukee, WI) and used as received.

5.3.2. Preparation of Microspheres

Microspheres of each polymer, 50:50 PLGA and SA-based PAE, were prepared as controls for the NGF-loaded polymer microspheres using a solvent evaporation method. A method to prepare SA-based PAE microspheres has been previously published[18] and modified here. For this study, polymer (0.1 g) was dissolved in dichloromethane (2 mL). The polymer solution was added to 1% PVA (30 mL) and homogenized (IKA T8 Ultra Turrax, Wilmington, NC) at 8,000 rpm for 1 minute. The resulting emulsion was poured over an additional 1% PVA (200 mL) and mechanically stirred for 3 hours at room temperature. The microspheres were isolated by vacuum filtration and dried overnight under vacuum.

5.3.3. Preparation of NGF-loaded Microspheres

The NGF-loaded microspheres were prepared by a solvent evaporation method. One milliliter of 10 μg/mL NGF was added to the polymer solution (SA-based PAE and 50:50 PLGA) and gently inverted to mix. The NGF solution also contained 0.1 % bovine serum albumin carrier protein (BSA) in PBS and was mixed with SA-based PAE (0.1 mg) in dichloromethane and vortexed lightly. The NGF/polymer mixture was added

dropwise to 30 mL 1 % PVA on ice and homogenized for 1 minute at 5,000 rpm. The resulting solution was poured over 200 mL 1 % PVA solution and mechanically stirred for 3 hours to remove dichloromethane and form microspheres. The microspheres were isolated by filtration, washed with water, and lyophilized overnight. The filtrate was diluted and examined by an ELISA to calculate the exact encapsulation efficiency of the NGF in the polymer. The value was calculated using the following equation:

$$\text{Encapsulation efficiency (\%)} = \frac{\text{Theoretical amount NGF loaded (mg)} - \text{Amount NGF in microsphere filtrate (mg)}}{\text{Theoretical amount NGF loaded (mg)}} * 100$$

5.3.4. SEM of Microspheres

The microsphere morphology was characterized by scanning electron microscopy (SEM). A thin layer of microspheres were affixed to a sample holder using non-conducting adhesive tabs (Electron Microscopy Services, Fort Washington, PA). An amalgam of Au-Pd was then sputtered onto the polymer samples (25 nm thickness) with a Baltec SCD 004 Sputter Coater. The samples were analyzed on an AMRAY 1830 I (AMRAY, Inc., Bedford, MA) with FlashBus FBG 4.2 software on Windows 2000 software to capture images.

5.3.5. *In Vitro* Degradation of Microspheres

Microspheres (20 mg) were placed in 15 mL centrifuge tubes and degraded in triplicate in 2 mL Dulbecco's PBS. The samples were incubated at 37 °C at 40 rpm and the media was exchanged at 4, 8, 12, 18, 24, 36, and 48 hours. Following the 48 hour

timepoint, the media was exchanged daily to continue to monitor the NGF and salicylic acid release for a total of 10 days. The samples were centrifuged (Hettich Zentrifugen EBA 12, Tuttlingen, Germany) at 3000 rpm for 10 minutes to remove the degradation media supernatant for analysis. The 2 mL PBS was replaced at each time point to maintain sink conditions. The spent degradation media was examined by ELISA to quantify the amount of NGF released and by HPLC to quantify the amount of salicylic acid released.

5.3.6. pH Measurement of Degradation Media

The pH of the degradation media was monitored at each time point during degradation with a Fisher Scientific Accumet AR15 pH meter (Pittsburg, PA). The pH at each time point is the average of three measurements from three samples.

5.3.7. Salicylic Acid Release from Microspheres

High pressure liquid chromatography (HPLC) was performed using a Waters 2695 Separations Module with a Waters 2487 Dual Wavelength Absorbance Detector set to 210 nm. Salicylic acid was separated on a C18 column (150 x 4.6 mm, 5 μm, Phenomenex, Torrance, CA) with a flow rate of 1 ml/min in an isocratic mobile phase of 75% 20 mM phosphate buffer solution pH 2.5 and 25% acetonitrile. Five point calibration curves were generated for each compound with concentrations ranging between 0.01 mg/ml and 0.4 mg/ml. The degradation media was diluted using PBS if needed to ensure measurements within the calibration curve and filtered through 0.45 μm

poly(tetrafluoroethylene) (PTFE) syringe filters (Nalgene, Rochester, NY). Full system automation and data analysis were completed using Empower 2 software Build 2154.

5.3.8. NGF Release from Microspheres

NGF release was quantified using an ELISA. The samples were diluted, as necessary, to keep NGF amounts within the calibration curve. A six-point calibration curve was used to quantify the NGF release. The experiment was run in triplicate and repeated in its entirety in duplicate. The 96-well ELISA plates were read using an EL808 Ultra Microplate reader (Bio-Tek Instruments, Winooski, VT) with KC Junior software.

5.4. Results and Discussion

5.4.1. Microsphere Characterization

The microspheres loaded with NGF were prepared with a range of sizes between 10 and 30 μm. Representative SEM images of the NGF-loaded SA-based PAE microspheres are shown in **Figure 5.2**. Upon drying, the solvent evaporation processing technique caused some very small pores to form on the microsphere surface. The pores were prevented in future samples by allowing the microspheres to stir longer in the PVA solution until all of the dichloromethane evaporated. The NGF encapsulation efficiency was calculated by measuring the amount of NGF remaining in the filtrate following microsphere preparation with an ELISA. This method was chosen, over other general

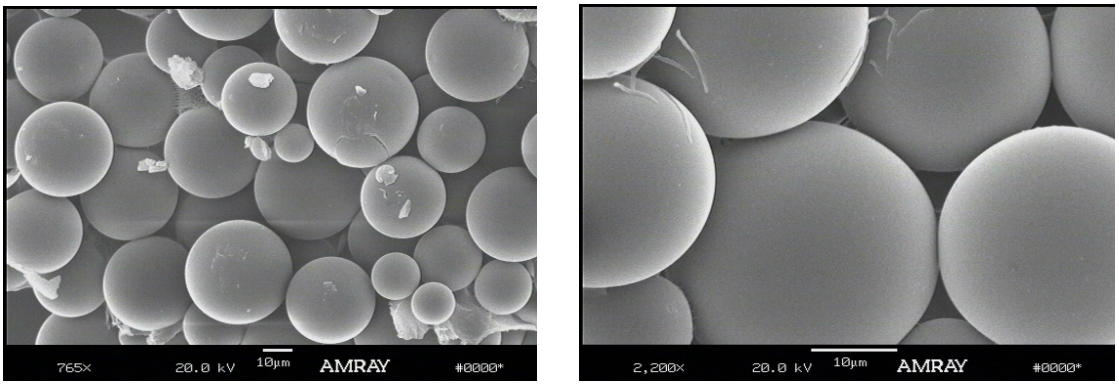

Figure 5.2. Representative SEM images of NGF-loaded SA-based adipic PAE microspheres. The average diameter of the microspheres was 20 µm.

protein measurement assays, such as the bicinchoninic assay (BCA), because it is specific for active NGF and does not measure the BSA used to stabilize the NGF or process-deactivated NGF. The average NGF encapsulation efficiency in the SA-based PAE was 72 %, which is comparable to reports of NGF encapsulation efficiency.[11,40]

5.4.2. *In Vitro* Degradation of NGF-loaded Microspheres

The NGF-loaded SA-based PAE microspheres were degraded in PBS at pH 7.4 and monitored for structural changes. Changes in pH of the degradation media were monitored as well because a significant pH drop may negatively affect the NGF stability. **Figure 5.3** shows representative SEM images of NGF-loaded microsphere degradation over 10 days. These images depict the development of a large pore network during the microsphere degradation, the result of water penetration into the microspheres. A larger portion of the microsphere begins to erode after 2 days degradation, while after 10 days, the pores permeate deep into the microsphere core. The pore network serves as the path for the simultaneous release of NGF and salicylic acid.

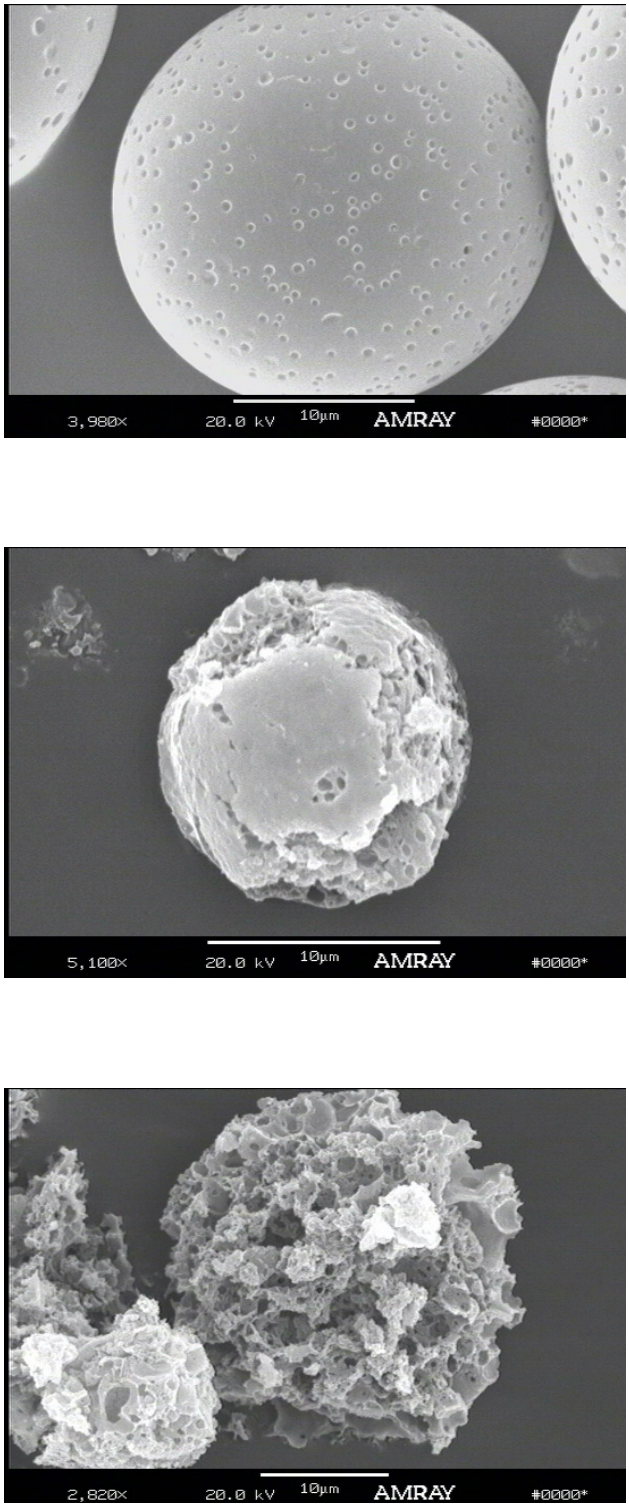

Figure 5.3. SEM images of NGF-loaded SA-based adipic polymer microspheres during degradation at 0 hours (top), 2 days (middle), and 10 days (bottom).

The pH change in the degradation media over 48 hours was monitored for the PLGA control and the SA-based PAE, and the pH values are reported in **Figure 5.4**. A decrease of about 1 pH unit for the SA-based PAE microspheres was observed while the pH of media exposed to PLGA remains near 7.6. The pH differences can be explained by the differences in molecular weight (M_w), crystallinity, and pKa for the two polymers. Specifically, the PLGA microspheres are expected to degrade slower than the SA-based PAE microspheres because it has a higher M_w crystalline domains,[41] and its breakdown products, lactic (3.85) and glycolic (3.83) acids, have slightly higher pKa values than

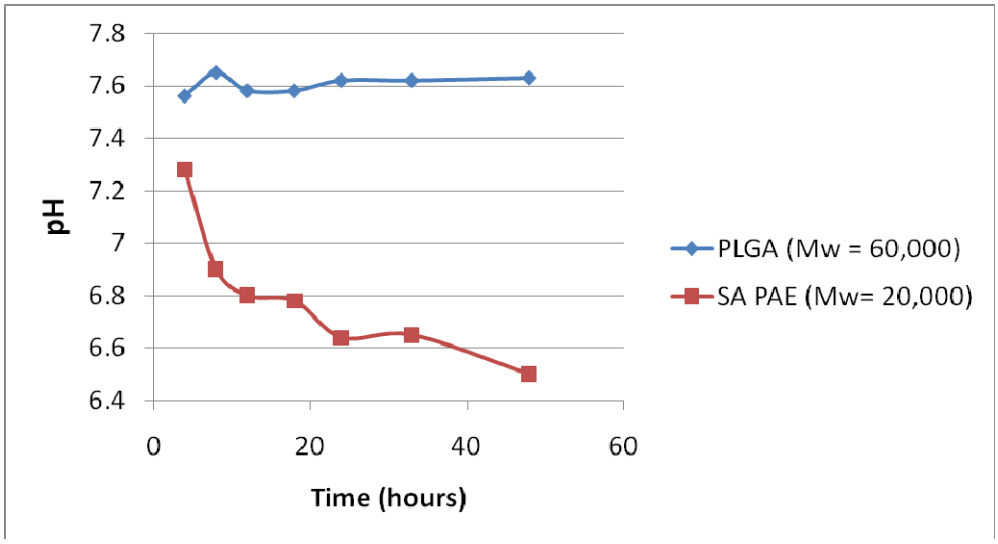

Figure 5.4. pH change in degradation media for the SA-based PAE and the PLGA during the initial 48 hours of degradation.

salicylic acid (2.97). The SA-based PAE is completely amorphous and thus allows water to penetrate beyond the microsphere surface relatively quickly. Although the SA-based

PAE microspheres show a decrease of one pH unit after 48 hours, they are expected to release NGF and SA in a controlled manner to positively influence nerve regeneration.

5.4.3. NGF Release from Microspheres

NGF release was quantified using an ELISA, which measures the amount of active NGF released into the media based on the rat β-NGF antigen binding to the goat anti-rat β-NGF antibody. The ELISA tests for active NGF only, and will not include bovine serum albumin (stabilizing protein) and inactive NGF, if present. The cumulative NGF release profile from the SA-based PAE and PLGA microspheres is shown in **Figure 5.5**. The curves show a near-zero order release with increasing amounts of NGF over the

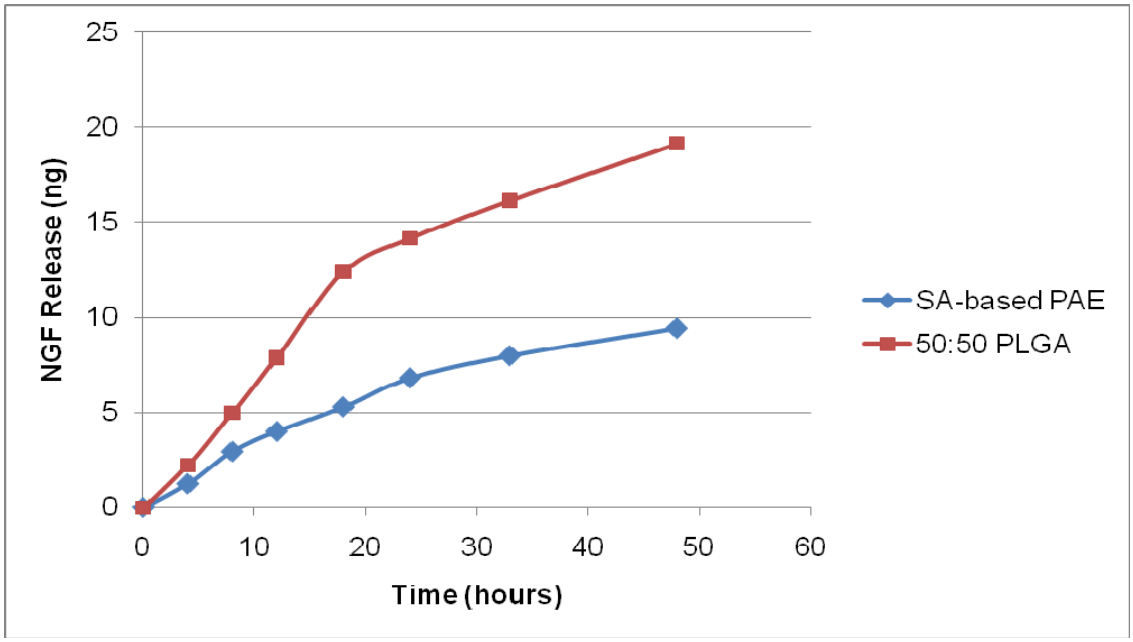

Figure 5.5. NGF release from SA-base PAE and PLGA microspheres over 48 hours.

48 hour time period resulting in approximately 5 % of the loaded NGF. Overall, the SA-based PAE microspheres released twice as much NGF as the PLGA microspheres. Song and Uhrich reported using a concentration of 12.5 ng/mL NGF to cell media to culture dissociated neurons.[42] Based on those previously reported methods, NGF release from the PLGA microspheres is slightly below the amount required for neuronal cell culture, while the SA-base PAE microspheres released slightly more than the required 12.5 ng/mL NGF.

Salicylic acid release is likely important for reducing inflammation during nerve regeneration. While PLGA degradation products tend to increase inflammation *in vivo*,[41,43] SA-based PAE should mitigate inflammation.[17] The cumulative salicylic acid release profile shows a lag phase for the initial 20 hours, and the start of a continuous release phase that continues in **Figure 5.6**, which shows cumulative salicylic acid release from the NGF-loaded SA-based PAE microspheres over 10 days. The final phase of the salicylic acid release is the plateau phase, in which the release rate levels off.

The salicylic acid and NGF release rates in **Figures 5.5 and 5.6** correlate with the pH measurements in **Figure 5.4**. Factors, such as pKa, molecular weight, and crystallinity, affect degradation and drug release rates in the same ways they affect the pH of the degradation media.[41] The NGF-based SA-based PAE microspheres release NGF and salicylic acid.

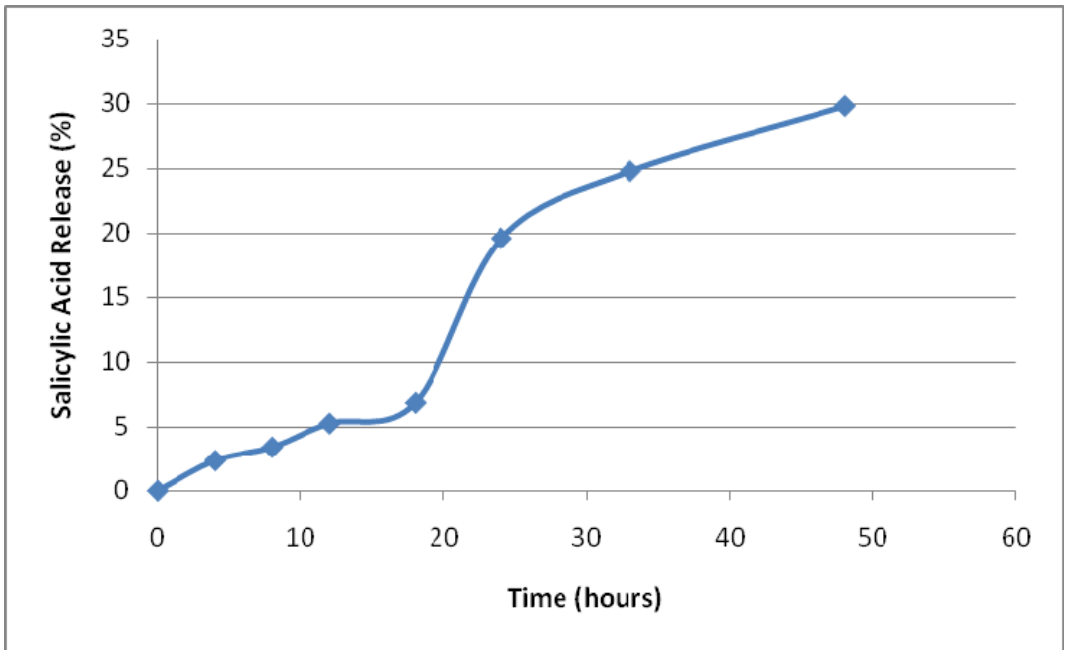

Figure 5.6. Salicylic acid release from the NGF-loaded SA-based PAE microspheres over the initial 48 hous of degradation.

5.5. Conclusions

SA-based PAE microspheres loaded with NGF were prepared at biologically relevant loadings while maintaining the protein activity. NGF release from the SA-based PAE microspheres was comparable to NGF release from PLGA (50:50) microspheres controls loaded with NGF. The NGF-loaded SA-based PAE microspheres may have more potential because of the ability to concurrently reduce inflammation caused by excess NGF. Future research will study the biological effects of the microspheres on dissociated DRGs to compare axonal outgrowth without the microspheres to outgrowth with both the NGF-loaded PLGA and SA-based PAE microspheres.

5.6. References

1. Arshady. Preparation of biodegradable microspheres and microcapsules: 2. Polylactides and related polyesters. J Controlled Release 1991;17(1):1-21.

2. Andrianov AK, Payne LG. Polymeric carriers for oral uptake of microparticulates. Adv Drug Deliv Rev 1998;34:155-170.

3. Makino K. Drug release from poly(lactide-co-glycolide) microspheres. Recent Res Devel in Polym Sci 2000;4:123-130.

4. Edlund U, Albertsson A-C. Degradable polymer microspheres for controlled drug delivery. Adv in Polym Sci 2002;157:67-112.

5. Varde NK, Pack DW. Microspheres for controlled release drug delivery. Exp Opin on Biol Ther 2004;4(1):35-51.

6. Freiberg S, Zhu XX. Polymer microspheres for controlled drug release. Int J Pharm 2004;282:1-18.

7. Mendez A, Camarata PJ, Suryanarayanan R, Ebner TJ. Sustained intracerebral delivery of nerve growth factor with biodegradable polymer microspheres. Meth Neurosci 1994;21:150-168.

8. Wong HM, Wang JJ, Wang C-H. In vitro sustained release of human immunoglobulin G from biodegradable microspheres. Ind Eng Chem Res 2001;40:933-948.

9. Hadlock TA, Sheahan T, Cheney ML, Vacanti JP, Sundback CA. Biologic activity of nerve growth factor slowly released from microspheres. J Reconstr Microsurg 2003;19(3):179-184.

10. Li Y, Jiang HL, Zhu KJ, Liu JH, Hao YL. Preparation, characterization and nasal delivery of α-cobrotoxin-loaded poly(lactide-co-glycolide)/polyanhydride microspheres. J Controlled Release 2005;108:10-20.

11. Gu H, Song C, Long D, Mei L, Sun H. Controlled release of recombinant human nerve growth factor (rhNGF) from poly[(lactic acid)-co-(glycolic acid)] microspheres for the treatment of neurodegenerative disorders. Polym Int 2007;56:1272-1280.

12. Schliephake H, Weich HA, Schulz J, Gruber R. *In vitro* characterization of a slow release system of polylactic acid and rhBMP2. J Biomed Mater Res 2007;83A:455-462.

13. Jaklenec A, Hinckfuss A, Bilgen B, Ciombor DM, Aaron R, Mathiowitz E. Sequential release of bioactive IGF-I and TGF-β_1 from PLGA microsphere-based scaffolds. Biomaterials 2008;29:1518-1525.

14. Li H, Chang J. pH-compensation effect of bioactive inorganic fillers on the degradation of PLGA. Composites of Science and Technology 2005;65(14):2226-2232.

15. van de Weert M, Hennink WE, Jiskoot W. Protein instability in poly(lactic-co-glycolic acid) microparticles. Pharm Res 2000;17(10):1157-1167.

16. Harten RD, Svach DJ, Schmeltzer R, Uhrich KE. Salicylic acid-derived poly(anhydride-esters) inhibit bone resorption and formation in vivo. J Biomed Mater Res 2005;72A(4):354-362.

17. Reynolds MA, Prudencio A, Aichelmann-Reidy ME, Woodward K, Uhrich KE. Non-steroidal anti-inflammatory drug (NSAID)-derived poly(anhydride-esters)in bone and periodontal regeneration. Curr Drug Deliv 2007;4(3):233-239.

18. Yeagy BA, Prudencio A, Schmeltzer RC, Uhrich KE, Cook TJ. Characterization and *in vitro* degradation of salicylate-derived poly(anhydride-ester microspheres). J Microencapsulation 2006;23(6):643-653.

19. Vane JR, Botting, R. M. Anti-inflammatory drugs and their mechanism. Inflammation Research 1998;47(Supplement 2):S78-S87.

20. Fu K, Klibanov AM, Langer R. Protein stability in controlled-release systems. Nat Biotechnol 2000;18:24-25.

21. Malik DK, Baboota S., Ahuja A., Hasan S, Ali J. Recent advances in protein and peptide drug delivery systems. Curr Drug Deliv 2007;4(2):141-151.

22. Bai X-L, Yang Y-Y, Chung T-S, Ng S, Heller J. Effect of polymer compositions on the fabrication of poly(ortho-ester) microspheres for controlled release of protein. J Appl Polym Sci 2001;80:1630-1642.

23. Yang Y-Y, Chung T-S, Ng NP. Morphology, drug distribution, and in vitro release profiles of biodegradable polymeric microspheres containing protein fabricated by double-emulsion solvent extraction/evaporation method. Biomaterials 2001;22:231-241.

24. Determan AS, Trewyn BG, Lin VS-Y, Nilsen-Hamilton M, Narasimhan B. Encapsulation, stabilization, and release of BSA-FITC from polyanhydride microspheres. J Controlled Release 2004;100:97-109.

25. Kipper MJ, Wilson JH, Wannemuehler MJ, Narasimhan B. Single dose vaccine based on biodegradable polyanhydride microspheres can modulate immune response mechanism. J Biomed Mater Res 2006;76A:798-810.

26. Chen F, Zhifen W, Wang Q, Wu H, Zhang Y, Nie X, Jin Y. Preparation and biological characteristics of recombinant human bone morphogenetic protein-2-loaded dextran-co-gelatin hydrogel microspheres, in vitro and in vivo studies. Pharmacology 2005;75:133-144.

27. Kim J-H, Taluja A, Knutson K, Bae YH. Stability of bovine serum albumin complexed with PEG-poly(L-histidine) diblock colpolymer in PLGA microspheres. J Controlled Release 2005;109:86-100.

28. Chen F, Zhao Y, Wu H, Deng Z, Wang Q, Zhou W, Liu Q, Dong G, Li K, Wu Z, Jin Y. Enhancement of periodontal tissue regeneration by locally controlled delivery of insulin-like growth factor-I from dextran-co-gelatin microspheres. J Controlled Release 2006;114:209-222.

29. Torres MP, Determain AS, Anderson GL, Mallapragada SK, Narasimhan B. Amphiphilic polyanhydrides for protein stabilization and release. Biomaterials 2007;28:108-116.

30. Sah H. Protein behavior at the water/methylene chloride interface. J Pharm Sci 1999;88(12):1320-1325.

31. Determan AS, Wilson JH, Kipper MJ, Wannemuehler MJ, Narasimhan B. Protein stability in the presence of polymer degradation products: Consequences for controlled release formulations. Biomaterials 2006;27:3312-3320.

32. Varon S, Conner JM. Nerve growth factor in CNS repair. J Neurotrauma 1994;11(5):473-486.

33. Raivich G, Kreutzberg GW. Nerve growth factor and regeneration of peripheral nervous system. Clin Neurol and Neurosurg 1993;95(Suppl):S84-88.

34. Lykissas MG, Batistatou AK, Charalabopoulos KA, Beris AE. The role of neurotrophins in axonal growth, guidance, and regeneration. Curr Neurovascular Res 2007;4(2):143-151.

35. Hefti FF, Rosenthal A, Walicke PA, Wyatt S, Vergara G, Shelton DL, Davies AM. Novel class of pain drugs based on antagonism of NGF. TRENDS in Pharmacological Sciences 2006;27(2):85-91.

36. Freund-Michel V, Frossard N. The nerve growthfactor and its receptors in airway inflammatory diseases. Pharmacol Therap 2008;117(1):52-76.

37. Griffin J, Song M, Carbone AL, Uhrich, KE. . In vitro dorsal root ganglia viability in a mimetic nerve guidance conduit environment. Polymer Preprints 2007;48(2):932-933.

38. Schmeltzer R, Anastasiou TJ, Uhrich KE. Optimized synthesis of salicylate-based poly(anhydride-esters). Polym Bull 2003;49(6):441-448.

39. Prudencio A, Schmeltzer RC, Uhrich KE. Effect of linker structure on salicylic acid-derived poly(anhydride-esters). Macromolecules 2005;38:6895-6901.

40. Xu X, Yu H, Gao S, Mao H-Q, Leong KW, Wang S. Polyphosphoester microspheres for sustained release of biologically active nerve growth factor. Biomaterials 2002;23(17):3765-3772.

41. Alexis F. Factors affecting the degradation and drug-release mechanism of poly(lactic acid) and poly[(lactic acid)-co-(glycolic acid)]. Polym Int 2005;54:36-46.

42. Song MJ, Uhrich KE. Optimal micropattern dimensions enhance neurite outgrowth rates, lengths, and orientations. Annals of Biomedical Engineering 2007;35(10):1812-1820.

43. Wong DY, Hollister SJ, Krebsbach PH, Nosrat C. Poly(ε-caprolactone) and poly(L-lactic-co-glycolic acid) degradable polymer sponges attentuate astrocyte response and lesion growth in acute traumatic brain injury. Tissue Eng 2007;13(10):2515-2523.

CHAPTER 6: THERMAL AND MECHANICAL PROPERTIES OF POLYANHYDRIDE BLENDS FOR NERVE GUIDANCE TUBES

6.1. Abstract

Blends of two polyanhydrides, poly(lactic acid anhydride) (PLAA) and poly(*o*-carboxyphenoxyxylene) (poly(*o*-CPX)), were fabricated into hollow nerve guidance tubes then characterized for changes in thermal and mechanical properties. The thermal properties of the raw polymers and the tubes were characterized, which included glass transition temperature (T_g) and decomposition temperature (T_d) measurements by differential scanning calorimetry (DSC) and thermogravimetric analysis (TGA), respectively. The polymer blend tubes were degraded, *in vitro*, for 4 weeks. During the degradation study, the mechanical strength of the tubes was characterized with compliance measurements in 3-point bending mode and water uptake monitored to determine the permeability and swelling. Future studies will assess the biological activity for nerve regeneration.

6.2. Introduction

Nerve guidance conduits containing new materials, such as biodegradable and natural polymers, are being studied by many researchers for nerve regeneration applications.[1-3] Naturally-derived materials have been approved for use, including Salumedica's Salubridge (Atlanta, GA)[4] and Integra's NeuraGen™ and NeuraWrap™

(Plainsboro, NJ).[5] Additionally, research efforts are focusing on synthetic materials such as poly(lactic acid), poly(glycolic acid), and copolymers of the two,[6-9] while other systems use poly(methyl methacrylate) copolymers[10] and poly(glycerol sebacate).[11] With these systems showing positive results, the next studies focus on blending polymers to achieve specific physical, thermal, and mechanical properties.

Polymer blending may be an important feature of new nerve guidance conduits to achieve the desired physical, thermal, and mechanical properties. Researchers have examined phase separation and drug distribution in polyanhydrides.[12-14] Physical properties, including mass loss and water uptake, have been correlated to mechanical properties.[15] Specifically, for nerve guide tubes, poly(glycolic acid) has been coated with collagen and then crosslinked,[16] but there was no physical blending of materials for the conduits. Polymer miscibility is important as nerve guidance conduits are developed with polymer blends for improved properties.

This chapter focuses on the development and characterization of a polymer blend with potential to guide nerve regeneration. The thermal and mechanical properties of the polymer blends were assessed prior to and during *in vitro* degradation. In the future, the nerve guidance conduits described here may be filled with the nerve growth factor (NGF)-loaded salicylic acid-based poly(anhydride-esters) (SA-based PAEs) microspheres described in Chapter 5 of this dissertation. This novel polymer blend tube, filled with NGF-loaded microspheres, has great promise to advance the field of nerve regeneration.

6.3. Materials and Methods

6.3.1. Materials

Poly(lactic acid anhydride) (PLAA) was provided by Bioabsorbable Therapeutics Inc. (BTI) (Menlo Park, CA) and is a propriety polymer. The iodinated salicylic acid-based polymer (iodo-SA PAE) and poly(*o*-carboxyphenoxyxylene) (poly(*o*-cpx) were prepared by previously described methods.[17,18] Hollow polymer tubes were manufactured at BTI using a melt extrusion process. Dulbecco's Phosphate buffered saline without Mg^{2+} and Ca^{2+} was purchased from MP Biomedicals (Solon, OH). All other reagents and supplies were purchased from Fisher Scientific (Fairlawn, NJ).

6.3.2. Scanning Electron Microscopy (SEM)

The polymer tube surface morphology was visualized using scanning electron microscopy (SEM; AMRAY 1830 I, Bedford, MA). The tubes were affixed to specimen mounts (Electron Microscopy Sciences, Fort Washington, PA) using non-conducting adhesive tabs (Electron Microscopy Sciences). Cross-section and surfaces of samples were gold-coated using a Sputter Coater (BALZER SCD 004; Baltec, Tuscon, AZ) and examined at an electron voltage of 20 kV. The images were captured with FlashBus FBG 4.2 software on Windows 2000.

6.3.3. Differential Scanning Calorimetry (DSC)

Samples of the unprocessed polymer, polymer tubes, and polymer-blended tubes were examined using DSC. The glass transition temperature (T_g) of each sample was

measured on a TA Instruments Q200 DSC (New Castle, DE). The polymer samples (5 mg) were heated under dry nitrogen gas with heating and cooling rates of 10 °C/min. Glass transition temperatures were calculated as the inflection point in the step change on the second heating cycle of a heat-cool-heat experiment.

6.3.4. Thermal Gravimetric Analysis (TGA)

TGA was performed using a Perkin Elmer TGA 7 analyzer with a TAC 7/DX instrument controller. Polymer samples (10 mg) were heated under dry nitrogen gas at a heating rate of 10 °C/min. Decomposition temperatures were defined as the onset of decomposition. Perkin-Elmer Pyris software was used for data collection on a Dell OptiPlex GX110 computer.

6.3.5. *In Vitro* Degradation

The polymer tubes were cut in half using a warm Accu-Knife™ (Control Co., Houston, TX). Each tube was 10 mm long and mass of approximately 40 mg. The tubes were degraded in 20 mL scintillation vials containing 10 mL Dulbecco's PBS without Ca^{2+} and Mg^{2+} for four weeks. The degradation study was conducted at 37 °C and 70 rpm in a New Brunswick Scientific Series 25 Controlled Environment Incubator Shaker (Edison, NJ). At weekly intervals, the PBS was exchanged to maintain sink conditions, and the polymer tubes were analyzed for water uptake and changes in mechanical properties.

6.3.6. Water Uptake

Water uptake was determined by obtaining the mass of each sample using an analytical balance (Mettler Toledo Columbus, OH). At predetermined time points during the degradation study, the samples were removed from the degradation media, rinsed in deionized water to remove residual phosphate salts, and patted with Kimwipes® (Kimberly-Clark, Neenah, WI). The water uptake was calculated using Equation (1):

$$WA(\%) = \frac{W_h - W_o}{W_o} \text{ X } 100 \qquad (1)$$

where *WA* is water absorbed by the sample or water uptake, W_h is the mass of the hydrated sample, and W_o is the mass of the sample prior to degradation. Five samples were measured and averaged for each time point (n = 5). Statistical error was shown by error bars denoting the standard deviation of the five measurements.

6.3.7. Dynamic Mechanical Analysis (DMA) by Three-Point Bending

Three-point bending testing was conducted on the 10 mm polymer tubes at each weekly time point (0, 1, 2, 3, and 4 weeks). The 5 mm bending platform with a 3 mm knife probe was calibrated prior to analysis. The testing method was a static force scan from 0 mN to 8000 mN at 400 mN/minute at 22 °C. The compliance was calculated as the initial slope of the static force, measured in milliNewtons (mN) versus the probe position movement in millimeters. The data was reported as the average compliance of five samples with error bars showing the standard deviation of the five measurements.

6.4. Results and Discussion

6.4.1. Hollow Polymer Tubes of PLAA, Poly(*o*-cpx), and Iodo-SA PAE

The polymer tubes were melt-extruded with dimensions of approximately 20 mm long, 0.22 mm thickness, and 3.5 mm inner diameter. Representative SEM images are shown in **Figure 6.1**.

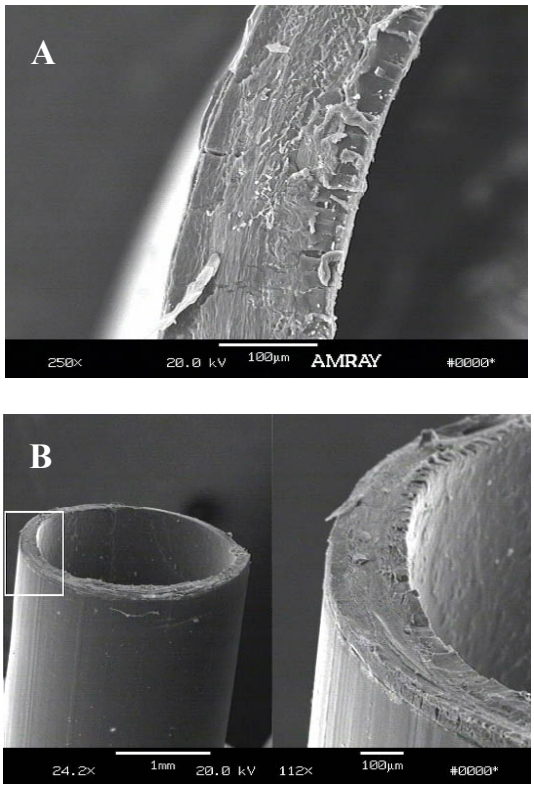

Figure 6.1. Representative SEM images of PLAA tubes. (A) cross section. (B) surface.

6.4.2. Thermal Characterization of Polymer Tube Blends

The thermal properties of the polymer tubes were characterized by DSC and TGA to determine whether the polymer blends in the tubes were miscible, and whether the melt extrusion processing damaged the polymer structure. A representative DSC thermogram is shown in **Figure 6.2**. The thermal properties are displayed in **Table 6.1**. The table compares the T_g and T_d values of the raw polymers, PLAA and poly(o-cpx), as well as blends of the two polymers in the form of hollow tubes. The blends of PLAA and poly(o-cpx) are labelled 15:85, 30:70, and 50:50 poly(o-cpx):PLAA. Two different T_gs are noted for the blends, but the decreased value shows that the polymers are interacting and partially miscible. The poly(o-cpx) may be acting as a plasticizer to effectively lower the T_gs of both polymers in the blends. Although a general lowering of

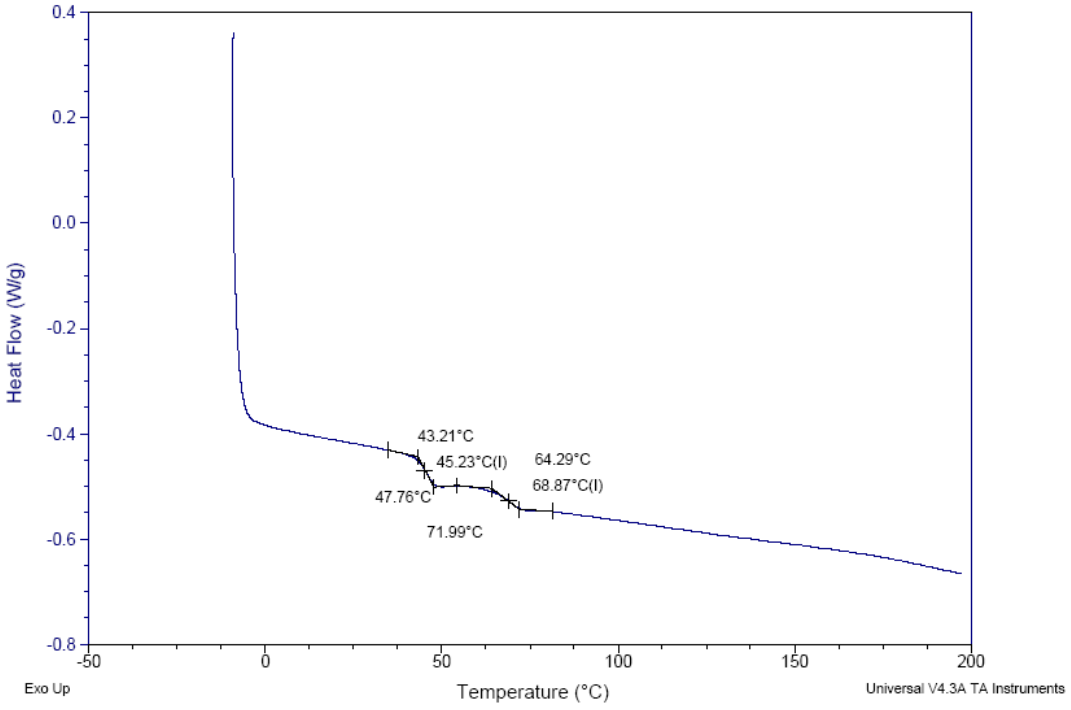

Figure 6.2. Representative DSC thermogram of 50:50 Poly(*o*-cpx):PLAA tube.

the polymer T_gs was noted, no trend was observed as the amount of poly(o-cpx) increased.

Table 6.1. Thermal analyses (DSC and TGA) of raw polymer and polymer tubes to monitor changes in Tg and Td as a result of processing. (* Thermal transition not observed)

Sample Composition	Sample Type	$T_{g\,1}$ (°C)	$T_{g\,2}$ (°C)	T_d (°C)
PLAA (BTI)	Raw Polymer	49.8	*	322
PLAA	Tube	50.5	*	322
Poly(*o*-cpx)	Raw Polymer	82.2	*	320
15:85 Poly(*o*-cpx):PLAA	Tube	47.2	66.3	312
30:70 Poly(*o*-cpx):PLAA	Tube	43.5	57.4	311
50:50 Poly(*o*-cpx):PLAA	Tube	45.2	68.8	314

Increasing the amount of poly(o-cpx) had no significant effect on the T_d of the blends, and polymer decomposition was not observed as a result of the melt extrusion processing technique.

6.4.3. Water Uptake of Polymer Tubes

The water uptake of the polymer tubes was monitored during the four week *in vitro* degradation study. Water uptake provides important information about water permeability and polymer degradation as a function of tube geometry. The water uptake

analysis is shown in **Figure 6.3**. Multiple facts are noted about the water uptake of the polymer tubes. Initially, the tubes containing 50:50 poly(o-cpx):PLAA had very little

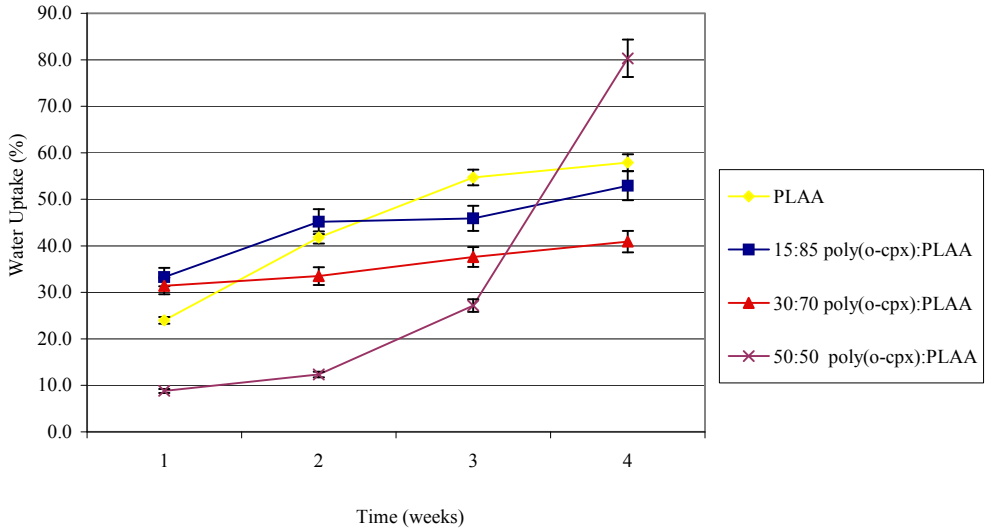

Figure 6.3. Water uptake of polymer blend tubes over 4 weeks.

water uptake. Generally, for the first three weeks of the study, as the amount of poly(o-cpx) increases, the water uptake decreases. These initial results are promising because significant tube swelling would have a negative effect on nerve regeneration, as the area where a tube would be placed may not be able to accomodate any tube swelling.

However, at week four, the 50:50 poly(o-cpx):PLAA tubes absorbed 80 % of their weight in water. It appears that at this point, the poly(o-cpx) begins to allow more water into its matrix as it begins to degrade quicker.

6.4.4. Mechanical Characterization of Polymer Tube Blends During *In Vitro* Degradation

The mechanical testing was conducted on the polymer tubes throughout *in vitro* degradation to determine their level of flexibility or compliance as applicable to nerve regeneration. The tube cannot be extremely stiff because this may cause brittleness as well as particulate generation at the injury site. Three-point bending analysis was performed to identify the most compliant tube composition. Digital images of the three-point bending setup during testing are shown in **Figure 6.4**. The image on the left of **Figure 6.4** shows the sample prior to testing, and the image on the right shows the sample during testing.

A representative plot of the three-point bending data to measure compliance is shown in **Figure 6.5**. The probe position is plotted versus the static stress values, and the inverse of the initial slope gives the compliance of the tubes. The data shown in

Figure 6.4. Representative images of 3-point bending testing performed on polymer tubes to measure compliance.

Figure 6.6 is a representative stress versus strain curve. The modulus of the tubes is calculated as the initial slope of the stress versus strain curve. The sample shown in **Figure 6.6** has high stress values and low strain which is indicative of a hard, brittle

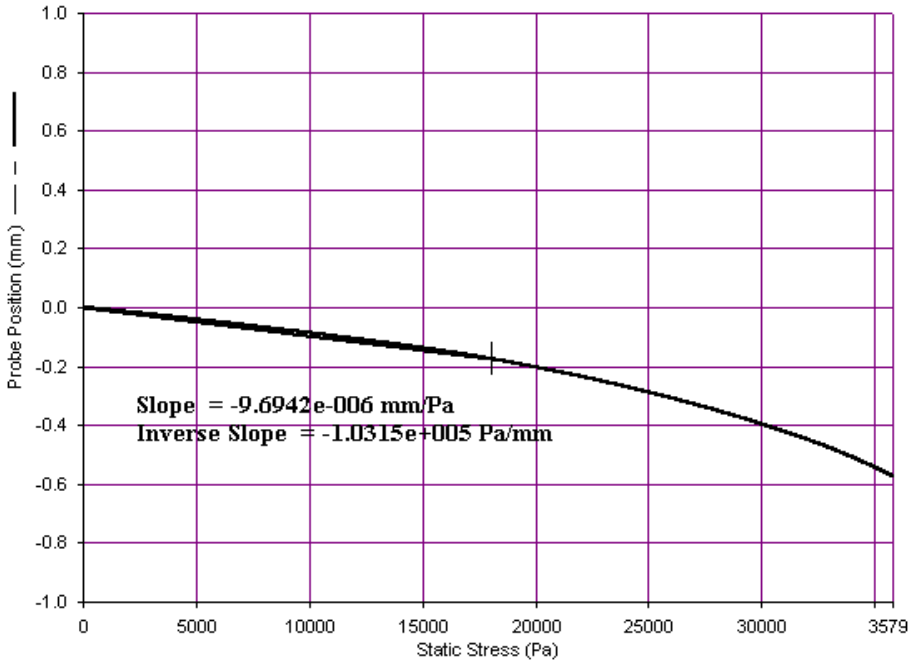

Figure 6.5. Representative plot of compliance testing data.

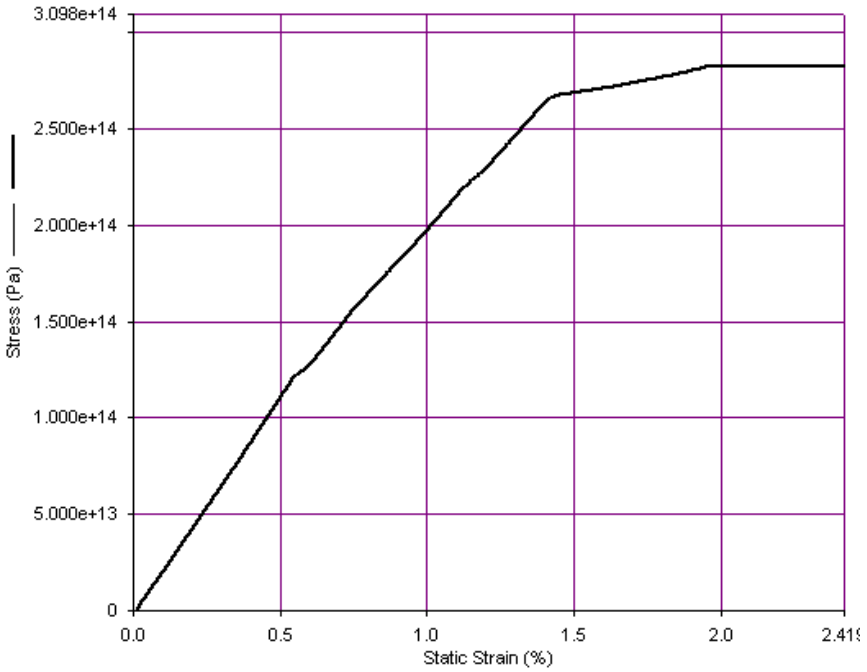

Figure 6.6. Representative stress vs. strain curve of a polymer tube tested using the 3-point bending geometry.

material with low toughness.[18] The compliance value was the focus of the mechanical testing in this chapter because it provides valuble insight into the flexibility of the tubes when they are placed at the injury site.

Initially, the compliance of an iodo-SA PAE tube was compared to that of a poly(o-cpx) tube to determine which material was most flexible. The iodo-SA PAE would be advantageous because it can be seen under x-ray once it is implanted in the body, while the poly(o-cpx) is know to have enhanced thermal and mechanical properties.[17] Therefore, the poly(o-cpx) may be useful by imparting strength and flexibility to the tubes. The results from those intial polymer tube testing studies are shown in **Figure 6.7**. Although the iodo-SA PAE has the advantage of radiopacity,[18]

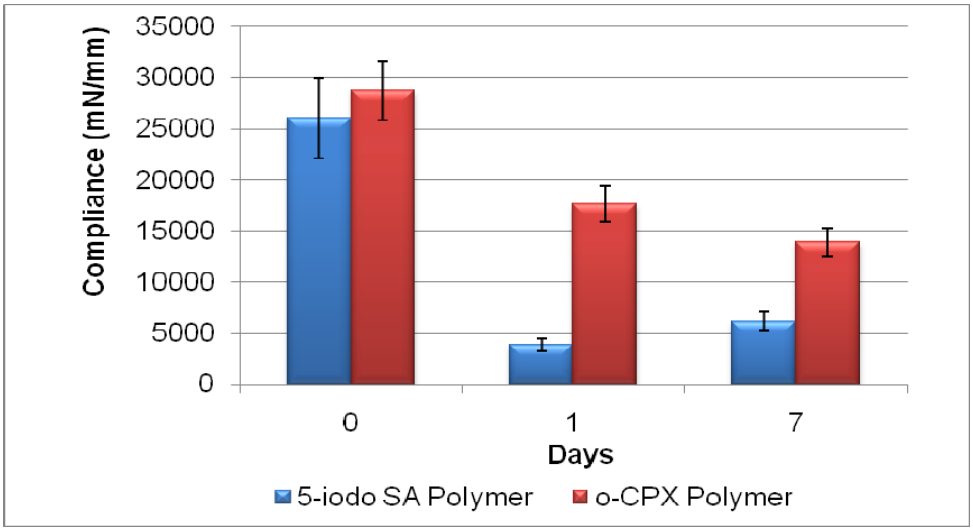

Figure 6.7. Compliance results for the 5-iodo SA polymer and the o-CPX polymer in 3-point bending testing mode.

it does not have the same compliance as poly(o-cpx). Prior to degradation, the two polymers appear to have the same compliance, but after one day and after 7 days in

aqueous media, a marked decrease in the iodo-SA PAE compliance was observed. Based on these results, the poly(o-cpx) tubes were the focus of the remaining mechanical testing studies.

The poly(o-cpx) was physically mixed with the PLAA to form hollow tubes containing, 15:85, 30:70, and 50:50 poly(o-cpx):PLAA. The compliance of each polymer blend was compared to PLAA polymer tubes. The complete results for the compliance testing during *in vitro* degradation for four weeks are depicted in **Figure 6.8**.

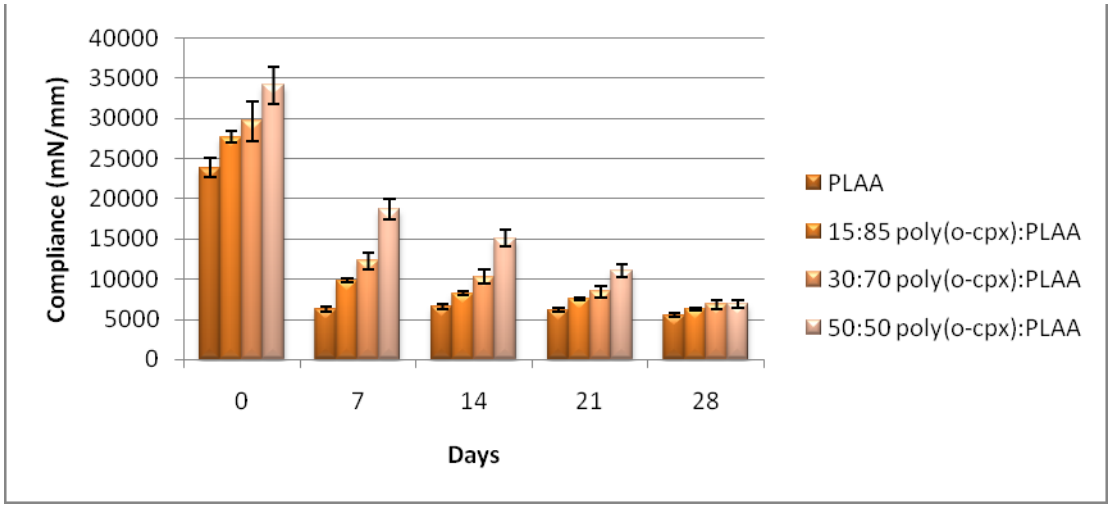

Figure 6.8. Compliance results for polymer tubes with increasing amounts of poly(*o*-cpx).

The general trend is that as the percentage of poly(o-cpx) is increased, flexibility increases. After four weeks in PBS pH 7.4, differences between the compositions are less significant, but the trend still holds that adding poly(o-cpx) imparts flexibility to the polymer tubes.

6.5. Conclusions

The hollow polymer tubes prepared by melt extrusion were characterized for the appropriate thermal, mechanical, and physical properties for nerve regeneration applications. The tubes do not undergo significant degradation during the melt extrusion process. Although the tubes that contain polymer blends are immiscible, the blends impart a plasticizer effect in which the polymers' T_gs are lowered and the tubes become more flexible. The compliance was quantified, the most flexible tubes may have the most relevance for nerve regeneration, as they can be manipulated for insertion. The hollow polymer blend tubes containing poly(o-cpx) and PLAA will be tested in future studies for neuron outgrowth. In terms of chemical and physical characterization, the tubes have the most promising properties for use as nerve guidance conduits.

6.6. Acknowledgements

The authors would like to thank Olex Hnojewyj and Tony Schaffer at Bioabsorbable Therapeutics, Inc. (Menlo Park, CA) for fabricating the hollow polymer tubes.

6.7. References

1. Ciardelli G, Chiono V. Materials for peripheral nerve regeneration. Macromol Biosci 2006;6:13-26.

2. Ma PX. Biomimetic materials for tissue engineering. Adv Drug Deliv Rev 2008;60:184-198.

3. Schmidt CE, Leach JB. Neural tissue engineering: Strategies for repair and regeneration. Annu Rev Biomed Eng 2003;5:293-347.

4. Salumedica Salubridge. www.salumedica.com/salubridgeinfodoc.htm.

5. Integra Neuragen. www.integra-ls.com/products/?product=88.

6. Goraltchouk A, Freir T, Shoichet MS. Synthesis of degradable poly(L-lactide-co-ethylene glycol) porous tubes by liquid-liquid centrifugal casting for use as nerve guidance channels. Biomaterials 2005;26:7555-7563.

7. Goraltchouk A, Scanga V, Morshead CM, Shoichet MS. Incorporation of protein-eluting microspheres into biodegradable nerve guidance channels for controlled release. J Controlled Release 2006;110:400-407.

8. Oh SH, Lee, JH. Fabrication and characterization of hydrophilized porous PLGA nerve guide conduits by a modified immersion precipitation method. J Biomed Mater Res 2007;80A(530-538).

9. Wang Y, Mano JF. Biodegradable poly(L-lactic acid)/poly(butylene succinate-*co*-adipate) blends: Miscibility, morphology, and thermal behavior. J Appl Polym Sci 2007;105:3204-3210.

10. Piotrowicz A, Shoichet MS. Nerve guidance channels as drug delivery vehicles. Biomaterials 2006;27:2018-2027.

11. Sundback CA, Shyu JY, Wang Y, Faquin WC, Langer RS, Vacanti JP, Hadlock TA. Biocompatibility analysis of poly(glycerol sebacate) as a nerve guide material. Biomaterials 2005;26:5454-5464.

12. Shen E, Pizsczek R, Dziadul B, Narashimhan B. Microphase separation in bioerodible copolymers for drug delivery. Biomaterials 2001;22:201-210.

13. Shen E, Kipper MJ, Dziadul B, Lim M-K, Narashimhan B. Mechanistic relationships between polymer microstructure and drug release kinetics in bioerodible polyanhydrides. J Controlled Release 2002;82:115-125.

14. Kipper MJ, Seifert S., Thiyagarajan P, Narasimhan B. Understanding polyanhydride blend phase behavior using scattering, microscopy, and molecular simulations. Polymer 2004;45:3329-3340.

15. Wan YZ, Wang YL, Xu XH, Li QY. *In vitro* degradation behavior of carbon fiber-reinforced PLA composites and influence of interfacial adhesion strength. J Appl Polym Sci 2001;82:150-158.

16. Tanaka S, Takigawa T, Ichihara S, Nakamura T. Mechanical properties of the bioabsorbable polyglycolic acid-collagen nerve guide tube. Polym Eng Sci 2006;46:1461-1467.

17. Anastasiou TJ, Uhrich KE. Novel polyanhydrides with enhanced thermal and solubility properties. Macromolecules 2000;33(17):6217-6221.

18. Carbone AL, Song, M, Uhrich KE. Melt condensation and solution polymerization of iodinated salicylate-based poly(anhydride-esters) as radiopaque biomaterials. Biomaterials 2008;in preparation.

CHAPTER 7: BASE HYDROLYSIS OF POLY(ANHYDRIDE-ESTERS) AND POLY(ANHYDRIDE-AMIDES)

7.1. Abstract

Salicylic acid-based poly(anhydride-esters) (SA-based PAEs) and ampicillin-based poly(anhydride-amides) (PAAs) were hydrolyzed in basic media (pH 10) to accelerate the degradation process. The salicylic acid release rates from the SA-based PAEs prepared by both melt-condensation and solution polymerization methods were compared. The ampicillin-based PAAs, prepared by solution polymerization, were also degraded; the release of ampicillin and its degradation products were monitored. The studies with the SA-based PAE proved that the salicylic acid release profiles are the same for both polymerization methods. The SA-based PAEs fully degraded into salicylic acid with no residual oligomers or unanticipated side products. The base hydrolysis of the ampicillin-based PAA showed that the β-lactam may hydrolyze prior to the amide hydrolysis in the diacid. For the ampicillin-based PAA, the major degradation products were the ampicillin diacid, instead of the free ampicillin. Overall, base hydrolysis of these polyanhydrides yielded valuable information as to whether the active compounds' structures change during polymer degradation and whether polymerization methods impact degradation rates and drug release rates.

7.2. Introduction

Polyanhydrides can be prepared by a number of different polymerization methods, including interfacial, melt-condensation, ring-opening, and solution.[1-7] Each of these polymerization methods may yield slightly different polymer properties. For example, melt-condensation polymerization usually yields higher molecular weight polyanhydrides than the solution polymerization method. However, heat-sensitive monomers may not be amenable to melt-condensation polymerization because the polymerization occurs at temperatures ranging from 160 °C to 180 °C. Although it may not be useful for all monomers, the melt-condensation method can be produced at a reproducible rate and on a larger scale. In contrast, solution polymerization requires exact stoichiometry and often yields lower molecular weight polymers, particularly when prepared on a small scale because any deviation from the required stoichiometry can lower the final molecular weight.

The Uhrich laboratory has developed and studied the synthesis and characterization of salicylic acid-based poly(anhydride-esters) (SA-base PAEs) for over a decade. The SA-based PAEs hydrolytically degrade to release salicylic acid, so it is important to compare the degradation and drug release profiles of polymers prepared by different polymerization methods. For thermally sensitive molecules, such as ampicillin, it is critically important to monitor changes in the drug structure and activity as a function of polymer synthesis, processing, and *in vitro* degradation.

Polyanhydrides are known to degrade faster under basic conditions,[8-11] the base-catalyzed hydrolysis breaks the anhydride bonds between the polymer repeat units. Other

researchers have monitored polymer degradation under basic conditions to accelerate degradation, and to develop mechanisms of base hydrolysis.[12-14] Additionally, researchers have studied the hydrolytic degradation of drug molecules such as ampicillin that degrade to yield the active, hydrolyzed form of the drug.[15-17] The SA-based PAEs and the ampicillin-based PAA were characterized in basic media to quickly and efficiently determine the final degradation products.

The objective of this chapter was to elucidate how polymer may be influenced by the polymerization method. Two polymerization methods, melt-condensation and solution are compared then degraded *in vitro* and compared again for degradation changes/differences. The ampicillin-based PAA was degraded *in vitro* as well to monitor ampicillin's sensitivity to heat resulting in changes in the chemical structure. Using base hydrolysis as a method to quickly analyze polymer degradation may be important as a potential screening mechanism regardless of the polymer structure.

7.3. Materials and Methods

7.3.1. Materials

The polymers, SA-based sebacic PAEs (**1** and **2** prepared by melt-condensation and solution polymerization, respectively) and ampicillin-based PAA (**3** prepared by solution polymerization), were prepared by previously described methods.[18-21] Sodium hydroxide (NaOH), hydrochloric acid (HCl), and all other reagents were purchased from Fisher Scientific (Fairlawn, NJ) and used as received.

7.3.2. Base-hydrolyzed Degradation

Ground polymers of **1**, **2**, and **3** (20 mg, n=3) were degraded in 10 ml aqueous NaOH solution (pH 10) over 5 days for polymers **1** and **2** and over 48 hours for polymer **3**. The media was replaced daily to maintain sink conditions. Samples were prepared in triplicate. The degradation media was stored at room temperature until HPLC analysis.

7.3.3. High-Pressure Liquid Chromatography Method

High-pressure liquid chromatography (HPLC) was performed using a Waters 2695 Separations Module with a Waters 2487 Dual Wavelength Absorbance Detector set to 210 nm. Salicylic acid was separated on a C18 column (150×4.6 mm, 5 μm, Phenomenex, Torrance, CA, USA) with a flow rate of 1 ml/min in an isocratic mobile phase of 75% 20 mM phosphate buffer solution (PBS) pH 2.5 and 25% acetonitrile. Five point calibration curves were generated for salicylic acid with concentrations ranging between 0.01 mg/ml and 0.4 mg/ml.

Ampicillin was separated on a C18 column (150×4.6 mm, 5 μm, Phenomenex, Torrance, CA, USA) with a flow rate of 1 ml/min in 20 mM monobasic potassium phosphate (KH_2PO_4) and methanol modified from a previous method.[22] A gradient method was used to separate ampicillin starting with 100 % 20 mM monobasic KH_2PO_4 for five minutes, then a 20 minute gradient to 50 % KH_2PO_4 50 % methanol for one minute, and finally a 14 minute gradient back to 100 % KH_2PO_4. Ampicillin eluted at about 17 minutes. Five point calibration curves were generated for ampicillin with concentrations ranging between 0.01 mg/ml and 0.4 mg/ml

Prior to injection, degradation study samples were neutralized to pH 7 with 1 M HCl solution, when needed, and diluted using PBS pH 7.4 to ensure measurements within the calibration curve and filtered through 0.45 μm PTFE syringe filters (Nalgene, Rochester, NY, USA). Full system automation and data analysis were completed using Empower 2 software Build 2154.

7.4. Results and Discussion

7.4.1. Comparison of SA-based PAE Degradation: Melt vs. Solution Polymerization

The release of the non-steroidal anti-inflammatory drug, salicylic acid (SA), from the polymer backbone was monitored during polymer degradation. SA release is directly dependent on the hydrolytic cleavage of the anhydride and ester bonds within the polymer backbone (see **Scheme 1.1** in Chapter 1). Given that the polymerization method appears to change the type and ratio of anhydride and ester bonds[21], we compared the hydrolytic degradation behavior of the melt-made (**1**) and solution-made (**2**) poly(anhydride-esters).

Poly(anhydride-esters) prepared by melt (**1**) and solution (**2**) methods were completely degraded in an alkaline solution. Degradation was monitored by HPLC; SA was the only aromatic product observed for polymers **1** and **2** by reverse phase chromatography, with a retention time of approx. 8 min. **Figure 7.1** shows representative HPLC chromatograms of the degradation media from each polymerization method. The chromatograms are overlaid to demonstrate that both polymerization methods yield

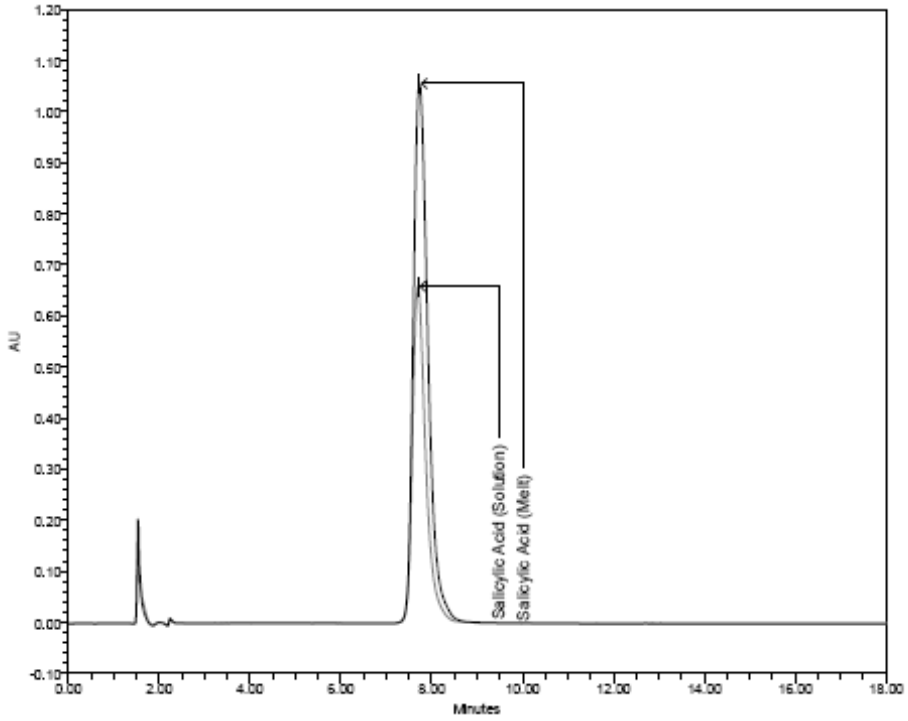

Figure 7.1. Representative HPLC separation of salicylic acid for both the melt-condensation and solution polymerization methods.

the same degradation product, SA. No additional aromatic degradation products were observed, demonstrating that regardless of the preparation method, both the melt-condensation (**1**) and solution (**2**) polymers degraded into SA. Note that sebacic acid is the other final degradation product, but is not a strong chromaphore and thus not observed.

Cumulative release curves of SA show similar profiles for PAEs prepared from either polymerization method (**Figure 7.2**). These results again demonstrate that polymer degradation is not affected by polymerization method.

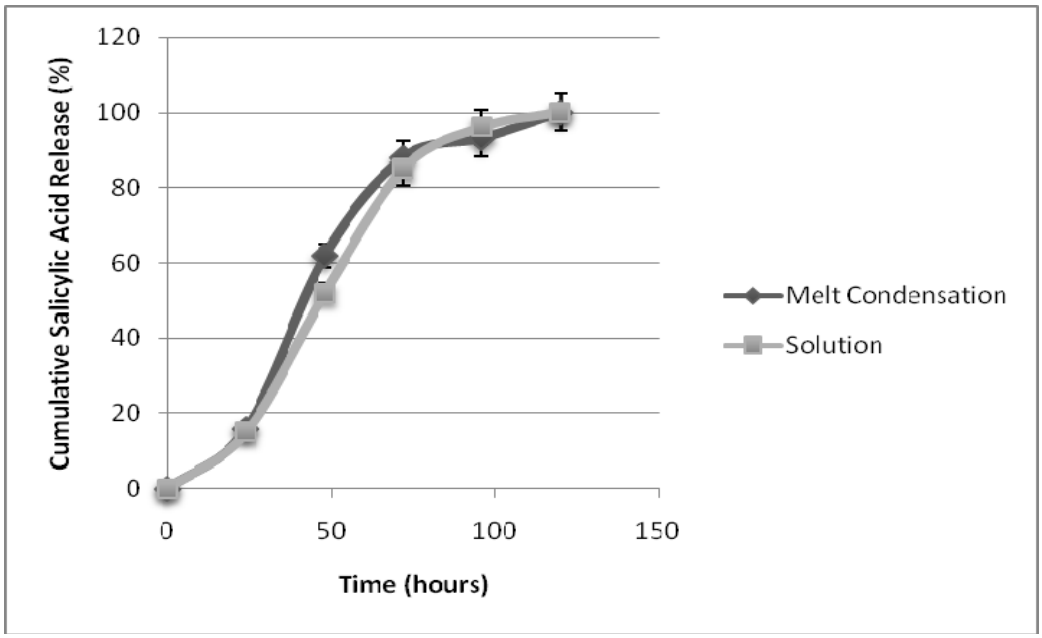

Figure 7.2. Cumulative profiles of salicylic acid released from melt-condensation (**1**) and solution (**2**) polymers upon base hydrolysis.

7.4.2. Ampicillin-based PAAs: Degradation

The ampicillin-based PAA is not amenable to complete degradation at physiological pH 7.4 because the amide bonds require more aggressive conditions, such as enzymes or extreme pH.[20,23] Previously, the polymer was found to release only ampicillin-based diacid.[20,24] Therefore, base hydrolysis was performed to fully degrade the polymer to free ampicillin. The cumulative ampicillin release over 48 hours is shown in **Figure 7.3**. Only about 20 % of the free ampicillin in the polymer was detected by this method. As a result, the chemistry of ampicillin degradation was examined in more detail.

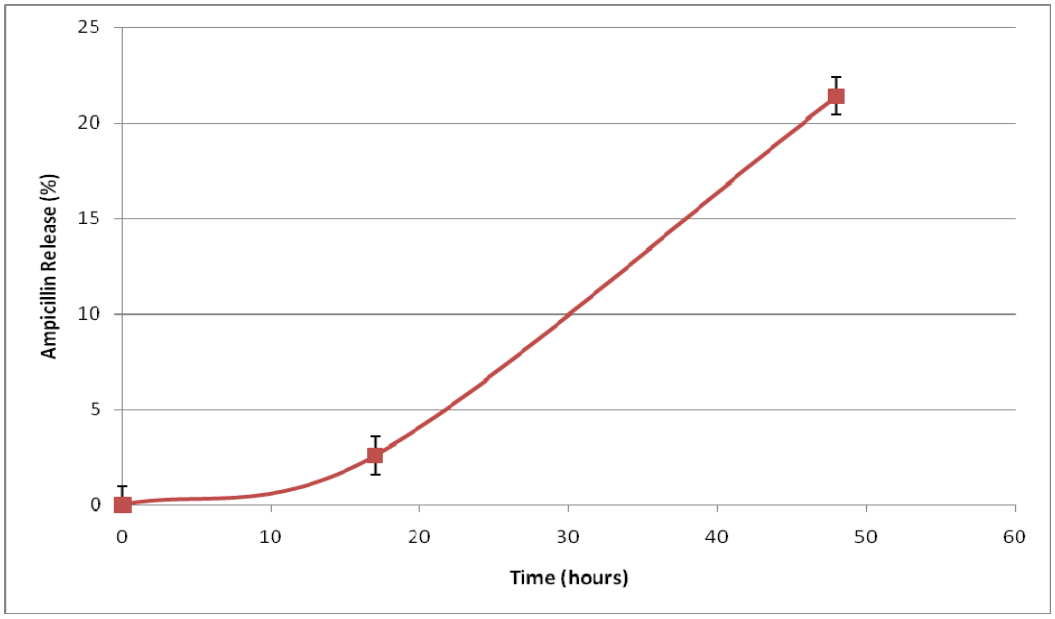

Figure 7.3. Cumulative free ampicillin release during base hydrolysis for 48 hours.

Based on the HPLC studies, the ampicillin is not stable in aqueous media and could not be detected before it degraded in solution. The β-lactam is known to hydrolyze to the active form of ampicillin, aminobenzyl-penicilloic acid (**Figure 7.4**).[25] During our experiments, a color change in the degradation media was noted from orange to yellow was noted, which may be an indication of the ampicillin degradation. Although the free ampicillin is not stable in aqueous media, this instability does not affect ampicillin's activity.[24] Additionally, the ampicillin-based diacid has shown activity against *Staphylococcus aureus*.[24]

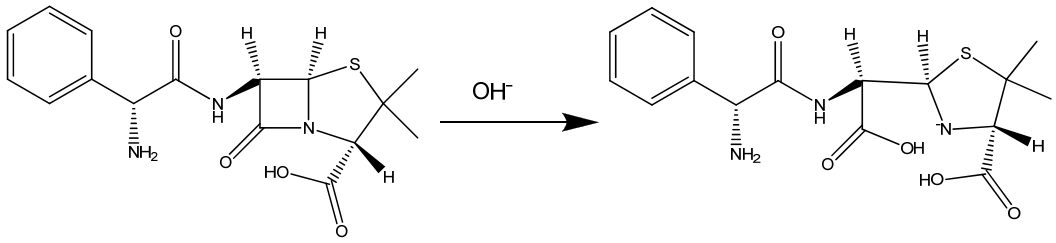

Figure 7.4. Synthetic scheme showing the decomposition of ampicillin in the presence of a strong base.

7.5. Conclusions

Regardless of the polymerization method, both the melt-made (**1**) and solution-made (**2**) SA-based PAEs completely hydrolyzed into SA under basic conditions. However, the ampicillin-based PAAs mostly degraded into the ampicillin-based diacid. Additionally, free ampicillin readily hydrolyzed further at the β-lactam to yield its own degradation product.

Although different mechanisms govern the synthesis of SA-based PAEs , HPLC results of the degradation media clearly indicate that the final degradation products are the same - salicylic acid. Furthermore, the SA-based PAEs degrade and release comparable amounts of salicylic acid, regardless of polymerization method.

7.6. References

1. Conix A. Aromatic polyanhydrides, a new class of high-melting, fiber-forming polymers. J Polym Sci 1958;29:343-353.

2. Leong KW, Simonte V, Langer R. Synthesis of polyanhydrides: melt-polycondensation, dehydrochlorination, and dehydrative coupling. Macromolecules 1987;20(4):705-712.

3. Domb AJ, Langer R. Polyanhydrides. I. Preparation of high molecular weight polyanhydrides. J Polym Sci, Part A: Polym Chem 1987;25:3373-3386.

4. Domb AJ, Ron E, Langer R. Poly(anhydrides). 2. One step polymerization using phosgene or diphosgene as coupling agents. Macromolecules 1988;21:1925-1929.

5. Yoda N, Miyake A. Synthesis of polyanhydrides. I. Mixed anhydrides of aromatic and aliphatic dibasic acids. Bulletin of the Chemical Society of Japan 1959;32:1120-1126.

6. Subramanyam R, Pinkus AG. Synthesis of poly(terephthalic anhydride) by hydrolysis of terephthaloyl chloride/ triethylamine intermediate adduct. Characterization of intermediate adduct. J Macromolec Sci, Chem 1985;A22(1):23-31.

7. Domb AJ, Amselem S, Shah J, Maniar M. Polyanhydrides: Synthesis and characterization. Adv in Polym Sci 1993;107:93-141.

8. Park E-S, Maniar M, Shah JC. Influence of physicochemical properties of model compounds on their release from biodegradable polyanhydride devices. J Controlled Release 1997;48(1):67-78.

9. Santos CA, Freedman BD, Leach KJ, Press DL, Scarpulla M, Mathiowitz E. Poly(fumaric-co-sebacic anhydride) A degradation study as evaluated by FTIR, DSC, GPC, and X-ray diffraction. J Controlled Release 1999;60(1):11-22.

10. Erdmann L, Uhrich KE. Synthesis and degradation characteristics of salicylic acid-derived poly(anhydride-esters). Biomaterials 2000;21(19):1941-1946.

11. Fu J, Wu C. Laser light scattering study of the degradation of poly(sebacic anhydride) nanoparticles. J Polym Sci, Part B: Polym Phys 2001;39(6):703-708.

12. Rahman M, East GC. Effect of applied stress on the alkaline hydrolysis of poly(ethylene terephthalate) at 40 °C: Relevance to medical textiles. J Appl Polym Sci 2006;102:4814-4822.

13. Shirahase T, Komatsu Y, Marubayashi H, Tominaga Y, Asai S, Sumita M. Miscibility and hydrolytic degradation in alkaline solution of poly(L-lactide) and poly(p-vinyl phenol) blends. Polym Degrad and Stabil 2007;92:1626-1631.

14. Witek E, Pazdro M, Botel E. Mechanism for base hydrolysis of poly(N-vinylformamide). J Macromol Sci: Pure & Appl Chem 2007;44(5):503-507.

15. Paternotte I, Fan HJ, Screve P, Claesen M, Tulkens PM, Sonveaux E. Syntheses and hydrolysis of basic and dibasic ampicillin esters tailored for intracellular Accumulation. Bioorganic and Medicinal Chem 2001;9:493-502.

16. Hou JP, Poole JW. Kinetics and mechanism of degradation of ampicillin in solution. J Pharm Sci 1969;58(4):447-454.

17. Rao SN, More O'Ferrall RA. A structure-reactivity relationship for base-promoted hydrolysis and methanolysis of monocyclic β-lactams. J Amer Chem Soc 1990;112(7):2729-2735.

18. Prudencio A, Schmeltzer RC, Uhrich KE. Effect of linker structure on salicylic acid-derived poly(anhydride-esters). Macromolecules 2005;38:6895-6901.

19. Schmeltzer R, Anastasiou TJ, Uhrich KE. Optimized synthesis of salicylate-based poly(anhydride-esters). Polym Bull 2003;49(6):441-448.

20. Prudencio A, Song, M, Uhrich KE. Synthesis of Novel Antimicrobial-Based Poly(anhydride-amides) and Antibacterial Assessment. Biomacromolecules 2007(under review).

21. Schmeltzer R, Johnson M, Griffin J, Uhrich KE. Comparison of salicylate-based poly(anhydride-esters) formed *via* melt-condensation *versus* solution polymerization. J Biomater Sci Polymer Edn 2008;in press.

22. Akhtar MJ, Khan S, Khan MAS. Determination of ampicillin in human plasma by high-performance liquid chromatography using ultraviolet detection. J Pharm and Biomed Analysis 1993;11(4/5):375-378.

23. Janda KD, Schloeder D, Bankovic SJ, Lerner RA. Induction of an antibody that catalyzes the hydrolysis of an amide bond. Science 1988;241(4870):1188-1191.

24. Johnson ML, Casas R, Patwardhan DV, Pollack SK. Ampicillin-based poly(anhydride-amide) coatings for medical implants. Polymer Preprints 2007;48(2):914-915.

25. Urbain JL, Wittich CM, Campion SR. *In vitro m*easurement of β-lactamase-catalyzed ampicillin hydrolysis by recombinant *Escherichia coli e*xtracts using quantitative high-performance liquid chromatography. Analytical Biochemistry 1998;260:160-165.

CHAPTER 8: ADDITIONAL STUDIES: SALICYLIC ACID ADMIXTURE AND RELEASE FROM SALICYLIC ACID-BASED POLY(ANHYDRIDE-ESTERS) AND POLYDIMETHYLSILOXANE (PDMS)

8.1. Abstract

Salicylic acid has been physically admixed into salicylic acid-based poly(anhydride-esters) (SA-based PAEs) and polydimethylsiloxane (PDMS). The samples were degraded *in vitro* to determine the effect of physically admixed salicylic acid on the polymer degradation and salicylic acid release rate. The salicylic acid (SA) and SA-based PAE- loaded PDMS was degraded over 24 hours, while the SA-loaded SA-based PAE was degraded over 72 hours. In the first part of this study, SA release was compared for SA-loaded and SA-based PAE loaded PDMS, and SA release was more controlled from the SA-based PAE. The second part compared SA-loaded and SA diacid-loaded SA-based PAE at 1, 5, and 10 wt %. The cumulative release profiles showed no significant change, but the lag phase was shortened for both the admixed SA and SA diacid.

8.2. Introduction

Drug release from polymer matrices is examined for controlled drug release systems,[1,2] where most systems release drugs based on diffusion from the polymer matrix. The diffusion-based drug delivery systems are typically composed of non-

degradable matrices.[3,4] Some degradable polymer systems release drugs based on erosion of the polymer matrix, while other systems release drugs based on a combination of diffusion and erosion mechanisms.[5]

SA-based PAEs can release physically admixed drugs based on a combination of diffusion and erosion mechanisms.[5] Additionally, as the SA-based PAEs degrade, they release salicylic acid by hydrolysis of the anhydride and ester bonds in the polymer backbone.[6]

By comparison, PDMS is a soft, permeable system that releases drugs based on the diffusion mechanism.[7,8] PDMS is non-degradable, so the matrix maintains its shape during degradation; the drug travels through the matrix and is released into the surrounding media.[9] PDMS has some water uptake, but this effect may be altered because of the influence of admixed drug.

This study has two parts: 1) examination of SA release from SA-loaded and SA-based PAE-loaded PDMS and 2) examination of SA release from SA-loaded and SA diacid-loaded SA-based PAEs. The salicylic acid release rates were compared to determine how the polymer permeability affects SA release. This study also provided insight about the affect of physically admixing additional salicylic acid into a polymer that already contains salicylic acid in its backbone SA-based PAE. In the future, additional amounts of salicylic acid may be admixed to determine whether there is any continued linearity or dose dependence on the salicylic acid release.

8.3. Materials and Methods

8.3.1. Materials

The SA diacid and SA-based PAE were prepared using previously described methods.[10,11] The polydimethylsiloxane (PDMS) was prepared from the SYLGARD® elastomer kit obtained from Dow Chemical (Midland, MI). All other chemicals were obtained from Aldrich (Milwaukee, WI) and used as received.

8.3.2. Methods

8.3.2.1. Preparation of Salicylic Acid-loaded PDMS Slabs

Two sets of drug-loaded PDMS slabs were prepared. The first set contained 10 wt% SA in the PDMS and the second set contained 10 wt% SA-based PAE in PDMS.

The silicone elastomer base (4 g) and curing agent (0.4 g) were mixed in a 50 mL beaker at a 10:1 ratio (w/w) and poured into a petri dish to set. For samples containing salicylic acid or polymer, the admixed component (0.44 g) was mixed at 10 wt% in the beaker with the elastomer base and curing agent prior to setting in the petri dish and stirred with a glass stirring rod. The PDMS samples were cured at 55 °C for 1 hour. After curing, the samples were cut into quarters and removed from the petri dish. Digital images were taken of the samples, and they were placed into individual 20 mL scintillation vials for *in vitro* degradation.

8.3.2.2. Preparation of SA-loaded and SA Diacid-loaded SA-based PAE Disks

The SA and the SA diacid were separately incorporated into the SA-based PAE at 1 %, 5 %, and 10 % (w/w). For each composition, polymer was heated in a 150 mL PTFE beaker (FisherBrand, Pittsburg, PA) with a heat gun for approximately 2 minutes or until the polymer began to flow at 65°C. Salicylic acid was added to the molten polymer and stirred for one minute with a glass stirring rod. The mixture was then cooled to room temperature and then ground for 30 seconds in a coffee grinder (Mr. Coffee, Rye, NY).

The ground salicylic acid or diacid-polymer mixture (45.0 ± 5.0 mg) was placed into an IR pellet die (International Crystal Laboratories, Garfield, NJ) and pressed at 4,000 psi at room temperature for 5 minutes in a Carver Press (Carver, Wabash, IN). The resulting disks were 6.0±0.2 mm diameter and 1.0±0.2 mm thick, as determined by vernier caliper measurements (Mitutoyo, Japan).

8.3.2.3. *In Vitro* Degradation

The PDMS samples loaded with SA and SA-based PAE were degraded in 20 mL scintillation vials containing 10 mL PBS pH 7.4. All degradation media for the PDMS samples was monitored for salicylic acid release by HPLC at 8 and 24 hours.

SA-loaded and SA diacid-loaded SA-based PAE samples were degraded in 20 mL scintillation vials containing 10 mL PBS pH 7.4. The degradation media for the SA-based PAE samples was monitored for salicylic acid release by HPLC at 4, 8, 12, 18, 24, 48, and 72 hours.

8.3.2.4. High Pressure Liquid Chromatography of Salicylic Acid

High-pressure liquid chromatography (HPLC) was performed using a Waters 2695 Separations Module with a Waters 2487 Dual Wavelength Absorbance Detector set to 210 nm. Salicylic acid was separated on a C18 column (150×4.6 mm, 5 μm, Phenomenex, Torrance, CA, USA) with a flow rate of 1 ml/min in an isocratic mobile phase of 75% 20 mM phosphate buffer solution (PBS) pH 2.5 and 25% acetonitrile. Five point calibration curves were generated for salicylic acid with concentrations ranging between 0.01 mg/ml and 0.4 mg/ml. Prior to injection, degradation study samples were filtered through 0.45 μm PTFE syringe filters (Nalgene, Rochester, NY, USA). Full system automation and data analysis were completed using Empower 2 software Build 2154.

8.4. Results and Discussion

8.4.1. Salicylic Acid and SA-based PAE Admixed into PDMS

Prior to and during degradation, digital images of the SA-based PAE and SA-loaded PDMS slabs were taken to monitor visual changes in the matrices. Representative images are shown in **Figure 8.1**. The PDMS samples containing admixed salicylic acid (top images of **Figure 8.1**.) were very sticky and tacky after the PDMS set, even before degradation. By comparison, the SA-based PAE-loaded PDMS samples were more

10 wt% SA in PDMS
0 hrs

10 wt% SA in PDMS
24 hrs

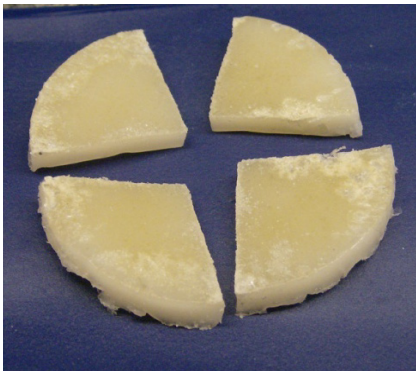

10 wt% SA-based PAE in PDMS
0 hrs

10 wt% SA-based PAE in PDMS
24 hrs

Figure 8.1. Digital images of PDMS loaded with 10 wt% SA-based PAE (top) and 10 wt% SA (bottom)

uniform and similar in structure to unloaded PDMS. Overall, few changes were visible over the 24 hour time period.

Quantitative changes were monitored by water uptake and mass loss measurements during the degradation. The SA-based PAE-loaded PDMS samples absorbed approximately 1 % of their weight in water, while the SA-loaded PDMS samples did not absorb water and lost about 2 % of their mass after 24 hours.

8.4.2. Salicylic acid Release from PDMS Matrix

Salicylic acid release from the PDMS loaded with salicylic acid and SA-based PAE is compared in **Figure 8.2**. Over the 24 hour time period, the physically admixed salicylic acid was released significantly faster than the salicylic acid from the SA-based PAE. While about 20 % of the admixed salicylic acid was released after 24 hours, only 3 % of the salicylic acid from the SA-based PAE was released in the same time period. Although the SA-based PAE releases salicylic acid in a slower, more controlled manner, the faster salicylic acid release may be useful for some applications requiring a burst release.

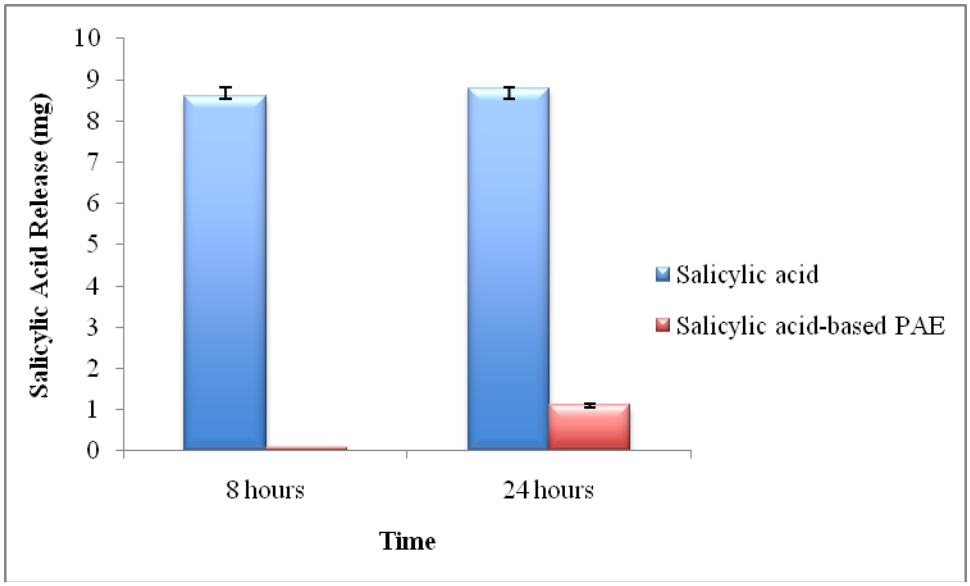

Figure 8.2. Salicylic acid release from PDMS samples loaded with SA and SA-based PAE.

8.4.3. Admixed SA and SA Diacid in SA-based PAEs on SA Release Rate

Although SA is already incorporated into the SA-based PAE backbone, admixing additional salicylic acid may increase the release rate and prevent a lag phase. **Figure 8.3**

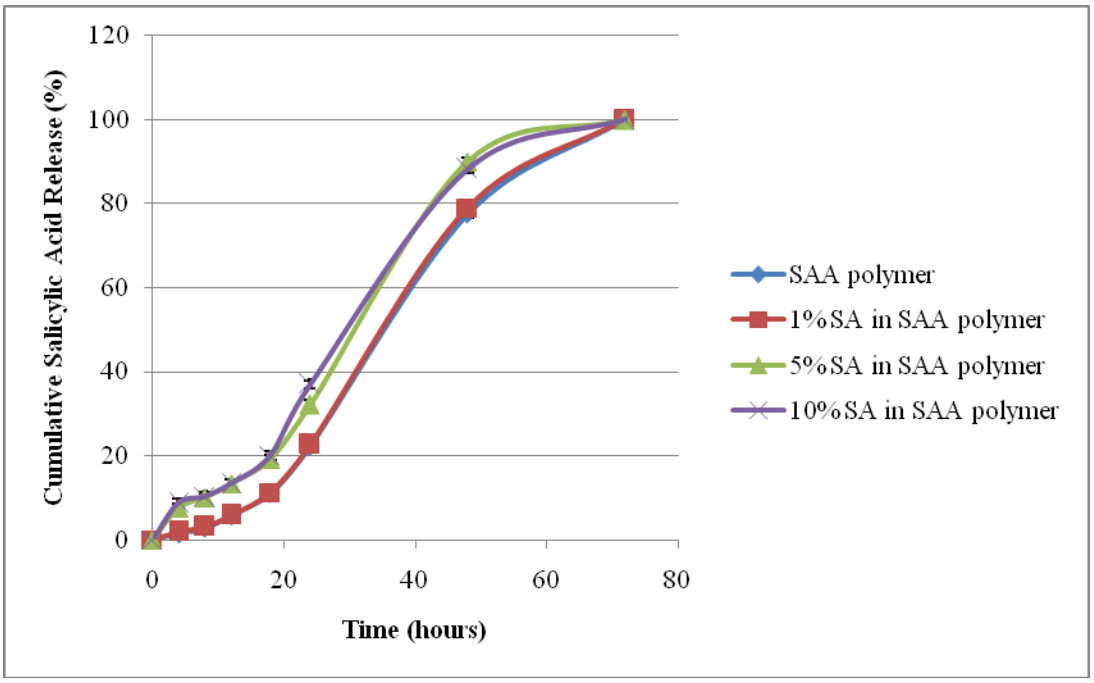

Figure 8.3. Cumulative SA release from SA-based PAE alone and admixed with additional SA over 72 hours.

depicts salicylic acid release over 72 hours when salicylic acid is admixed in the SA-based PAE. **Figure 8.4** shows salicylic acid release over 72 hours when SA diacid is admixed in the SA-based PAE. Overall, no significant difference in the release profile of salicylic acid is observed in the tested compositions.

However, when the initial 24 hours is examined, differences are readily observable; the lag phase of salicylic acid is reduced as the admixed salicylic acid or diacid content is increased. The free admixed salicylic acid was released at a slightly faster rate than the admixed diacid because the diacid requires additional time for the ester bonds to hydrolyze (see **Scheme 1.1** in Chapter 1).

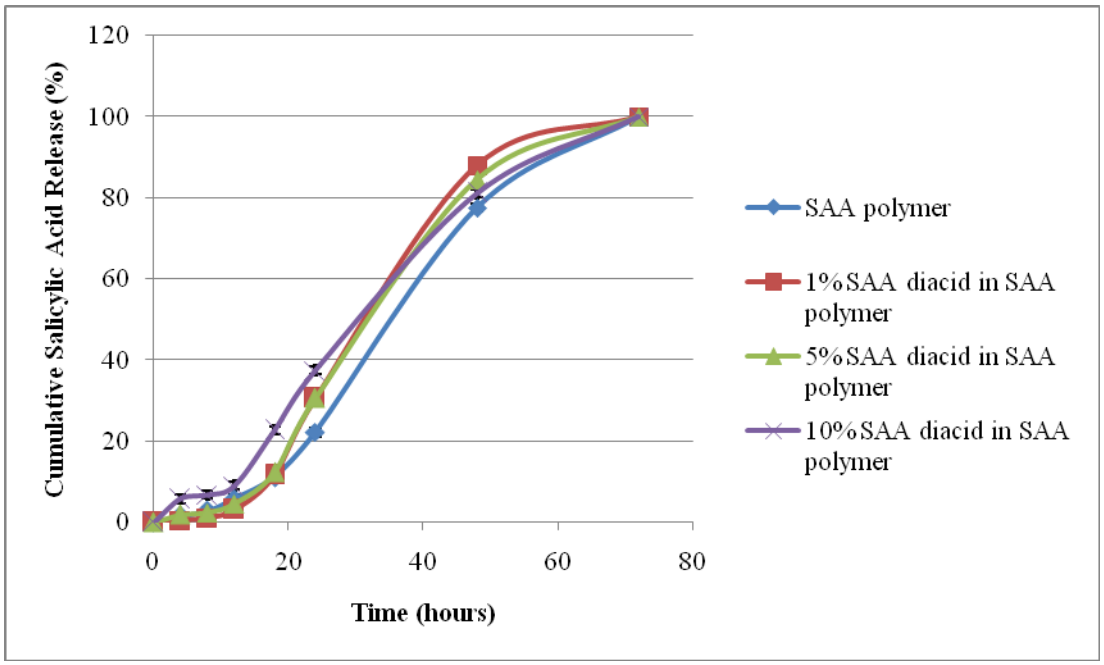

Figure 8.4. Cumulative SA release from SA-based PAE alone and admixed with various percentages (1, 5, and 10 %) SA diacid over 72 hours.

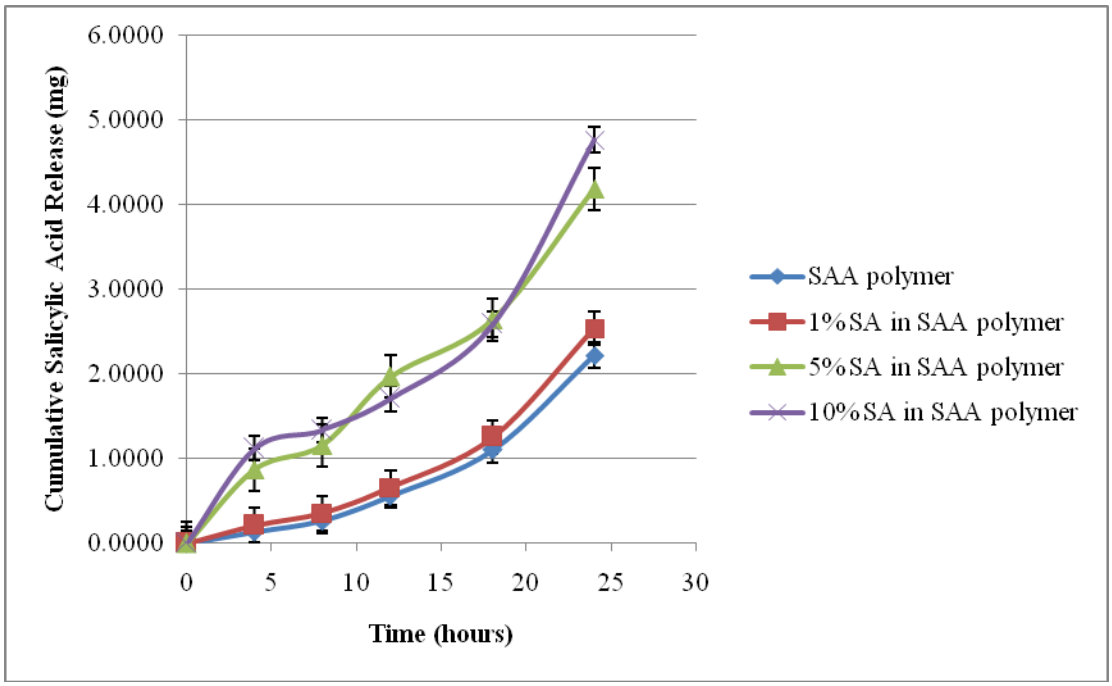

Figure 8.5. Cumulative SA release over 24 hours from SA-based PAE admixed with varying amounts of SA (1, 5, and 10 %).

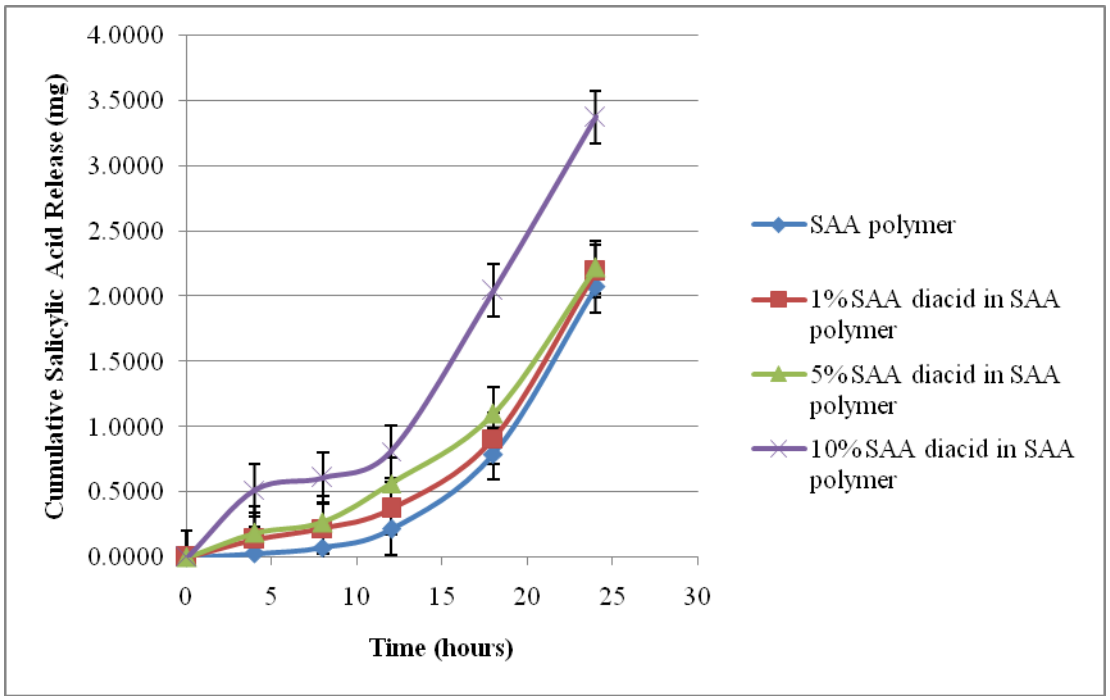

Figure 8.6. Cumulative SA release over 24 hours from SA-based PAE loaded with SA diacid (1, 5, and 10 %).

8.5. Conclusions

By chemically incorporating SA into a polymer, the resulting release of SA is prolonged relative to physically admixed SA. Generally, salicylic acid release is more controlled when it is released from the SA-based PAE within another, non-degradable delivery matrix, such as PDMS. In comparison, salicylic acid admixed in PDMS does not show the same controlled release profile, and has over 15 % of its salicylic acid released within the first 8 hours.

Additionally, when salicylic acid or salicylic acid-based adipic diacid are admixed into SA-based PAE, the overall degradation rate is unchanged, but the initial 24 hours

show a dose dependent increase in salicylic acid release. Admixing salicylic acid into the SA-based PAEs may be a way to overcome the initial lag phase in these degradable systems.

8.6. References

1. San Roman J, Gallardo A, Elvira C, Vazquez B, Abraham GA. Resorbable polymeric delivery systems based on physical absorption/diffusion versus dhemically controlled delivery systems. Biodegradable Systems in Tissue Engineering and Regenerative Medicine 2005:281-299.

2. Chopra SK. Procise:drug delivery systems based on geometric configuration. Drugs and Pharmaceutical Sciences 2003;126:35-48.

3. Ulman KL, Lee C-L. Drug permeability of modified silicone polymers. III. Hydrophilic pressure-sensitive adhesives for trandermal controlled drug release applications. J Controlled Release 1989;10(3):273-281.

4. Akdemir ZS, Kayaman-Apohan, N. Investigation of swelling, drug release, and diffusionbehaviors of poly(N-isopropylacrylamide)/pol(N-vinypyrrolidone) full-IPN hydrogels. Polym for Adv Tech 2007;18(11):932-939.

5. Johnson ML, Uhrich KE. Concurrent release of admixed antimicrobials and salicylic acid from salicylate-based poly(anhydride-esters). J Biomed Mater Res 2008;accepted.

6. Erdmann L, Uhrich K. Synthesis and degradation characteristics of salicylic acid derived poly(anhydride-esters). Biomaterials 2000;21:1941-1946.

7. Van Dyke ME, Clarson SJ, Arshady R. Silicone biomaterials. PBM Series-Introduction to Polymeric Biomaterials 2003:109-135.

8. Kokubi T, Kim H-M, Kawashita M. Novel bioactive materials with different mechanical properties. Biomaterials 2003;24(13):2161-2175.

9. Tarantino R, Adair D, Bolton S. In vitro and in vivo release of salicylic acid from povidone/polydimethylsiloxane matrices. Drug Development and Industrial Pharmacy 1990;16(7):1217-1231.

10. Schmeltzer R, Anastasiou TJ, Uhrich KE. Optimized synthesis of salicylate-based poly(anhydride-esters). Polym Bull 2003;49(6):441-448.

11. Prudencio A, Schmeltzer RC, Uhrich KE. Effect of linker structure on salicylic acid-derived poly(anhydride-esters). Macromolecules 2005;38:6895-6901.

APPENDIX 1: SYNTHETIC SCHEMES OF POLYANHYDRIDES STUDIED

A1.1. Synthesis of Salicylic acid-based Adipic Poly(anhydride-ester) by Melt-Condensation Polymerization[1,2]

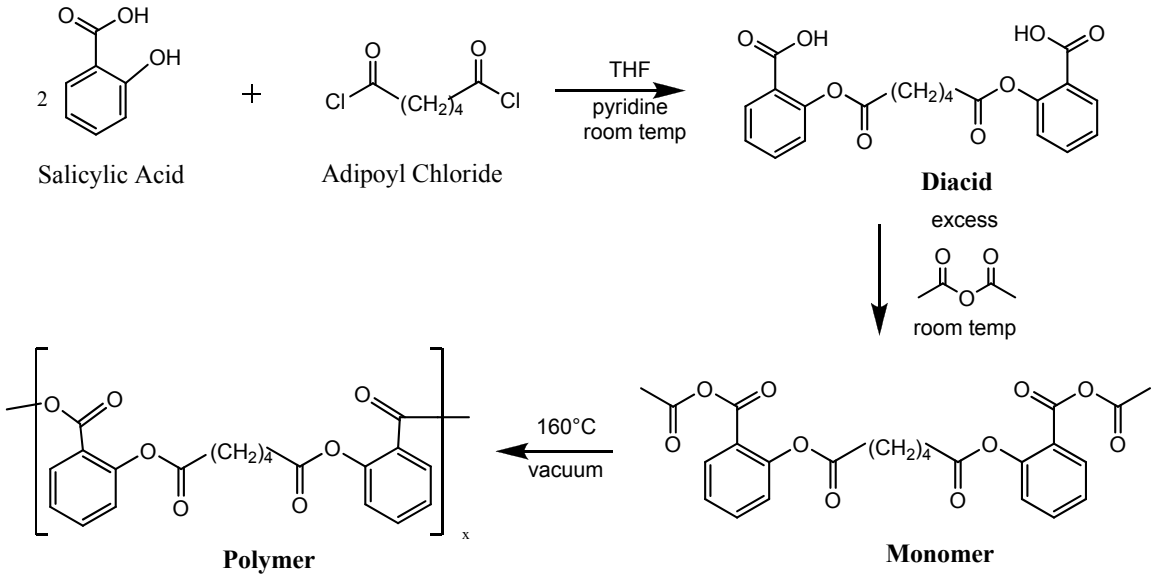

A1.2. Synthesis of Poly(*o*-carboxyphenoxy-*p*-xylene) by Melt Condensation Polymerization[3]

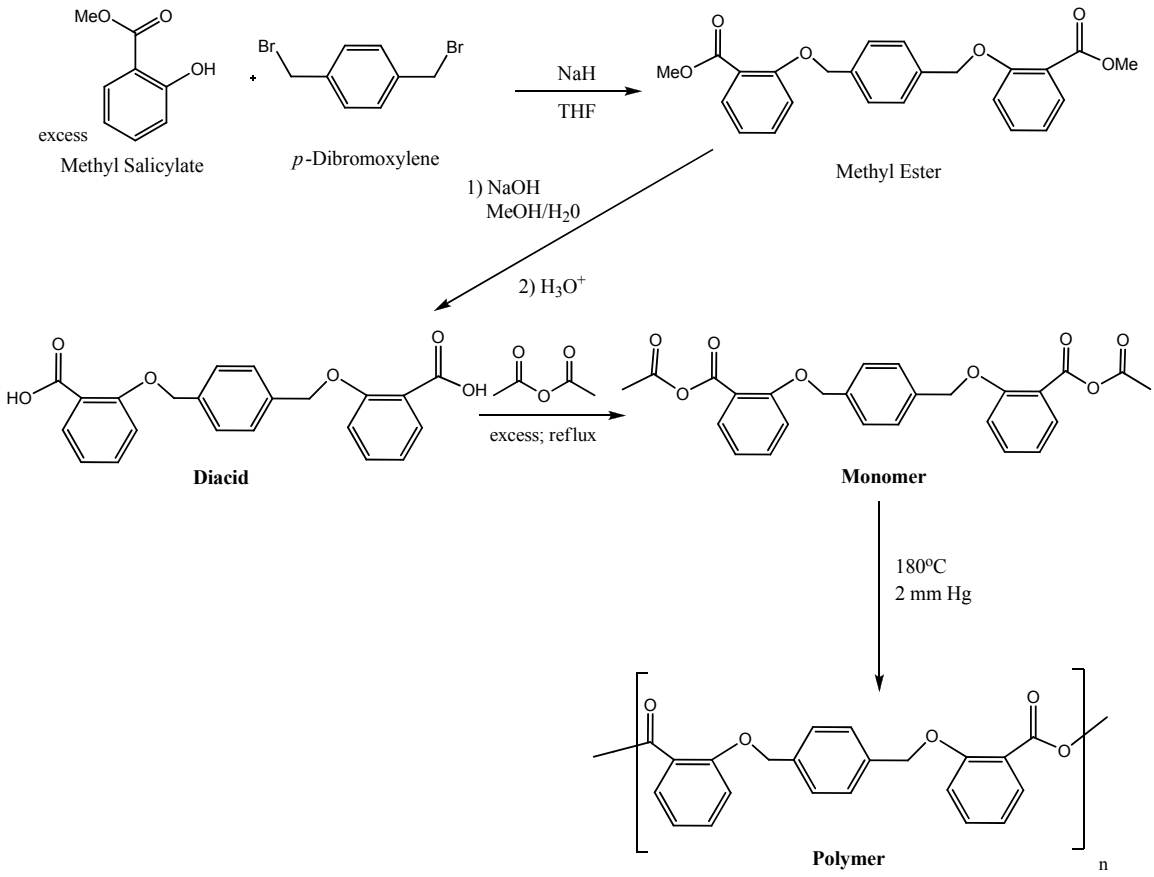

A1.3. Synthesis of Salicylic Acid-based Sebacic Poly(anhydride-ester) by Melt-condensation and Solution Polymerization Methods[1,2,4]

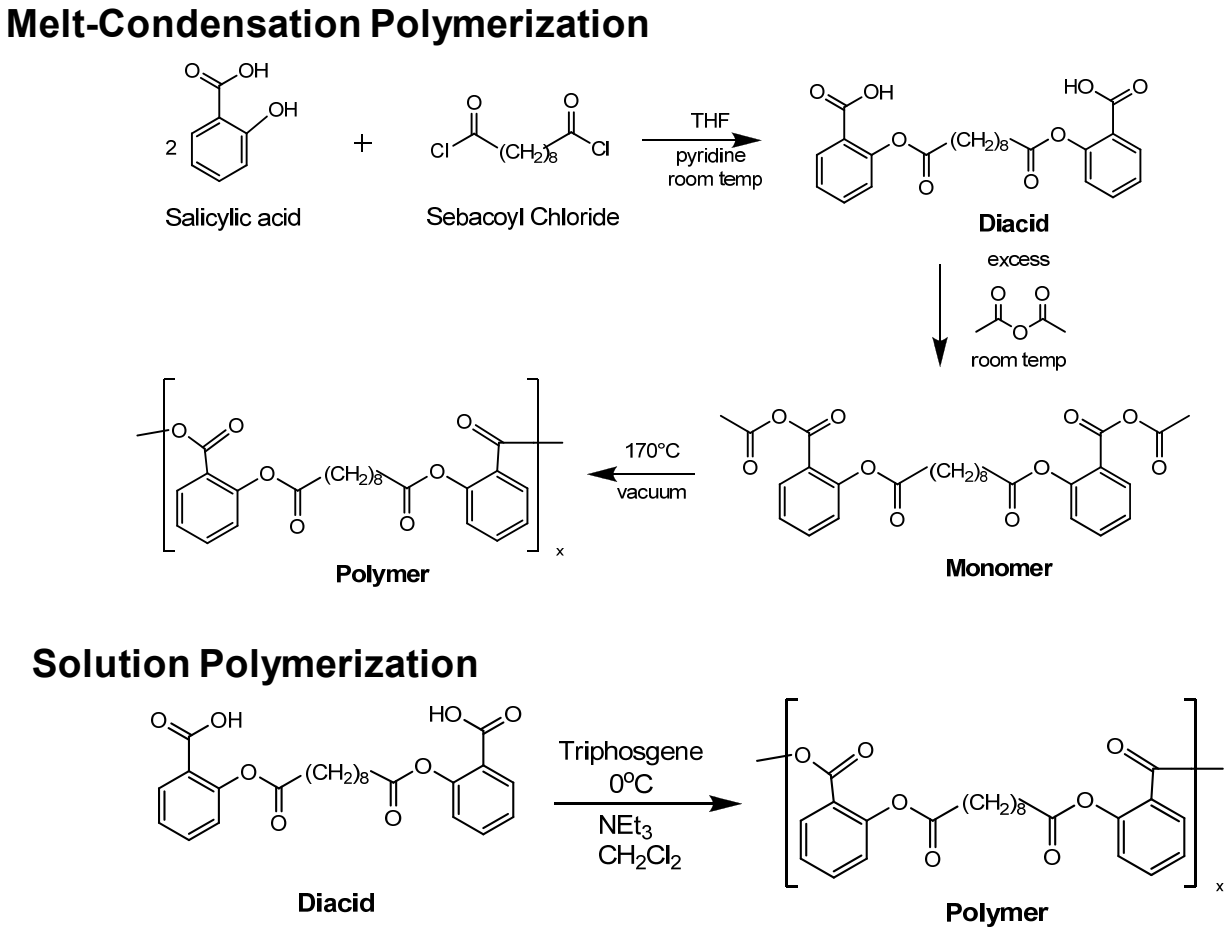

A1.4. Synthesis of Ampicillin-based Poly(anhydride-amide) by Solution Polymerization[5]

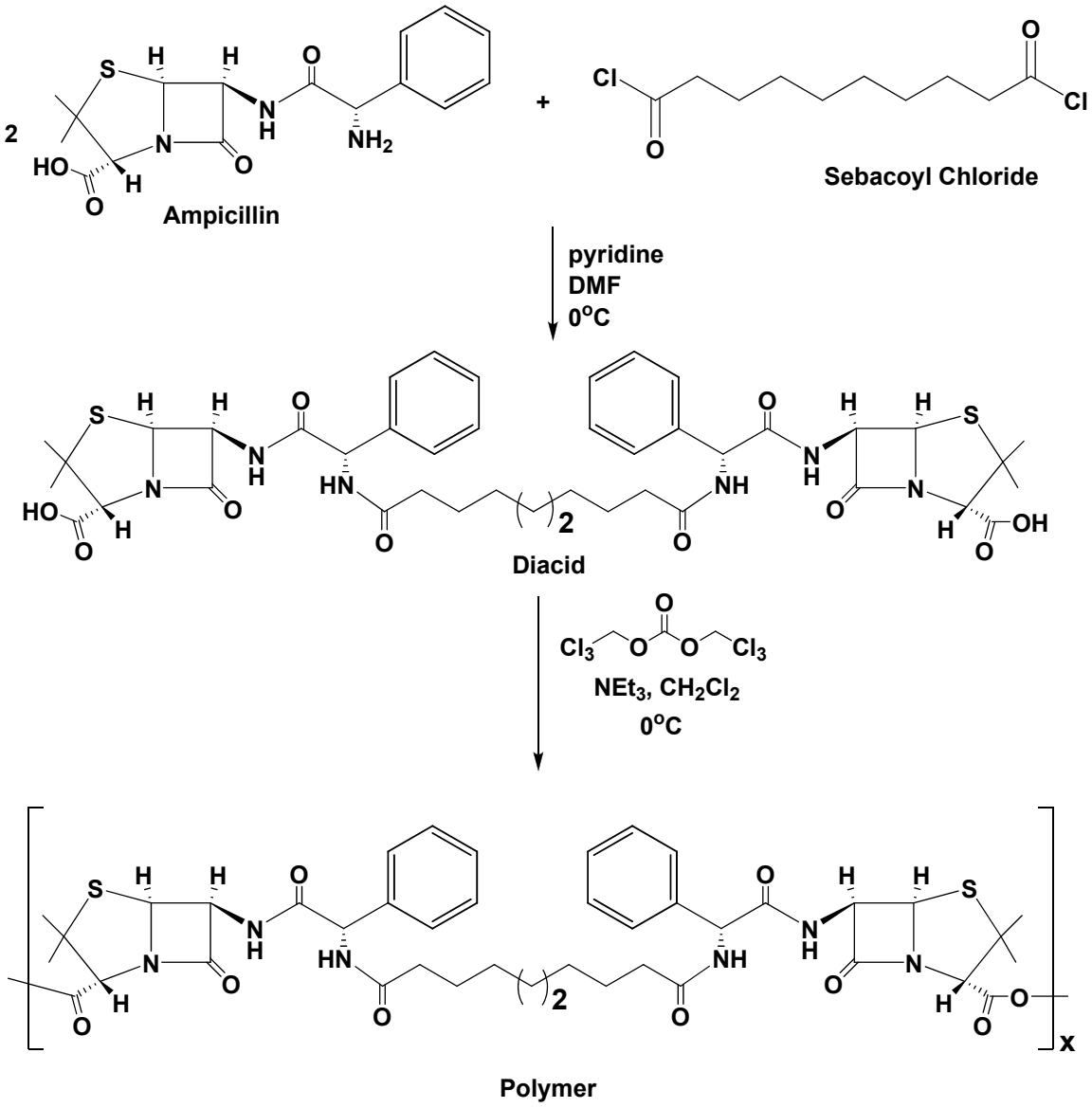

A1.5. References

1. Schmeltzer R, Anastasiou TJ, Uhrich KE. Optimized synthesis of salicylate-based poly(anhydride-esters). Polym Bull 2003;49(6):441-448.

2. Prudencio A, Schmeltzer RC, Uhrich KE. Effect of linker structure on salicylic acid-derived poly(anhydride-esters). Macromolecules 2005;38:6895-6901.

3. Anastasiou TJ, Uhrich KE. Novel polyanhydrides with enhanced thermal and solubility properties. Macromolecules 2000;33(17):6217-6221.

4. Schmeltzer R, Johnson M, Griffin J, Uhrich KE. Comparison of salicylate-based poly(anhydride-esters) formed *via* melt-condensation *versus* solution polymerization. J Biomater Sci Polymer Edn 2008;in press.

5. Prudencio A, Song, M, Uhrich KE. Synthesis of novel antimicrobial-based poly(anhydride-amides) and antibacterial assessment. Biomacromolecules 2007(under review).

CURRICULUM VITA

Michelle Linette Johnson

EDUCATION:

9/2004 – 5/2008	Rutgers, The State University of New Jersey, Piscataway, NJ Ph.D. Candidate, Department of Chemistry and Chemical Biology
8/1998 – 5/2002	University of Virginia, Charlottesville VA, B.S. Chemistry

POSITIONS HELD:

9/2005 – 5/2008	Graduate Fellow Department of Chemistry and Chemical Biology Rutgers University, Piscataway, NJ Research Advisor: Kathryn E. Uhrich, Ph.D.
5/2006 – 9/2006	Research Intern, CDRH/OSEL/DCMS Food and Drug Administration, Rockville, MD Supervisor: Dinesh V. Patwardhan, Ph.D.
5/2005 – 9/2005	Graduate Assistant Department of Chemistry & Chemical Biology Rutgers University, Piscataway, NJ
9/2004 – 5/2005	Teaching Assistant Department of Chemistry & Chemical Biology Rutgers University, Piscataway, NJ
6/2004 – 8/2004	Research Intern, Merck Summer Internship Rutgers University, Piscataway, NJ
6/2002 - 5/2004	Research Associate Clearant, Inc, Gaithersburg, MD

PUBLICATIONS:

Schmeltzer RC, **Johnson M**, Griffin J, Uhrich KE. "Comparison of Salicylic Acid-Based Poly(anhydride-esters) Formed Via Melt-Condensation vs. Solution Polymerization Processes," *Journal of Biomaterials Science: Polymer Edition*, **2008**, in press.

Johnson ML, Uhrich KE. "Concurrent Release of Admixed Antimicrobials and Salicylic Acid from Salicylate-Based Poly(anhydride-esters)," *Journal of Biomedical Materials Research,* **2008**, accepted.

Johnson ML, Patwardhan DV, Piracha NZ, Uhrich KE. *"In Vitro* Degradation of Ampicillin-Based Poly(anhydride-amide) Coatings for Medical Devices," in preparation.

Johnson ML, Uhrich KE. "Thermal and Mechanical Properties of Polymer Tubes for Nerve Regeneration," in preparation.

Johnson ML, Uhrich KE. "NGF Protein Encapsulation and Release from Salicylate-Based Poly(anhydride-esters)," in preparation.

Johnson ML, Uhrich KE. "Salicylate-Based Poly(anhydride-ester): Hydroxyapatite Composites: Characterization and Degradation," in preparation.